Journal of Computer-Aided Molecular Design
https://doi.org/10.1007/s10822-018-0134-x

PERSPECTIVE

Force field development phase II: Relaxation of physics-based criteria… or inclusion of more rigorous physics into the representation of molecular energetics

A. T. Hagler[1,2]

Received: 5 March 2018 / Accepted: 18 July 2018

Abstract
In the previous paper, we reviewed the origins of energy based calculations, and the early science of FF development. The initial efforts spanning the period from roughly the early 1970s to the mid to late 1990s saw the development of methodologies and philosophies of the derivation of FFs. The use of Cartesian coordinates, derivation of the H-bond potential, different functional forms including diagonal quadratic expressions, coupled valence FFs, functional form of combination rules, and out of plane angles, were all investigated in this period. The use of conformational energetics, vibrational frequencies, crystal structure and energetics, liquid properties, and ab initio data were all described to one degree or another in deriving and validating both the FF functional forms and force constants. Here we discuss the advances made since in improving the rigor and robustness of these initial FFs. The inability of the simple quadratic diagonal FF to accurately describe biomolecular energetics over a large domain of molecular structure, and intermolecular configurations, was pointed out in numerous studies. Two main approaches have been taken to overcome this problem. The first involves the introduction of error functions, either exploiting torsion terms or introducing explicit 2-D error correction grids. The results and remaining challenges of these functional forms is examined. The second approach has been to improve the representation of the physics of intra and intermolecular interactions. The latter involves including descriptions of polarizability, charge flux aka geometry dependent charges, more accurate representations of spatial electron density such as multipole moments, anisotropic nonbond potentials, nonbond and polarization flux, among others. These effects, though not as extensively studied, likely hold the key to achieving the rigorous reproduction of structural and energetic properties long sought in biomolecular simulations, and are surveyed here. In addition, the quality of training and validation observables are evaluated. The necessity of including an ample set of energetic and crystal observables is emphasized, and the inadequacy of free energy as a criterion for FF reliability discussed. Finally, in light of the results of applications of the two approaches to FF development, we propose a "recipe" of terms describing the physics of inter and intramolecular interactions whose inclusion in FFs would significantly improve our understanding of the energetics and dynamics of biomolecular systems resulting from molecular dynamics and other energy based simulations.

Keywords Force fields · Force field derivation · Potential functions · Van der Waals · Hydrogen bond · Drug discovery · Molecular dynamics · Molecular mechanics · Protein simulation · Molecular simulation · Nonbond interactions · Combination rules · Polarizability · Charge flux · Nonbond flux · Polarizability flux · Free energy · Coupling terms · Cross terms · AMBER · CHARMM · OPLS · GAFF · AMOEBA · SDFF · CFF · VFF · Consistent force field · Electrostatics · Multipole moments · Anisotropic nonbond potentials · Quantum derivative fitting · QDF

Abbreviations

AG	Arithmetic–geometric
Ala	Alanine
AMBER	Assisted model building with energy refinement
AMOEBA	Atomic multipole optimized energetics for biomolecular applications
AUE	Absoluter unsigned error
BCC	Bond charge correction

✉ A. T. Hagler
athagler@gmail.com

[1] Department of Chemistry, University of Massachusetts, Amherst, MA 01003, USA

[2] Present Address: Valis Pharma, San Diego, CA, USA

Published online: 30 November 2018

BNS	Ben Naim–Stillinger
C22	CHARMM22
CASP	Critical assessment of protein structure prediction
CFF	Consistent force field
CHARMM	Chemistry at HARvard Macromolecular Mechanics
CHELPG	Charges from electrostatic potentials using a grid-based method
CHEQ	Charge equilibration method
CMAP	Grid based energy correction map
CNDO	Complete neglect of differential overlap
COMPASS	Condensed-phase optimized molecular potentials for atomistic simulation studies
CVFF	Consistent valence force field
DFT	Density functional theory
DMA	Distributed multipole analysis
DZVP	Valence double-zeta plus polarization
ECEPP	Empirical conformational energy program for peptides
EHT	Extended Hückel theory
ESP	Electrostatic potential
EVB	Empirical valence bond
FEP	Free energy perturbation
FF	Force field
FQ	Fluctuating charges
FRET	Forster resonance energy transfer
GAFF	General AMBER force field
Gly	Glycine
GROMOS	GROningen MOlecular Simulation
hCatL	human Cathepsin L
HF-SCF	Hartree–Fock self-consistent-field
Hyp	Hydroxyproline
IDP	Intrinsically disordered protein
LCAO	Linear combination of atomic orbitals
LJ	Lennard-Jones
LP	Oxygen lone pair
MC	Monte Carlo
MCMS FF	Momany, Carruthers, McGuire, and Scheraga force field
MCY	Matsuoka–Clementi–Yoshimine
MD	Molecular dynamics
MDDR	MDL drug data report
MDL	Molecular Design Limited
MEP	Molecular electrostatic potentials
MM	Molecular mechanics
MMFF	Merck molecular force field
NMA	*N*-methylacetamide
OPLS	Optimized potential for liquid simulations
OPLS-AA	OPLS all atom
OPLS-AA	OPLS-AA/L OPLS all atom FF (L for LMP2)
PCILO	Perturbative configuration interaction using localized orbitals
PDB	Protein data base
PEFC	Potential Energy Function Consortium (Biosym)
PMF	Potential of mean force
POL3	Polarizable water model (3)
PP_{II}	Polyproline II conformation
QCPE	Quantum chemistry program exchange
QDF	Quantum derivative fitting
QDP	Charge dependent polarizability
QM	Quantum mechanics
RESP	Restrained electrostatic potential
RMS	Root mean square
RMSD	Root mean square deviation
RMSE	Root mean square error
SAMPL	Statistical assessment of the modeling of proteins and ligands (competition)
SAXS	Small angle X-ray scattering
SCF-LCAO-MO	Self-consistent field-linear combination of atomic–molecular orbital
SDFF	Spectroscopically determined force fields (for macromolecules)
SIBFA	Sum of interactions between fragments ab initio (computed)
SPC	Simple point charge (water model)
ST2	Four point water model replacing Ben-Naim Stillinger (BNS) model
STO	Slater-type atomic orbitals
SWM4-NDP	Simple water model with negative Drude polarization
TIP3P	Transferable intermolecular potential three point
TTBM	Tri-*tert*-butylmethane
TZVP	Triple-zeta plus valence polarization (basis set)
UB	Urey–Bradley
UBFF	Urey Bradley force field
VDW	Van der Waals
VFF	Valence force field
WH	Waldman–Hagler

1 **Introduction**

1.1 Rigorous optimization of the 12-6-1 quadratic diagonal FF, and characterization of its capabilities and deficiencies

1.2 Simple 12-6-1 quadratic diagonal FFs (as used in standard biomolecular FFs) are not adequate to achieve quantitative accuracy

1.3 Abandoning representations based on Physics for hybrid physics-based/empirical FFs. Polarizability and Empirical correction factors

2 **AMBER—empirical adjustments: on tweaking of torsional parameters to compensate for deficiencies in representation of physics**

2.1 ff14ipq/ff15ipq

2.1.1 J-coupling and secondary structure propensities—convergence issues
2.1.2 Protein stability—trajectories longer than 10 μs required

2.2 AMBER-FB15/TIP3P-FB

2.2.1 Stability of seven proteins over short trajectories
2.2.2 Temperature dependence of secondary structure in two peptides
2.2.3 CMAP in AMBER

2.3 Energetics, crystal structures and sublimation energies: a forgotten and missed powerful resource
2.4 AMBER—introducing polarizability
2.5 On the use of different data sets: a problem that permeates the FF development field and sabotages rigorous comparisons of the accuracy of FFs

3 **CHARMM—empirical adjustments: introduction of grid-based correction factors**

3.1 CHARMM22/CMAP
3.2 Rigorously comparing FFs

3.2.1 Lysozyme

3.3 C22/CMAP—extension to other families
3.4 On the immense value and validityof experimental crystal structure and thermodynamics for FF assessment
3.5 C36: further reparametrization of sidechain torsion potentials and the CMAP correction
3.6 C36m: demonstration of the need to improve the representation of the physics (atomic multipole, polarizability, charge, nonbond, and polarization fluxes, etc.) in protein and peptide FFs

3.6.1 The need for μs and longer simulations in testing FFsbased on protein stability

3.7 Thermodynamic data is essential in assessing the validity of FFs

3.7.1 Summary: physics in current 12-6-1 fixed charge FFs is incapable of reliably accounting for peptide and protein properties

3.8 Drude polarizable FF

3.8.1 A major concern—omission of flexible geometry and charge flux
3.8.2 Hydrocarbons
3.8.3 Observation of consequences of omission of charge flux
3.8.4 Internal parameters
3.8.5 Benzene
3.8.6 Extension of Drude FF to additional functional groups and proteins
3.8.7 Danger of deriving a FF from one or two compounds
3.8.8 A reparametrization of the amide FF

3.9 Drude-2013 protein force field

3.9.1 A third reparametrization of the amide FF
3.9.2 Polarizability results in degradation of Fit

3.10 Summary of Drude FF development for organic compounds and proteins. Polarizability does not lead to a general improvement of FF performance—often degrades fit

3.10.1 Inadequate training sets can lead to future failures and need for reparametrization

3.11 CHARMM polarizable charge equilibration FF

3.11.1 Significant deviations remain, indicating flaws in CHEQ FF
3.11.2 CHEQ and other FFs (other than OPLS) have difficulty accounting for energetics of tetra-ala conformers
3.11.3 Puzzling results—does the grid based correction factor, CMAP, improve accuracy?
3.11.4 On abandoning combining rules for vdW interactions and introduction of phase dependent polarizabilities
3.11.5 Summary, CHEQ FF

4 **OPLS**

4.1 OPLS2.0
4.2 OPLS-AA/M

4.2.1 Ala tetrapeptide and NMR properties
4.2.2 Limited size and information content of observables considered

4.3 OPLS2.1 and 3: a hybrid physics based—free energy function

4.3.1 Secondary structure propensities of three peptides—low resolution observables
4.3.2 Crystal structure, a more rigorous test
4.3.3 Information available from secondary structure propensities—necessary but not sufficient
4.3.4 Energetic and structural observables
4.3.5 Protein stability
4.3.6 A relative free energy perturbation tool for lead optimization
4.3.7 A prospective study—FEP is a valuable tool for lead optimization
4.3.8 Cancellation of errors makes free energy a poor criterion for FF validity

4.4 Summary of quadratic diagonal fixed charge FFs. The end of the road?

5 **Expanding the physics represented in force fields: charge, nonbond and polarizability fluxes and anisotropic nonbond interactions**

5.1 CFF

5.1.1 Charge flux—geometry dependent charges
5.1.2 Analytical representation of charge flux—a significant improvement without computational cost
5.1.3 Anisotropy of nonbond parameters: extracting parameters and functionality of pairwise nonbond interaction terms in FF from ab initio energy second derivatives
5.1.4 Annihilating all terms but the single O–O pairwise interaction in the dimer
5.1.5 Flux terms revealed by Hessian elements
5.1.6 Anisotropy of nonbond repulsion

5.2 Nonbond and polarizability flux
5.3 SDFF: the most complete formulation of a FF to date, in terms of capturing the physics of inter and intramolecular interactions

5.3.1 Multipoles, polarizability and charge flux in SDFF

5.4 AMOEBA

5.4.1 AMOEBA parametrization
5.4.2 Valuable information in discrepancies
5.4.3 The Ala tetrapeptide benchmark
5.4.4 Several studies point to the contribution of polarizability in ionic protein ligand interactions
5.4.5 Reparametrization of the AMOEBA protein FF
5.4.6 A puzzling outcome

5.5 Optimization protocols—factors in the methodology that will affect the quality of the FF

6. **Summary and conclusions: reconciling the physics based force fields with the underlying physics**

6.1 Quadratic diagonal FFs
6.2 Early attempts to better account for the physics: CFF and MM2/3

6.2.1 Second wave of development, an increasing divergence in approaches—the 2000's
6.2.2 Path one: a shift from physics-based to empirical-based potentials, while implementing polarizability
6.2.3 AMBER, OPLS, torsion parameter adjustment versus CMAP

6.3 Polarizability, necessary but not sufficient?
6.4 The second path: expanding the physics represented by the force field
6.5 CFF: charge, nonbond and polarizability fluxes: their time has come

6.5.1 Second derivatives extract energetics of single atom–atom interactions and individual valence coordinate deformations from the total energy function

6.6 SDFF
6.7 AMOEBA

7 **The future—a recipe for a physics based potential achieving experimental accuracy?**

7.1 Components of the physics currently unaccounted for in most "standard" FFs and likely required to achieve experimental accuracy in biomolecular force fields

1 Introduction

As described in the previous paper [1], the "birth" of Molecular Mechanics, occurred roughly over the decade spanning the mid 1950s to the 1960s with the pioneering publications of Westheimer [2] and Allinger [3] involving manual calculations, followed by the introduction of computers to calculate molecular energies from analytical representations by Hendrickson [4], and the important recognition that energy minimization was more robustly carried out in Cartesian rather than internal coordinates [5]. The first phase of FF development, began almost immediately following these pioneering studies. The first efforts at rigorously representing the physics of molecular conformation and interaction came from several labs including those of Lifson [6–8], Allinger [9, 10], Scheraga [11, 12] and others [13] in the late 1960s to early 1970s. These studies led in the following decade to the emergence of "protein" FFs including AMBER [14], CVFF [15, 16] and CFF93 [17], CHARMM [18], GROMOS [19], and OPLS [20], as well as the MMX series of FFs by Allinger [21].

These FFs were refined over the subsequent years, though as noted in previous paper [1], even in these early days there was a subtle difference in overall objectives and therefore methodology. Thus AMBER, CHARMM, GROMOS and OPLS developers were, for the most part, focused on applications to proteins, which, because of computational constraints, led to emphasizing "simplicity" in the FF representaion [22] i.e., using a "minimal" FF. This was manifested in the initial FFs by ignoring nonpolar hydrogen atoms (the "united atom approximation"), and in subsequent versions by adherence to the simple quadratic diagonal form. (This is not to say accuracy was not also a concern and significant effort was expended to optimize these simplified force fields to reproduce experimental data).

On the other hand, the emphasis in the early development of the MMX and CFF force fields was primarily concerned with improving the representation of the physics of molecular interactions, with computational economy a secondary concern. For example in the earliest days Lifson and Warshel noted that certain deviations in molecular properties reported on the need for representation of the physics of coupling between torsion angles and the two valence angles they contain [23]. Hagler and Lifson probed the energies and structures of crystals to reformulate the representation of the physics of hydrogen bonding [16, 24, 25]. Allinger carried out perhaps the most systematic and extensive development of FFs. He gathered discrepancies arising from application of each generation of the MMX FFs [10, 21, 26, 27] (over 5–10 years), analyzed these for the physics missing in his FF representation, such as various intramolecular couplings, reformulated the representation and rigorously tested the new FF against all data used in previous generations as well as additional data. Similarly, Hagler et al. also accounted for the known physics of intramolecular coupling by introducing a large number of valence interaction terms (cross terms) in their CFF force field, examined deficiencies in the representation of the physics of out-of-plane deformations and discarded the "improper torsion" for a more physical description of the out-of-plane coordinate [28], and interrogated the properties of rare gas interactions to establish more accurate combination rules [29]. It should be emphasized that all these FFs were targeted to treatment of proteins and other biological systems, including later versions of the Allinger FFs [30].

1.1 Rigorous optimization of the 12-6-1 quadratic diagonal FF, and characterization of its capabilities and deficiencies

Over the years spanning their introduction in the 1980s to the late 1990s and early 2000s the minimal, diagonal quadratic FFs were further optimized, against experimental and QM data. The first major step was the restoration of nonpolar hydrogen atoms into the molecular structures, implemented in AMBER [31] in 1986, CHARMM in 1992, though not published until 1998 [22], and OPLS in 1996 [32], Gromos is an outlier in this respect as it still uses "united atoms" [33]. The FFs were refined over this period, and converged toward the end of the century with the publication of the CHARMM22 FF [22] (C22) in 1998, AMBER ff99 [34] and GAFF force fields [35] in 2000 and 2004 respectively, and the OPLS-AA [32] and OPLS-AA/L [36] FFs in 1996 and 2001. As noted in the previous paper, these studies, published within a few years of each other, were all well designed, methodical optimizations of the parameters for the respective quadratic FFs. The observable to parameter ratio was large and the resulting force fields were stringently tested against an extremely comprehensive set of experimental and quantum mechanical properties of a variety of molecular systems including isolated molecules, liquids and crystals outside the training set. The set of training and validation data used in these studies is worth noting as they should set a standard for future developments, and as in Allinger's approach it would have been worth incorporating and adding to these in future assessments of FF accuracy.

For example, in perhaps the most comprehensive study Karplus and coworkers invoked gas-phase structures from microwave and electron diffraction data and crystal structures from X-ray data, supplemented by QM data, and vibrational frequencies from IR and Raman spectroscopy and

(scaled) QM calculations, along with solution and crystal spectra for systems where gas phase data wasn't available, to determine intramolecular force constants and reference values. Relative conformational energies, and barriers, of a variety of model compounds were also used in optimizing and testing the parameters. Nonbond parameters were obtained from extensive QM calculations of dimer interaction energies and structures as well as QM and experimental dipole moments. These were then refined by fitting heats of vaporization and molecular volumes of aliphatic and polar neutral compounds as well as some crystal heats of sublimation and unit cell parameters.

The FF was then tested by comparing calculated results with a large set of experimental and QM properties outside the training set. This included energies and geometries of NMA–Water and NMA–NMA dimers, and heats of vaporization and volume of neat NMA, as well as heat of solution of NMA in water. Structures of crambin, BPTI, and carbonmonoxy myoglobin in vacuo and simulations of crystals of three tripeptides, six cyclic peptides, crambin, BPTI and carbonmonoxy myoglobin, were compared with experimental structures.

Though not quite as extensive, the data sets used in the parametrization of the AMBER [34, 35] and OPLS FFs [32, 36], were also quite large (and for the most part distinct from each other and the observables used in the derivation of CHARMM22). The Amber data set consisted primarily of experimental conformational energies, structures and vibrational frequencies of a limited set of representative compounds to derive the intramolecular force constants [37]. The torsion potentials and charges were then refined based on experimental and QM conformational energies from 82 small molecules, six alanine dipeptides and 11 tetrapeptides, and QM electrostatic potentials [34]. OPLS exploited QM calculations on a set of some 50 organic compounds to derive torsion potentials, along with experimental heats of vaporization and densities of 34 organic liquids [32]. All OPLS amino acid torsion parameters as well as the nonbond parameters of sulfur containing amino acids were refined by fitting the torsions to 108 dipeptide and ten Ala tetrapeptide energies, as well as two QM dimerization energies, and experimental heats of vaporization and densities of four sulfur containing compounds [36].

The reason for listing the observables that went into the derivation of these FFs is twofold: As noted, the first is to highlight the extensive set of both experimental and QM data that formed the basis of these FFs, and allow for comparison with current FF development studies. The second is to show the quality of the derivations and the validity of the assessment of the capabilities and limitations of the 12-6-1 quadratic diagonal functional form.

1.2 Simple 12-6-1 quadratic diagonal FFs (as used in standard biomolecular FFs) are not adequate to achieve quantitative accuracy

These exhaustive studies, both individually and taken together, demonstrate that many features of biomolecular systems can be captured by this simple representation, and useful *models* can result. *However*, equally clear is that, they rigorously and definitively, demonstrate that this simple representation categorically falls significantly short of achieving quantitative accuracy (e.g. deviations of several kcal and 20–30% or more in different observables are commonly encountered [1, 22, 32, 34, 36, 37]) This has been recognized earlier by several groups, for example, Karplus et al. noted several times that significant deviations in particular calculated observables, pointed to possible limitations in the functional form and commented [22],

> … the present method provides an approach for identifying limitations in the potential function and correcting them after detailed examination

Likewise MacKerell et al. acknowledged the inability of the physics described by the simple diagonal FF form to account for peptide and protein conformation, by introducing an empirical grid-based correction factor (CMAP), discussed below, to adjust the inherent inaccuracies in the FF [38, 39].

Kaminski et al. commented [36]

> A major problem with all widely used protein force fields is the functional form of the potential energy. At present, this functional form" (i.e. quadratic diagonal FF) "has significant restrictions…. We and others have shown that, unless the functional form is modified to be more realistic, some errors in energetics cannot be overcome.

Others, including Mu et al. [40] Cardamone et al. [41] and Pierro end Elber [42] have also called attention to deficiencies inherent in this simple form. The inadequacy of this simple approximation is not surprising given it is an inherently crude approximation of both the intra and intermolecular forces. For example, the atomic spatial electron density is not spherical, resulting in atomic multipoles and anisotropic repulsion, and changes with both geometry (charge flux) and environment (polarizability), none of which can be accounted for by a single fixed point charge [43]. Use of the single inverse 6th power term for dispersion, inverse 12th power repulsion rather than an exponential form, are both approximations without a firm theoretical foundation, especially at short distances [43, 44]. The lack of coupling and the use of the same van der Waals approximation for intra molecular interactions as for intermolecular interactions further impact the accuracy achievable with this simple function.

Recognizing the severe limitations of the simple form, FF developers embarked on developing representations that more faithfully recapitulated experimental results, and more reliably predicted properties of molecular and biomolecular systems. The divergent approaches described above, i.e., a focus on improving the representation of the physics vs focusing on simple representations and speed were magnified in the subsequent years and persist in the present. Thus, generally the AMBER, CHARMM, and OPLS schools directed their efforts to "correcting" the simple form. This was done by abandoning the "physics-based" FF representation and creating a hybrid empirical/physics based functional form employing correction factors or error functions derived by essentially creating a torsion dependent function which when overlaid on the physics-based potential reproduced the observed values of the systems being simulated.

Over the same period, the MMX and CFF schools, continued to focus on further improvement of the representation and coverage of the components comprising the physics of molecular interactions and deformations. These effort were also reflected in the MMFF [45], SDFF [46], AMOEBA [47] FFs which emerged in response to these limitations. Both approaches are reviewed in the following.

1.3 Abandoning representations based on physics for hybrid physics-based/empirical FFs. Polarizability and Empirical correction factors

In the years since the publication of the classic papers described above, the school exploiting these simplified representations has taken a twofold approach in attempting to improve their reliability. The first is to account for polarizability in the energy expression [48–51] using a variety of approximations [50, 52–54], to improve the representation of the physics of molecular interactions. The second is to introduce empirical torsion based error functions to compensate for errors inherent in these simplified force fields. It should be noted that although there has been a huge effort devoted to inclusion of polarizability into FF representations, the vast majority of simulations still employ the fixed charge model.

2 AMBER—empirical adjustments: on tweaking of torsional parameters to compensate for deficiencies in representation of physics

Following the publication of FF99 in 2000 [34], a series of studies, which have continued to the present [55] have been devoted primarily to modifying the torsion correction in order to correct discrepancies that appeared in previous applications of the 12-6-1+ diagonal representation to proteins. The empirical nature of torsion potential correction factors has been noted by several FF developers, for example Ceruti et al. [56] stated

> "…the role of the torsion Fourier series is to **artificially** correct errors in the nonbonded electrostatic and van der Waals interactions between atoms on either end of a dihedral; the PES of a rotatable bond is mostly captured by the nonbonded parameters." (emphasis added)

In 2006 Hornak et al. [57] reviewed and compared eight variants of the AMBER FF proposed in the intervening years. Each of these emphasized modifications of the ϕ-ψ dihedral potentials. He pointed out that:

> "All these previous modifications" (of torsion potentials) "were aimed at correcting an apparent problem encountered with a specific system. The heuristic approaches that were employed might have improved that specific weakness but a more systematic revision was clearly necessary to quantify the problem and address the issue with generality and transferability in mind"

Hornak et al. then carried out another extensive systematic reparametrization of the torsion terms in an attempt to improve these potentials. As seen by the numerous subsequent studies that revisited this problem and reparametrized yet again these torsion parameters, for example those cited by Debiec et al. [58] Lopes et al. [59] and Wang et al. [55] the effort is much like that of Sisyphus, condemned to repeatedly push a boulder to the top of a hill only to have it roll down again each time. As noted by Hornak et al. [57] the torsion angle functions modified to fix one property, inevitably fail when applications to another set of systems are carried out, demanding further modifications, and the process is repeated, seemingly ad infinitum.

The basic problem is that the torsion correction is not robust enough to correct for the deficiencies in the intra and intermolecular physics, such as description of spatial electron density, coupling, charge flux, etc. which will have very different functional forms. Thus, when exploring other domains of configurational space the periodic torsion "correction term" will deviate from the coordinate dependence of the missing interactions.

2.1 ff14ipq/ff15ipq

Recently another reparametrization of a fixed charge AMBER FF (ff14ipq/ff15ipq) was undertaken [56, 58], motivated primarily by the desire to implement a set of charges that reflect the polarized state of molecules in the condensed phase. This was accomplished by fitting the electrostatic

potential of model compounds such as peptides in vacuo and polarized by a reaction field corresponding to that produced by a time averaged water density. The average of these charges yields the energy of the corresponding polarizable system. In addition to reformulating the charges, many new Fourier series torsion terms were added including different torsional potentials for different amino acids. This raised the total unique torsion terms to 900 from the 67 in the ff99SB force field [57]. The ff15ipq FF also invoked the SPC/Eb water model [60], based on its ability account for rotational diffusion of proteins in water. The torsion and angle bending constants were fit to an immense set of ~250,000 QM conformational energies of short peptides, calculated at the MP2/cc-pVTZ level. RMS deviations in the relative energies were still large, varying from 1.3 kcal/mol for the neutral amino acids to 2.4 kcal/mol for the positively charged amino acids. Maximum deviations ranged between 3 and 4 kcal/mol, though these comprised a small percentage of structures. The addition of the large set of torsion error functions seems to have played a major role in the fitting as the torsion contribution to the energy is much larger than in previous AMBER FFs, often by a factor of two [56].

The FF was tested by assessing its ability to account for a diverse set of experimental and QM properties. One of the motivations for the reparametrization was to address the problem of over-stabilization of salt bridges by ff14ipq [56]. To correct this deficiency, it was found necessary to empirically correct (increase) the radii of hydrogen atoms bonded to nitrogen in both the protein backbone and side-chains. The resulting FF was used to simulate the bound fraction of three pairs of oppositely charged amino acid side-chain analogues: guanidinium-acetate, butylammonium-acetate and imidazolium-acetate. A very useful aspect of the assessment was comparison of simulations of the same systems with a variety of standard force fields [61] including two polarizable FFs (CHARMM Drude-2013 and AMOEBA). Results were in reasonable agreement for the first two systems (for which experimental data is available), where ff15ipq performed as well or better than the other fixed charge FFs. Interestingly both polarizable FFs outperformed the fixed charge FFs. This is gratifying as the contribution of polarization would be expected to be most pronounced in charged systems.

2.1.1 J-coupling and secondary structure propensities—convergence issues

A further test of ff15ipq was carried out by comparing calculated and experimental J-coupling constants for the Ala_5 peptide [62]. Again, the coupling constants were reproduced reasonably well by the FF, with several problematic observables noted. The FF performed comparably to other fixed charge FFs, some of which included these observables in the training set. Next, the ability of the FF to account for secondary structure propensities in oligopeptides was investigated. **α**-helical propensity was gauged by comparing the results of μs MD simulations of the peptides Ace-GGG-$(KAAAA)_3$-K-NH_2 (K19) and Ace-$(AAQAA)_3$-NH_2 in aqueous solution and comparing with experimental helicities. Qualitatively the results mirror experiment in that the K19 peptide is found to be more helical than Ace-$(AAQAA)_3$-NH_2 at 300 °K. However, as the authors point out, even these 4 μs simulations "are not sufficiently long to obtain converged estimates." This can be seen in part from the trajectory of K19 where, though it is ~40% helical, this is almost entirely in the initial 1.2 to 1.3 μs and only brief excursions into this state by short peptide substructures occur for the remainder of the trajectory. Another manifestation of the convergence issue is that K19 appears to be as much or more helical at 305 °K than at 275 °K, contrary to the experimental results (which shows a T_m of ~282 °K [63]). Thus, as the authors point out, more extensive simulations are required to confirm these conclusions. Similar simulations were carried out on three model β-hairpin systems to assess the ability of the FF to account for β-sheet propensities. As with the α-helical simulations, convergence was an issue and though some encouraging qualitative results emerged, anomalies were also noted. Conclusive results await further work.

2.1.2 Protein stability—trajectories longer than 10 μs required

ff15ipq was also evaluated by assessing its ability to account for protein stability. To accomplish this, simulations of the Trp-cage miniprotein and six small globular proteins (BPTI, villin, GB3, ubiquitin, binase, and lysozyme) were carried out. Six 4μs calculations were carried out for the Trp-cage over a temperature range of 275–325 °K, while the globular proteins were simulated for 2–10 μs at temperatures between 298 and 303 °K. The melting temperature of the Trp-cage was found to be ~318 °K in good agreement with the experimental T_m of 315 °K. Most of the six globular proteins are stable and remain within 1–1.3 Å of their experimental structure. A notable exception is binase where an RMSD of 3.4 Å was observed (Fig. 1). It was noted that the largest deviations occurred in loop regions, typical for simulations of globular proteins, but even the core diverged significantly when compared to the other structures, exhibiting an RMSD of 1.9. Another significant excursion from the experimental structure occurred in the ubiquitin trajectory. The overall RMSD for this protein was 1.2 Å however in the last 2μs of the 10 μs trajectory a transition to a structural state ~2 Å from the experimental structure occurs. An analogous but smaller excursion occurs at ~9 μs in the trajectory of GB3 (Fig. 1). Again, convergence is an issue in determining whether these are simply transient fluctuations, and the

structure will return, or they are initial transitions to alternative states.

An important aspect of this work is the extension to additional biophysical properties such as NMR relaxation parameters [15] N R1 and R2, [15] N–1H, heteronuclear NOEs, and protein rotational diffusion constants. Overall the mean absolute percentage errors in the calculated values of R1 and R2 were found to be reasonable (10 and 12%) for GB3 and ubiquitin respectively, and average deviations of 8 and 19% for R2. However, several residues display much larger deviations from experiment, ranging from 20 to 47%. Heteronuclear NOE values are more problematic, displaying overall errors of 22 and 30% for the two proteins. Finally, reasonable rotational diffusion constants were calculated for ubiquitin, GB3, and binase (deviations from 14 to 22%), though these had to be calculated in several independent NVE ensembles to avoid perturbations by the thermostat.

The implications of the deviations in these NMR properties as a probe of the quality of the FF and the correlation with errors expected in other calculated structural and thermodynamic properties is not entirely clear at this stage.

Overall the calculations employed to derive and validate the ff15ipq force field represents a tour de force. Hundreds of microseconds of simulations enabled the calculation of stability of salt bridges, conformational equilibria of peptides, structural stability of proteins and elegant calculations of NMR observables, all compared with corresponding experimental data. In addition, many of these properties were simulated with several other standard force fields allowing for a direct comparison of their relative abilities to account for these properties.

On the other hand, as noted above for other force fields, the flip side of calculating this impressive set of properties, is that most of the more standard experimental observables used in the validation of previous FFs were not addressed. It would be extremely useful to reproduce critical properties such as heat of vaporization, dimerization energies, solvation free energies and crystal properties, especially those reported on in previous generations of AMBER and other FFs. Many of these observables are also more intimately related to the most common applications of these FFs. Finally, because the cost of calculating properties which require 10 s of microseconds of simulation is substantial, their number is severely limited. Thus, the benchmark used for validation contained 15 J-coupling constants and 13 other observables, 5 of which, the secondary structure propensities, didn't converge. In addition, 15 qualitative observables, i.e., conformational preferences of amino acids in oligopeptides compared to those observed in protein loops, were investigated. (For comparison the validation benchmark for the vdW parameters alone [64] in the polarizable AMBER FF contained a total of 64 well determined thermodynamic properties comprised of densities, solvation energies, and vaporization energies). Comparison can also be made to the recent derivation of C36m where, as discussed below, properties of a large set of 15 peptides and 20 proteins were employed to document deficiencies in the FF [65]. This included stabilities of 15 folded proteins, though these were simulated only for a μs, which based on the results displayed in Fig. 1, may be insufficient (though it was long enough to reveal problematic systems).

In summary, though ~ 900 additional torsion correction parameters were added, based on the comparisons carried out in the study, and the deviations from experiment detailed, it appears that ff15ipq is comparable to other fixed charge quadratic diagonal FFs. Though It does not seem to be demonstrably superior.

2.2 AMBER-FB15/TIP3P-FB

Another reparametrization of the AMBER FF has been carried out more recently [55]. A major focus of this study was the use of quantum derivative fitting [28, 66] in the optimization of the FF. In this application only Cartesian first derivatives of the energy (forces) were exploited, along with energies and vibrational frequencies [55]. In this case valence parameters were optimized, starting with parameters from ff99SB [57], while the nonbond parameters were transferred without further modification. The Lorentz–Berthelot combining rules for mixed van der Waals interactions (arithmetic mean for radius, geometric mean for well-depth), and improper torsion for out of plane description are used. These have been shown to be flawed representations (combining rules [29, 67]; out-of-plane coordinate [28, 68]) and will indubitably result in errors in other parameters in order to compensate.

An attractive aspect of this study was the comparison of results with seven FFs. In addition assessment with four water models (TIP3P [69], TIP3P-FB [70], TIP4P-Ew [71], TIP4P-FB [70]) was carried out. It was found that the optimal results with the derived FF were obtained when used in combination with the TIP3P-FB model and the resulting FF was labelled AMBER-FB15/TIP3P-FB.

2.2.1 Stability of seven proteins over short trajectories

Though the comparison of water models and a variety of FFs provides useful information, the downside is that computational costs limit the validation of the FF to a small set of systems. Thus, the stability of only eight proteins was evaluated, and the simulations were limited to ~ 500 ns. As seen from Fig. 1 [58] discussed above, and the results of Huang et al. [65] 500 ns is insufficient to fully assess protein stability. As the authors point out however, lack of stability in a short trajectory indicates errors in the FF. Limited experience including the studies cited [58, 65], indicate that

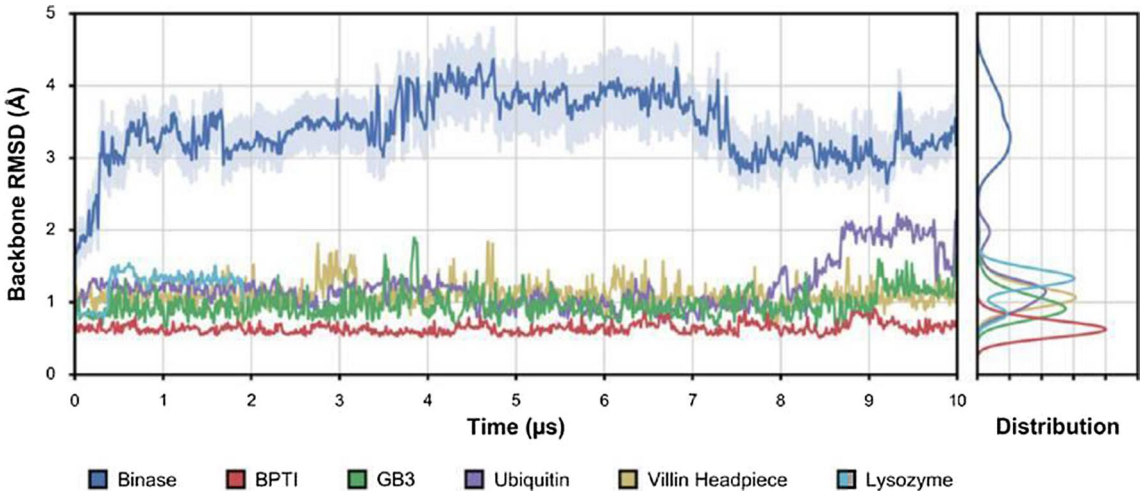

Fig. 1 Backbone RMSD of six globular proteins from experimental structure. Note the excursions to higher RMSDs for ubiquitin (at ~8 μs) and GB3 (at ~9 μs). Reproduced with permission from Debiec et al. [58]

in general one or two proteins out of seven will probe FF errors, and even in the relatively short trajectories carried out here, this seems to hold as well The reason for this is uncertain, but may lie with such factors as disulfide constraints, intrinsic stabilities, or simply the random initial velocities applied. In this case lysozyme is the problematic system (RMSD approaching 2.3 Å RMSD over the final 200 ns). Ubiquitin also seems to show a possible transition to an alternate state with a larger RMSD at ~300 ns. Small amplitude fluctuates around an RMSD of 0.8 Å occur for the first 300 ns, followed by a seeming transition to ~1.4 Å and larger excursions over the following 200 ns. This is reminiscent of the behavior of ubiquitin with ff15ipq [58] (Fig. 1), albeit much sooner in the trajectory. Overall the results with AMBER15-FB/TIP3P-FB are comparable to the other FFs and water models investigated.

Because of the inadequacy of even microsecond simulations, though large deviations in protein structure (> 2–2.5 Å) are a valuable property to reveal errors in FFs, lack of deviations do not attest to the accuracy of the FF. For the latter, it is likely that trajectories of many 10 s of μs to perhaps milliseconds will be required.

NMR properties of these proteins were also assessed. For example, 3J scalar couplings were calculated from the trajectories and compared with experiment for four of the proteins. The fit was comparable to that achieved with other AMBER FFs, with root mean square errors of ~1 Hz, though much larger deviations were observed (~2–2.5 Hz) for some residues. In general, NMR parameters are used to probe and determine structure. As the structures of these proteins are known from X-ray to atomic resolution, and the simulation may be compared to these experimental structures, it is not clear that the NMR properties add significantly to the FF evaluation.

2.2.2 Temperature dependence of secondary structure in two peptides

In addition to the stability of globular proteins the FF was assessed by calculating secondary structure propensities as a function of temperature for the helical peptide Ac-(AAQAA)3-NH2, and the β-hairpin CLN025 [72]. Although, the performance was somewhat improved relative to the other AMBER FFs, significant deficiencies remained. Thus, AMBER-FB15 significantly underestimates the slope in both curves, relative to experiment. This results, for example in the underestimation of the folded fraction of CLN025 by 15% at 280 °K and overestimation by roughly a factor of 2 (40 vs. 20% exptl) at 370 °K. An examination of the fraction of peptide folded versus the water–peptide interaction energies for the four water models, revealed that, as might be expected, they are inversely proportional.

Finally, the radius of gyration of GB3 the denaturated state ensemble for was calculated with the seven peptide models and four water models and compared with experiment. The simulated structure was too compact with all FFs (17.7 Å in AMBER15-FB vs experimental value of between 22 Å from FRET and 26 Å SAXS). All FFs gave comparable results, though several were in better agreement.

In summary, the AMBER15-FB/TIP3P-FB FF seems to give comparable results to other contemporary FFs, but does not seem to offer any clear advantage to the latter. Deficiencies inherent in the common functional form remain. It is somewhat difficult to make a comprehensive comparison to other FFs because of the relatively small validation set, and short time scale of the simulations. For example, in the recent derivation of the C36m FF [65], the stability of 15 globular proteins over a μs was assessed as opposed

to the 7 structures considered here which were simulated for ~500 ns. Similarly, populations of the folded states of 4 β-hairpins and radius of gyration of four peptides were compared to experiment, among many other properties. These allowed for a thorough documentation of the deficiencies in the FF.

2.2.3 CMAP in AMBER

The inability of torsion corrections to produce acceptable agreement with experiment over a wide range of properties and systems recently led to several groups abandoning this approach in AMBER and resorting to the more all-encompassing grid based CMAP [73] correction factors [74, 75].

2.3 Energetics, crystal structures and sublimation energies: a forgotten and missed powerful resource

Omissions common to many recent FF assessments is the lack of energetic observables and atomic resolution data of small peptides and organic compounds. As discussed in more detail below, assessment of energetics of helix formation [62] and folding [76] demonstrate conclusively that FFs which can reproduce protein stabilities, secondary structure propensities, and NMR solution properties can still result in unacceptably large errors in energies. In addition, there is a pervasive lack of crystal structure observables in contemporary FF assessment. Thus, for example, the crystal structure of CLN025 is presented in the same paper [72] that the experimental helix propensities of the peptide are determined. This is much more information rich data than the solution data, to test FFs.

Relative inter and intramolecular forces can be assessed based on the structure and conformation of the molecule in the crystal [77, 78]. Peptide crystals often contain water molecules and thus provide atomic resolution probes into the validity of water peptide interactions. Peptide [22, 79–84] and small model compound [24, 25, 85–92] crystals had been used for years to assess FFs. There is also a huge literature on the derivation and testing of FFs from crystal properties in the field of packing mode predictions [93–97]. As noted these systems are more information rich than solution properties, while cheaper to compute. Furthermore they lend themselves to interrogation, yielding insight into deficiencies in the FF and more importantly ways to correct the representation, much in the way Lifson [23] and Allinger [91] examined deviations from experimental properties and corrected the FF representation. An analogy might be the ability to understand protein function. Though many spectral approaches including light scattering were used to investigate proteins it wasn't until X-ray diffraction elucidated the atomic structure that we gained insight into the underlying architecture of proteins and its relation to function. In much the same way, by examining the discrepancies in intermolecular (or intramolecular) structure observed in these crystal simulations, for example, CH···O distances that are too large, or H-bonds that are too long, or distorted, or benzene packing which distorts the herringbone structure, or has correct structure but underestimates sublimation energy, etc. we can intuit discrepancies in the functional form and test enhancements. This simply can't be done with solution properties since we don't know underlying discrepancies in interatomic or intramolecular geometry at the atomic level. Thus, we may get correct heats of vaporization, or density for example, but they may correspond to the wrong structure. It is not clear why this valuable assessment information seems, for the most part, to have been forgotten/abandoned in assessing contemporary biomolecular FFs, but it is clearly a handicap in both deriving and assessing these energy functions.

2.4 AMBER—introducing polarizability

AMBER was one of the first FFs to add polarizability into the energy expression [34, 98] employing an induced atomic dipole model [49, 53] for representing the polarization. The polarizabilities were derived by fitting to QM and experimental conformational energy differences of 60 organic pairs [1, 34]. Unfortunately, inclusion of polarizability actually resulted in degradation of the fit, though when torsion parameters were allowed to vary simultaneously the situation improved somewhat [34]. Nevertheless, this presaged future results as discussed below; namely, though inclusion of polarizability is important in certain systems, e.g. those containing charge–nonpolar interactions, in general its inclusion has not yielded the improvement in accounting for experimental or QM properties hoped for.

In 2011–2012 Wang et al. carried out a series of rigorous studies to derive a polarizable AMBER FF using the induced dipole method [64, 99–101]. In the first study, they parametrized atomic polarizabilities by fitting to an extensive set of 420 experimental molecular polarizabilities. Several models were tested including the effect of the inclusion or exclusion of 1–2 and 1–3 interactions, and various scaling factors for the 1–4 interactions were examined. In the second paper the performance of the various polarizable models were tested by comparing the dimerization energy calculated with these models to QM dimerization energies calculated at the MP2/aug-cc-pVTZ level. In addition results were compared with two fixed charge AMBER FFs, ff99 [34] and ff03 [102]. Here too, a very large set of dimers comprising 481 amino acid main- chain and side-chain analog pairs were used to test the various models.

This work provides a thorough characterization of the performance of various polarization models given the large set of dimer interaction energies treated. Overall a reasonable

agreement to the QM energies was found with the best of the 12 polarization models considered (RMS error of 1.41 kcal/mol). However, 44 of the 481 dimers returned deviations greater than 2.5 kcal/mol in the dimerization energy. As noted above, the elucidation of such problematic systems is perhaps the most valuable result of FF assessment studies. They provide critical observables for deriving and testing future FFs (this of course holds only if proposed enhanced FFs exploit these information rich systems as discussed below).

Based on the results of the calculations, it was concluded that inclusion of polarizability "notably improved accuracy in comparison with the fixed charge models". It would appear however, that this conclusion is deeply flawed. This is based on the fact that the conclusion was drawn by the fit to dimerization energies calculated at the MP2/aug-cc-pVTZ level as noted above. The electrostatic parameters for the polarizable model were calculated at the same MP2/aug-cc-pVTZ. *However, for the fixed charge FFs, ff99 and ff03 models, the charges were calculated at the original HF/6-31G*, and B3LYP/cc-pVTZ//HF/6-31G** levels respectively*. Thus, it is not surprising that the energies resulting from these charges are significantly inferior in fitting MP2/aug-cc-pVTZ energies. This clearly does not necessarily represent a deficiency in the fixed charge model as much as incompatible charges. In fact, the deviations reported far exceed deviations found in the original papers, as well as in other 12-6-1 FFs, though for a different set of observables. To validly compare a fixed charge model to a polarizable model one would need to optimize the parameters against the same training set, in this case consistently using the same basis set to derive the charges as that used to calculate energies. Furthermore, the magnitude of the errors quoted are inconsistent with those obtained by fixed charge FFs, including AMBER, both prior to and subsequent to this work. For example the studies of free energy of hydration of small solutes [103] and a study on the transport and thermodynamic properties of ionic liquids using the GAFF force field [104], both containing similar functional groups yield much smaller errors than those which would be expected from the above study [100].

The work was extended to comparing four polarizable water FFs, two 3-site and two 4-site models [64]. It was found that the FFs were able to account for the density and heat of vaporization of water, but were unable to reproduce dynamic and temperature dependent properties of the liquid.

This was followed by a reparametrization of the vdW parameters [101]. Again, an impressively large set of both QM and experimental observables were used in deriving and testing of these parameters. The training set consisted of 1639 QM interaction energies of model compounds, along with densities, and heats of vaporization of 25 pure organic liquids. The validation set consisted of densities of 34 pure liquids, heats of vaporization of 33 pure liquids, and solvation free energies of 15 compounds. A reasonable agreement with both QM and experimental data was obtained. For example, the percentage errors in the densities ranged from 3.17 to 4.50%, and RMSDs in dimer interaction energies and heats of vaporization ranged from ~1.56–1.66 and 1.62–2.61 kcal/mol respectively, for various polarizable models [101]. As in the original assessment of polarization without optimization of the vdW parameters [100], the reproduction of the thermodynamic properties is reasonable, though the magnitude demonstrates that significant deficiencies in the FF remain.

Also, as with the original assessment, it was concluded that the addition of polarizability significantly improves the performance over additive FFs. The basis of the conclusion, however, is again highly problematic. For the additive F99/GAFF [35] potential, charges were again determined from the original 6-31G* ESP as opposed to the more accurate MP2/aug-cc-pVTZ electrostatic potentials used for the polarizable models. For the hydration free energy calculations the TIP3P water potential [69] was used while the polarizable water FFs were based on the POL3 model [105]. Thus, one could rigorously draw the conclusion that the polarizable FF derived here outperforms the F99/GAFF potential, but to rigorously assess the improvement to be obtained from inclusion of polarizability both the additive and polarizable FFs would have to be optimized against the same training set, using the same basis set for calculation of charges, and tested against the same validation set.

This is dramatically illustrated by the results of a contemporaneous study from one of the labs in which the additive GAFF force field was evaluated [106]. The authors found that the percentage error in the calculated densities of 71 organic liquids to be 4.43% which dropped to 3.43% when two outliers and four high pressure densities were excluded. *Furthermore, the Heats of Vaporization were reproduced with an RMSD of only 1.2 kcal/mol i.e. better accuracy than achieved with the polarizable FFs*. These simulations were carried out without optimization of vdW parameters, which, it was speculated, would further improve the fit to experiment. Thus, if these studies were the basis, *the opposite conclusion would be drawn*, i.e. not only does polarizability not improve the performance, but it led to a degradation of the fit.

2.5 On the use of different data sets: a problem that permeates the FF development field and sabotages rigorous comparisons of the accuracy of FFs

The source of the discrepancy between the assessment of GAFF by Wang and Hou [106] on the properties of the 71 compounds and the results presented in the polarizability study [101] is not clear, but obviously has significant consequences for the assessment of the contribution of

polarizability to improving the accuracy of FFs. It most likely arises from a combination of the use of different observables and test systems in the two FFs. This also serves to emphasize a problem that permeates FF development and especially comparisons among them. Different labs, and even the same labs in deriving improved FFs, employ different data sets both to derive and test the FF. This makes a truly rigorous comparison virtually impossible, and results in a plethora of papers reporting on FF derivations which are claimed to be superior to previous versions of the same FF as well as others in the literature. Inevitably these are superseded, as in the case of the AMBER FFS discussed above, it would have been interesting, and important to go back and test the FFs against the experimental and QM data used in the derivation of previous versions of published FFs including e.g. the excellent data set reported in the CHARMM22 derivation [22]. Likewise, subsequent AMBER as well as other FFs would do well to compare results with the extensive data set developed in the previous AMBER papers among others—especially for reported observables which the FF were unable to account for. And as discussed above to include both crystal structure data (such as that addressed in the CHARMM22 paper [22] and the references cited above), and a significant set of thermodynamic observables.

Adopting this practice, which is basically the CFF approach of Lifson [7, 107] would to a large extent reduce the need for subsequent reparametrizations as the increased diversity of the validation set would reveal errors occurring in these systems at the time of the FF development. The observation by Allinger [108] remains ever more relevant today.

> … It is easy to see now why different force fields were able to give good results in different areas, but not "consistent" results. Because the force fields were fit to limited data sets, they usually fit them well. But the force fields used limited parameter sets and formulations, and hence while they could fit well over a local area, they could not fit well in general.

Enlarging the set and diversity of observables to include in addition those from previous studies would involve more effort for the individual study, but reduce overall effort in that many errors occurring in subsequent applications would be eliminated, and the need for series of corrections, as discussed for example, by Hornak [57], reduced or obviated. In addition, it is the only way to rigorously ascertain whether an "improved FF" is truly more accurate than previous versions.

A corollary to the use of larger and more diverse validation sets is the interrogation of discrepancies that have arisen in previous FFs, or arise in fitting the validation set, to improve the representation of the physics, as well as force constants.

3 CHARMM—empirical adjustments: introduction of grid-based correction factors

3.1 CHARMM22/CMAP

MacKerell et al. [38] took an alternative approach to correct deficiencies in the CHARMM functional form. Rather than relying on the torsion potential to act as an error function, they implemented a grid of energy correction factors for the peptide backbone (CMAP). This was carried out by calculating difference maps of the Ala, Gly, and Pro ϕ–ψ maps calculated with CHARMM22 (C22) and the corresponding QM ϕ–ψ maps (calculated at the LMP2/cc-pVQZ//MP2/6-31G* level). The grids were calculated at 15° increments, which yielded an additional 625 parameters to fit the ϕ–ψ energy surface for Ala and 325 for Gly. The final continuous map of correction factors was obtained by carrying out two-dimensional "bicubic" interpolation between the grid points. By definition when the CMAP energies are added to those obtained with CHARMM22 it produces an essentially identical ϕ–ψ energy surface to that obtained by QM.

This is obviously a more all-encompassing empirical error function than the use of torsion functions. These functions correct for errors in nonbond and electrostatics as pointed out by others, and we would add lack of coupling terms, inaccurate combination rules and out-of-plane representations, charge, polarizability and nonbond flux, etc. As noted above with respect to the torsion corrections, *the problem is that the distance and coordinate dependence of the correction factor matrix will differ from the corresponding distance and coordinate dependence of these other terms*. Thus, for example, if there is a deficiency in the representation of electrostatics these correction factors won't help with discrepancies in the interaction of sequentially distant residues in a protein which come into proximity.

This in fact was observed when the CMAP correction was tested by a fit to crystal structures of seven proteins. It was found that systematic deviations in MD structures persisted. Further optimization of the CMAP correction grid was required which was carried out manually to reduce the RMSD between time averaged MD and crystal structures of the seven proteins. This resulted in a reasonable fit to the protein structures (1.6 Å or less for all heavy atoms) although it should be noted that these were extremely short simulations (1 ns) and increased divergence from the crystal structure is likely to occur with increasing simulation times, as discussed above.

The FF was then tested by solution simulations of three protein structures not included in the parametrization. Throughout, the RMSDs from experiment were somewhat larger than for the set used to optimize the parameters (~ 1.7 to 2.5 Å or more for all heavy atoms, based on the backbone and sidechain deviations). These larger deviations are somewhat troubling and may have resulted, as hypothesized, because the simulations were somewhat longer (5 ns, with the final 3 ns used for analysis).

3.2 Rigorously comparing FFs

Though the CMAP corrected C22 FF seemed to offer some improvement over the uncorrected FF based on these proteins, as noted above with regard to the AMBER FFs, one really can't rigorously conclude that it is indeed superior. Especially since the CMAP potential was directly trained on the these protein, while the CHARMM22 FF was trained against many other observables and protein systems were only one of the validation sets [22]. One would need to test the FF against the many observables considered in the CHARMM22 derivation and testing, especially the problematic systems noted there [22]. Of special importance in this regard are the alanine dipeptide crystal, and the three tripeptides and six cyclic peptide crystal structures. These are likely to occupy different regions of phase space and might well be better test systems, though clearly comparison of the whole set of observables would be optimal. The apparent abandonment by current workers in the field of the principles of FF development of the previous century, especially as espoused by Allinger, whereby refinements of one generation of a FF was tested on all observables used previously and additional tests were added, is unfortunate. It has led to less well validated FFs, and the proliferation of refinement papers, duplication of efforts which might/would have been avoided by more rigorous testing.

3.2.1 Lysozyme

Buck et al. [39] carried out a further simulation of Lysozyme with C22/CMAP and again compared the performance with the C22 FF. This time the protein was simulated in aqueous solution rather than the crystal and longer, though still extremely short 25 ns trajectories were obtained. The RMSD of Cα atoms was 0.9 Å, significantly better than the 1.8 Å resulting from the C22 FF. Interestingly, the C22/CMAP RMSD was slightly better than the previous result from a shorter crystal simulation. Given that solution simulations are being compared to crystal structure, and this second simulation is significantly longer one would expect the resulting RMSD to be much larger than the previous short crystal simulation. A contributing cause is very likely that the RMSD is calculated for the Cα atoms rather than the backbone or backbone sidechain atoms. The former will give significantly smaller deviations.

In addition to comparing RMSDs, order parameters were also calculated with both FFs, and, as with the structure better agreement with experiment was found with the CMAP correction. The authors conclude that the CMAP correction yields an improved description of protein dynamics, which arises from its ability to better reproduce ab-initio surfaces, including those from OPLS and AMBER. However, it had been shown previously by one of the authors that the OPLS-AA/L FF [36] reproduced the QM energies of the Beachy [109] test set of Ala tetrapeptides significantly better than C22/CMAP RMSD 0.56 versus 1.67 kcal/mol [110]. Thus, there must be more going on here, which begs elucidation. Finally, it is dangerous to draw conclusions from the simulation of a single system. When multiple systems are considered, often though many are fit well others show large deviations, as for example seen in the first paper where the three test protein simulations displayed much larger deviations than the other seven proteins [38], and more recently by Debiec et al. [58] and Huang et al. [65] as well as others.

3.3 C22/CMAP—extension to other families

MacKerell and coworkers went on to extend the additive CHARMM FF to additional families in a series of extensive studies. For a review of this research see the recent comprehensive review by Vanommeslaeghe and MacKerell [111]. For example in the 2009 study by Hatcher et al. [112], a CHARMM FF was derived for acyclic polyalcohols, acyclic carbohydrates and Inositol. The methodology used in this study is representative of that used for all the functional groups. Initial bond and angle internal parameters were transferred from values in similar families and then modified based on comparison of calculated structures with those found in a survey of the Cambridge Structural Database (CSD), and vibrational frequencies of model compounds. Nonbond parameters were transferred from the hexapyranoses [113]. There they were obtained by fitting the structure and energetics of dimers of water and model compounds obtained by HF/6-31G(d) QM calculations with energies scaled by a factor of 1.16 and H-bond distances reduced by 0.2 Å to account for polarization in the condensed phase [113]. In deriving the nonbond parameters, water was represented by the TIP3P water model. This has the advantage of obtaining consistent parameters for use in aqueous solutions represented by TIP3P, but the disadvantage of introducing errors in the carbohydrate FF to compensate for deficiencies in the water model [114, 115], which would need to be corrected if a different water model were exploited.

The nonbond parameters were tested by comparison with the QM energies and hydrogen bond distances of 24

dimers of water with the polyalcohols, threitol, ribitol, allitol and altritol as well as inositol, scaled as described above. The results are mixed, with several large discrepancies revealed. The energies of eight of the 24 complexes deviate from the QM values by 10–63% with the largest deviation observed in a ribitol-water H-bonded dimer in which the water acts as the proton donor, where the QM energy is − 2.3 kcal/mol while the FF yields a much more stable dimer of − 3.8 kcal/mol, a difference of 1.5 kcal/mol. The authors suggest that since for the most part the larger errors occur in weaker H-bonded orientations of the water alcohol dimer, and that the more favorable dimer configurations will "dominate," these deviations are acceptable. However, there are several reasons why this is cause for concern. First and foremost, the magnitude of these errors is telling us that there are major deficiencies in the representation of the energy surface. It is impossible to predict, a priori, how these deficiencies in the FF will manifest themselves in simulations of complex systems. It should be noted that, as stated elsewhere in this perspective but worth emphasizing, errors such as these are extremely valuable, as the deficiencies they reveal are the basis for improving the representation of the underlying physics of the interaction. The analysis of such deviations and subsequent modification of the description of the underlying physics, is the entire basis of the derivation of the MMX series of FFs by Allinger and the CFF force field of Lifson.

Secondly, and of equal importance, is that these are minimized, isolated dimer structures. The dynamic trajectory of liquid systems will traverse less stable regions of the energy surface, and in addition constraints imposed by competing interactions in the condensed phase may well exclude the ideal minimized geometries. Thus, in some systems of interest it is possible that the "low energy" dimer configurations exhibiting the large deviations could be prevalent, especially if they are significantly stabilized by the errors in the FF as seen here. Thus, the deviations have immense utility as probes into the inadequacies in the representation of the physics, and a basis for improvement in this representation, but the assumption that they will not be reflected in results of future applications seems perilous.

A further test of the potentials was carried out by simulating the heat of vaporization and volume of glycerol. Again, significant deviations were uncovered, − 14.2% in ΔH_{vap}, and + 4.8% in the volume. The authors note that the error in ΔH_{vap} could arise from over stabilization of intramolecular H-bonds in the gas phase due to overly polarized hydroxyls in the FF needed to represent interactions in the condensed phase. This hypothesis was assessed by using the trajectory of a glycerol molecule taken from the liquid, where intermolecular H-bonds would destabilize the intramolecular bonds, to calculate the gas phase energy. As would be expected this increased $\Delta H_{vap,}$ and brought it to within 2% of the experimental value. The reasoning is certainly plausible, though a better test might have been just to use charges obtained from the unscaled QM to obtain the gas phase properties. The liquid trajectory might well produce an overly destabilized set of "gas phase" configurations. In addition, the hydroxyls in the gas phase are also polarized by intramolecular hydrogen bonding. Other rationales for the discrepancy are equally plausible, however. It could be simply that the potential functions are inadequate. Given the dimer results this is cause for concern. In addition, as the authors point out, over polarization in the gas phase does not account for the 5% error in the volume. In general, the cohesive energy of the liquid is inversely proportional to the volume, consistent with the underestimation of ΔH_{vap}. Taken together these factors point to some deficiency in the FF.

Following the parametrization of the nonbond parameters, torsion parameters were obtained by fitting QM potential scans of six polyalcohols. Geometries of the polyols were optimized at the MP2/6-31G(d) level at 15° intervals and single point energies of the relaxed structures were than calculated at the RIMP2/cc-pVTZ level of theory. In all the energies of over 1700 conformers were obtained. Large deviations were observed with RMS errors in relative energies of 2.5, 1.6 and 1.9 kcal/mol found for the $n = 6,5,4 CH_2OH(CHOH)_{n-2} CH_2OH$ alcohols respectively. Since the conformational energies were cutoff at 15 kcal/mol, without knowing the distribution of energies if we conservatively assume the average energy is 10 kcal/mol, this would correspond to errors of 16–25%. Individual errors of course can be much larger than the mean square. Thus, for example, in inositol, the QM energy of the conformer corresponding to $\phi(C_1–C_2–C_3–C_4) = 0$ is ~ 1 kcal/mol while the energy calculated from the FF is ~ 9 kcal/mol, a 900% error. A slightly less extreme, but no less consequential example occurs in glucitol where the QM energy of the cis conformer about $O_1–C_1–C_2–O_2$ is ~ 2.5 kcal/mol while the corresponding energy obtained from the FF is ~ 9 kcal. These deviations would clearly have severe ramifications in the calculated properties of systems containing these functionalities. *In the two cases cited the favorable configurations become inaccessible*.

These errors in conformational energies are attributed to two factors. The first is that the dihedral parameters are optimized against all stereoisomers of the 6-carbon polyols simultaneously. This is a puzzling rationalization as the transferability of parameters of functional groups is one of the core foundations of classical FFs. If parameters are not transferable between stereoisomers, which have identical covalent bonding they certainly won't be transferable to biological systems of interest. The second rationale is, as in the case of ΔH_{vap}, the overly-polarized hydroxyls lead to stronger H-bonds that are broken in the region of the energy

barriers increasing the energy relative to the minimum. This is also problematic in that as we have seen in the cases of inositol and glucitol cited above, it is the low energy conformations that are destabilized. Furthermore, the QM energies are scaled by 16%, which is unlikely to cause the large errors of over 100% or more seen here. In any case the hypothesis could be easily tested by deriving the "unpolarized" hydroxyl parameters by fitting the unscaled QM energies and recalculating the torsion profiles.

3.4 On the immense value and validity of experimental crystal structure and thermodynamics for FF assessment

Additional tests were carried out on extremely informative crystal observables by simulating the crystal structures of 11 polyols, and comparing with experiment. As noted above, crystal systems provide perhaps the most critical test (or training data) for assessing both intra and intermolecular potential functions. They are far less expensive to simulate than the corresponding liquid, while at the same time providing close to an order of magnitude more observables. Thus, from a single constant pressure simulation of a crystal one obtains 1–6 lattice parameters (cubic-triclinic lattices), positon and orientation of the asymmetric unit, relative orientations of interacting molecules, interatomic distances including H-bond lengths and angles, molecular structures including torsion angles, and sublimation energies, all of which can be compared with experiment. The balance of intermolecular and intramolecular forces is exquisitely revealed by the effect different packing modes have on the molecular conformation [77, 78, 116]. A comparable liquid simulation yields for the most part two observables; ΔH_{vap} and liquid density. But even here though ΔH_{vap} might be fit, there is no way of knowing whether the underlying liquid "structure" is correct. Thus, one may achieve a good fit to ΔH_{vap} with erroneous intermolecular interactions, similar to the situation where one reproduces the binding energy of a ligand to a protein for the wrong pose. The latter does not validate the FF.

The calculated unit cell vector lengths and cell volume were compared with experiment. Consistent with what was observed with the liquid volumes, the unit cell volumes were systematically too large, with an average deviation of 7%. Unfortunately, though available [117] the fit of sublimation energies to experiment was not calculated. In addition in this case it might have been worthwhile to calculate heats of fusion, which are also available for these systems [117], and would eliminate the problems of intramolecular H-bonds in the gas phase inherent in the ΔH_{vap} comparison. It also might have been worthwhile to examine the structures of the polyalcohols in the crystal. This might have given some insight into the underlying intermolecular interactions responsible for the systematic positive deviations in liquid and crystal volumes. It should be noted that improvement in these latter observables was achieved with the subsequent Drude polarizable FFs for acyclic polyalcohols [118], and hexopyranoses [119].

The authors suggest that the deviations in volume may be due to the inapplicability of a FF derived from liquid properties to crystals. This concept appears from time to time and is both puzzling and problematic. Its basis is unclear, and would uproot many of the applications of these FFs if true. After all, a folded protein is more similar to a solid than a liquid. Atoms have well defined positions as defined by both NMR and crystallography (ergo RMSDs), and they diffract. (Protein crystal structures contain a large amount of mother liquor and much of it is disordered or solvent like and thus the environment in the crystal is similar to solution—further supported by the fact that solution and crystal structures are essentially the same.) This is why simulations of protein in aqueous solution are compared to crystal structures. Thus, if it were true that "liquid" FFs are not applicable to solids, then they are not applicable to globular proteins or other structured biomolecules—basically what they are being derived for.

Furthermore, the assumption that the microenvironment of compounds in the liquid phase is materially different than that in the solid is flawed. The liquid microenvironment is similar to that in the crystal, especially close to the melting point. For example, the microenvironment of water in the liquid, on average is close to a tetrahedral structure with the water molecule having ~4 nearest neighbors at roughly H-bonding distance, as evidenced by the radial distribution function—basically, the structure of ice [120]. Thus, it is likely that the microenvironment of the hydroxyls and methylene groups in the liquid polyalcohols is more similar to their environments in crystals of the same compound than to that of liquids of myo-inositol, or hexapyranoses to which the FF is also applied. Moreover, the whole point of including a variety of liquids, or crystals, is to make sure the FFs can reproduce the energy surface over a range of distances and orientations, as exhibited for example by H-bonded or hydrophobic interactions in a protein as well as interactions between more distant neighbors.

In conclusion, though the fit to the FF reveals large deviations, an impressive range and number of observables is exploited which can form the basis for needed refinement.

3.5 C36: further reparametrization of sidechain torsion potentials and the CMAP correction

Subsequent applications to proteins and model peptides revealed significant deficiencies in the CHARMM potential, even with the CMAP correction [62, 121]. To address this,

Best et al. [122] undertook a reparametrization of the backbone and sidechain torsion potentials in amino acids with the resulting FF termed C36. Backbone torsions were revised by optimizing the CMAP grid derived previously [38] to fit the NMR scalar coupling constants of Ala_5, and then further adjusted to fit chemical shift data of the helical oligopeptide Ac-$(AAQAA)_3$-NH_2. Not surprisingly given the relatively few observables in this data set and the large number of parameters involved in the 2D CMAP grid, agreement with experiment was good. It was also much improved over the previous C22/CMAP CHARMM potential and several AMBER potentials, though again this is to be expected as the latter were not parametrized specifically to fit this data.

Sidechain χ_1 and χ_2 optimization was carried out by first fitting to QM energies of configurations of dipeptides excluding Gly and Pro. These were generated by sampling χ_1 and χ_2 at 15° increments for the three backbone configurations, α_R, β and α_L. Deviations from the QM energies *less than 12 kcal/mol* ranged from RMSDs of 1 to 2 kcal/mol for the different conformers. These are somewhat misleading however, as deviations for particular classes of configurations were much higher. For example, RMSDs of the side chain conformer energies for the α_L backbone conformer of ~ 3–6 kcal/mol for Asn, Cys, Gln, Leu, Phe, Met, and Val were observed and the deviations for the charged residues were even larger. Although these were the most extreme errors, large deviations were also observed for configurations corresponding to the critical α, β backbone conformers as well, with many errors of 3–4 kcal/mol and more [122].

MD simulations of denatured ubiquitin and GB1 in 8M urea revealed discrepancies between the calculated and experimental χ_1/χ_2 distribution as determined by NMR. This may be reflecting, in part, the observed discrepancies in energy alluded to above. The parameters were than further adjusted to reconcile these deviations. Though the fit is better than those obtained with CHARMM22 and AMBER FFs, again this is to be expected as they were not fit to this data, and it is not clear how much this improved fit will manifest itself in applications to other systems.

A concern to fitting these data is that the FF used to represent urea will play a significant role in the resulting conformational properties of the peptide. It would be useful to assess the accuracy of this FF as well. There are both X-ray and neutron diffraction studies of the urea crystal at a variety of temperature yielding both the structures and thermal motions of the crystal [123]. Furthermore sublimation energy [124, 125] and vaporization energies of urea (http://webbook.nist.gov/cgi/cbook.cgi?ID=C57136&Mask=4#ref-8) are available. These make excellent observables to derive or optimize the FF used for urea. In addition urea is an intriguing system in and of itself as it is the only known crystal where the carbonyl oxygen accepts four H-bonds, two in the plane of the molecule and two perpendicular to the plane [123]. Thus it makes an excellent test case for H-bond potential functions [124].

A related concern as noted above, is the use of a particular water FF, in this case the TIP3P water, in the water-model compound dimers, for parametrization of the non-bond parameters (for example see Plana et al. [126]). This results in any errors in the water FF being absorbed by the parameters of the model compound, thus introducing errors in these parameters. These will manifest themselves for example, in residue–residue interactions in proteins etc. It also has the disadvantage of requiring a reparametrization of the entire FF for all functional groups if a more accurate FF for water is invoked.

Further assessments were made on a number of systems: First simulated coupling constants of short peptides ($Ala_{3,5,7}$, Gly_3, Val_3, and GPGG) were compared with experiment. Though the Ala results were in good agreement, χ^2 values < 1, the results for the remaining peptides were less good $\chi^2 > 2$. The FF was also tested by its ability to reproduce the structure of a dimeric coiled-coil (PDB 1U0I). A backbone RMSD of 2–2.5 Å and heavy atom RMSD of 3–3.5 Å represents an improvement over results obtained by previous FFs [122], though it is still large for a small protein (42 residues). In addition, when one helix of the simulated structure was aligned with the experimental structure, the RMSD of the second helix ranged from 3 to 5 Å yielding another measure of the discrepancy.

Simulations of eight protein crystals revealed a slight degradation in the fit to the sidechain torsion angles. Average deviations for all ϕ, ψ angles and those in α helices and β strands for the eight proteins were presented. Average deviations tend to obfuscate the magnitude of the deviations as positive and negative deviations cancel, but even with this, problems were revealed. Thus, even when taking the average, several of the eight proteins displayed deviations in ϕ, ψ of 6–11°. Though standard deviations are given, a better measure might be the averaged unsigned deviation. Comparison of sidechain J-coupling constants for folded and unfolded proteins with experiment revealed similar concerns. Thus χ^2 values of the amino acids of 2.2–18 were observed which, though an improvement over C22, indicate large remaining deviations in the protein structure. It is not clear why deviations in sidechain configurations of folded proteins were not compared directly to the X-ray results, as was done for the backbone angles. Calculated NMR data is model dependent and less precise than the corresponding crystal structure and therefore less informative as to the underlying interactions which may be inadequately represented by the FF. To this point the common use of averages and RMSDs in the community, *to the exclusion of analyzing individual large deviations*, is lost information and a lost opportunity for the improvement of FFs. Though many properties may be fit well, it is

the large discrepancies which reveal inadequacies in the force constants or functional form, and form the basis for correction, and improvement of *both* the parameters and functional form [7, 23, 26, 108].

Overall results with the CHARMM36 FF showed improvement over the previous CHARMM22/CMAP version, especially with regard to the problem of over prediction of helix. Interestingly similar improvement in the prediction of helix propensity was achieved by Piana et al. [76] who removed the CMAP correction for all residues except Gly and Pro, replacing it with optimized torsion parameters (partial charges on Asp Glu and Arg and sidechain torsions on Asp were also refined). The FF was labelled C22*.

Nevertheless, large deviations in energetic and structural properties remained in C36. This is a fundamental problem and intrinsic to the simple quadratic, diagonal functional form employed to represent the energetics of these systems. This functional form is simply incapable of accurately representing the structural and thermodynamic properties of biomolecular systems as has been noted in various studies and alluded to above. The authors also comment on this in discussing deviations in side chain angles:

> … This is due to poor reproduction of the local minima required to better reproduce the high-energy regions, a compromise that is due to inherent limitations in the form of the potential energy function that limits the ability to match the entire energy surfaces.

Unfortunately, it is virtually impossible to predict in what applications these large deviations will manifest themselves, and thus the repeated occurrence of ill- behaved systems, such as over-prediction of helices, and the repeated reparametrization of FFs. Given this experience, and the size of the documented deviations, it is only to be expected that history will repeat itself. The only true solution is to improve the representation of the physics as discussed in the section "Expanding the physics represented in force fields: charge, nonbond and polarizability fluxes and anisotropic nonbond interactions" below.

3.6 C36m: demonstration of the need to improve the representation of the physics (atomic multipole, polarizability, charge, nonbond, and polarization fluxes, etc.) in protein and peptide FFs

As noted above, the expectation that the documented deficiencies in C36, would manifest themselves in some unpredicted erroneous behavior, analogous to the experience with the series of error correction functions in CHARMM and AMBER discussed above, was realized recently. A study of intrinsically disordered proteins (IDPs) with a variety of force fields revealed that revising the nonbond parameters of the CH_2 group to correct bias to right handed helix in the C22/CMAP potential resulted in the C36 FF having a bias to left-handed helices [127]. Applying a variety of FFs, Rauscher et al. [127] carried out an extensive analysis of five model disordered peptides ranging in length from 15 to 50 residues, employing radius of gyration and similar NMR observables to those used by Best et al. [122] and others [76, 128]. They noted that the reason for the bias for α_L propensity in C36 was twofold: first different oligopeptides were studied in the C36 optimization; and second though 30% of the HEWL C36 ensemble contained left-handed α-helix [127], 200 ns of MD were required before the α_L forms, longer than the trajectory carried out by Best et al. [122]. This problem was emphasized by Debiec et al. who found that even 4 μs was not sufficient to achieve convergence of several oligopeptides [58], raising an obvious concern in drawing conclusions from much shorter simulations.

To correct the propensity for left handed helices Huang et al. [65] re-optimized the CH_2 nonbond CMAP potential to reduce the predicted α_L probability of the FG-nucleoporin (FG) peptide to 1.1%, using the reweighting scheme of Li and Brüschweiler [129]. In addition, as noted by Piana et al. [76] modifications in the carboxylate and guanidinium potentials were required to decrease the strength of salt bridges. Unlike Piana et al. who modified the charges, specific pair parameters were introduced for the guanidinium nitrogen and carboxylate oxygens in this study. Though both modifications achieve the desired reduction in the strength of the salt bridge, it is a bit concerning as the consequences of these changes will be very different in the context of other interactions involving these residues. It would seem that extensive additional testing, for example by simulating peptide crystals containing these groups, would be extremely desirable to distinguish between these corrections. Use of more accurate combination rules [130–132] might also obviate the need for specific pairwise potentials.

The modified FF labelled C36m, was tested against an impressive validation set comprised of 15 peptides and 20 proteins. The properties of IDPs were provided by small angle X-ray scattering (SAXS) and NMR as customary in recent studies of these systems [76, 122, 128]. NMR observables included J coupling constants, chemical shifts, residual dipolar couplings, and order parameters. Protein simulations assessed stability of structure along 1 μs trajectories, the free energy of folding of the villin headpiece and folding of two designed peptides.

The study provides a valuable set of tests to characterize the FF, and document deficiencies in the fixed charge, 12-6-1, diagonal quadratic form, which may inform the development of more accurate forms. That the correction of the erroneous bias for α_L was achieved, was shown by the results of simulations of four IDPs, where the artifactual average α_L population of ~20% obtained with C36 was reduced to ~5%,

close to the experimentally observed value. Probative information is provided by a number of results. Simulation of the four β-hairpins with C36m resulted in folded state populations of chignolin and CLN025 of ~3 and 40% respectively, far below the experimental populations of ~60 and 90%. The rate of loop closure in the four peptides $C(AGQ)_nW$, n = 1–4, as measured by the rate of tryptophan quenching by the N-terminal cysteine, though reasonable for the smaller two peptides was far too high for the larger chains. This is interpreted as the ensembles being too collapsed. Thus, again, remaining deficiencies indicate flaws in the FF, which might inform approaches to refine the representation of the physics and parameters.

3.6.1 The need for μs and longer simulations in testing FFs based on protein stability

Crystal simulations also revealed deficiencies in the empirical energy surface. The RMSDs of the C_α atoms of the C-terminal domain of TFIIF and bovine ICaBP, reached 4–5 Å as seen in Fig. 2. In addition, the RMSD of deoxy-myoglobin oscillated about 3 Å, and those of lysozyme and dethiobiotin synthetase drifted toward 2.5–3 Å toward the end of the trajectory and may not have converged (Fig. 2). These deviations, larger than those seen in the past may well be due to the long 1 μs trajectories, and demonstrate the need for even longer trajectories (or enhanced sampling techniques), if the "stability" of crystal structures is to be used in assessing FFs. This is also consistent with the simulations carried out by Debiec et al. [58] where results suggest that even 10 μs is not sufficient to ensure convergence of protein structure as seen in Fig. 1. It is likely that the constraints imposed by tertiary structure and perhaps crystal packing, will slow down the drift of proteins from their initial starting structure, and tens to hundreds of μs may be necessary to obtain the true measure of deviations in these systems. Even so, the deviations observed here give grave cause for concern, and imply the need for including better descriptions of the physics in the FF. We note that these are RMSD of the Cα atoms, backbone RMSDs are likely to be larger and RMSDs of all heavy atoms larger yet. An RMSD of ~3 to 4 indicates that individual deviations of 6–7 Å will not be unusual and at this point it is questionable that one can describe the structures as similar.

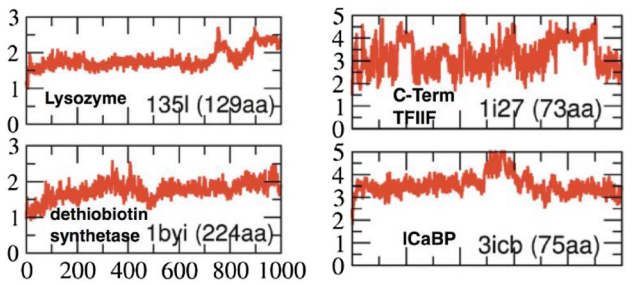

Fig. 2 Trajectories of lysozyme (135I), and dethiobiotin synthetase (1byi) indicating continuing divergence at 1 μs, while the trajectories of the C-terminal domain of human transcription factor IIF (1i27) and bovine intestinal calcium-binding protein (3icb) reveal discrepancies of 3–5 Å demonstrating the FF is incapable of accounting for protein structure. Reproduced with permission from Huang et al. supplementary material [65]

Another important observable calculated in this study is the free energy of folding of the Villin headpiece subdomain HP36 [65]. Although, as noted above, and seen from the discussion, a large number of discriminatory observables have been evaluated in this study, one class missing is a set of thermodynamic data, especially energy or enthalpy. These are key properties in validating or discrediting FF functions. The calculated free energy of the villin headpiece of ~4.1 kcal/mol, is an improvement on the value of −4.9 kcal/mol, obtained with C36, but still indicates the folded state to be ~75% more stable than the experimentally observed stability of −2.4 kcal/mol.

3.7 Thermodynamic data is essential in assessing the validity of FFs

In regard to the critical importance of energetic observables, it is instructive to consider similar thermodynamic comparisons carried out recently with a variety of FFs. Examples include Piana et al. [76] on the folding free energy of a fast folding variant of the villin headpiece [76], simulations of the thermodynamics of helix coil equilibrium [133] and host guest ligand binding [134]. These studies yield important information on the assessment of validity, or inadequacy of FFs. Such studies are essential for the faithful evaluation of the accuracy of FFs. This is demonstrated by the results of these studies presented in Table 1.

As can be seen by these results there is still a long way to go in achieving FFs that can account for the energy surface of peptide systems with even moderate accuracy. The importance of these studies is demonstrated emphatically by the calculated thermodynamics of the fast folding variant of the villin headpiece by Piana et al. [76] presented in the first section of Table 1. Thus, for example, Lindorff-Larsen [128] compared eight FFs based on their ability to account for the NMR properties of ubiquitin and GB3, secondary structure propensities of two oligopeptides, and the ability to reach "a folded state" for the villin headpiece in 10 μs and the WW domain in 50 μs. Two of the eight FFs had a "perfect score", ff99SB*-ILDN [133], and CHARMM22* [76] (C22*), both parametrized against NMR data and secondary structure propensity of oligopeptides. It was concluded from these comparisons that FFs are improving with time. However as noted, the

Table 1 Evaluating force fields: accuracy of simulations of thermodynamics of folding, helix coil transitions and ligand binding

System	Force field	T°K	ΔH kcal/mol	−TΔS kcal/mol	ΔG kcal/mol
HP35	ff03[b]	390	9.70		0.21
Folding[a]	ff99SB*-ILDN[c]	380	19.70		0.70
	CHARMM27[d]	430	19.30		0.51
	CHARMM22*[a]	360	17.00		1.00
	Experiment[e]	370	*25.00*[n]		*0.80*
–(AAQAA)$_n$[f]					
Helix initiation	ff03[b]	300	0.44	0.11	
	ff99sb[g]	300	0.90	0.32	
	ff03*[f]	300	0.72	0.28	
	ff99sb*[f]	300	0.71	0.26	
	Experiment[h]	300		*1.98*	
Helix extension	ff03[b]	300	−0.99	0.41	−5.30
	ff99sb[g]	300	0.23	0.09	−5.70
	ff03*[f]	300	−0.61	0.54	−3.60
	ff99sb*[f]	300	−0.47	0.47	−3.30
	Experiment[h]	300	*−1.28*	*1.13*	
Host–guest binding[i]					
OAH-G4	GAFF[j]/TIP3P[k]	298	−15.46	3.12	−12.34
	GAFF[j]/OPC[l]	298	−9.22	−2.13	−11.35
	Experiment[m]	298	*−14.80*	*5.43*	*−9.37*
OAH-G5	GAFF[j]/TIP3P[k]	298	−5.57	1.11	−4.46
	GAFF[j]/OPC[l]	298	−5.60	−0.82	−6.42
	Experiment[m]	298	*−9.90*	*5.40*	*−4.50*
OAMe–G3	GAFF[j]/TIP3P[k]	298	−9.46	2.12	−7.34
	GAFF[j]/OPC[l]	298	−6.94	−1.88	−8.82
	Experiment[m]	298	*−6.62*	*0.68*	*−5.94*

[a]Piana [76], [b]Duan [102], [c]Best [133], Piana [76], Lindorff-Larsen [135], [d]MacKerell [38], [e]Kubelka [136], [f]Best [133], [g]Hornak [57], [h]Rohl [137], [i]Yin [134] hosts octa acid (OAH) and tetra-endo-methyl octa-acid (OAMe), G3,G4,G5 are ligands, [j]Wang [35], [k]Jorgensen [69], [l]Izadi [138], [m]Sullivan [139], [n]Experimental values italicized

observables used to score the performance are similar to the observables used to parametrize the FF, while, for example in the case of C22* versus C22 [22], where there is the largest difference in score, the observables fit in the original C22 derivation have not been recalculated with the modified FF. Thus, if scored on those observables, an entirely different conclusion might be drawn.

Furthermore, as seen from the comparison in Table 1, the fit to the thermodynamics has deteriorated on going from the CHARMM27 [38] FF (C27, derived in 2004) to the revised C22* FF (2011), though both yield unacceptably large deviations, 5.7 kcal/mol (23%) and 8 kcal/mol (32%) in the enthalpy respectively. There is no clear criteria for accuracy required for general applicability of FF methods to molecular systems, though Stouch has suggested that accuracy to ~0.5 kcal/mol is an appropriate target [140]. The errors in these studies are an order of magnitude larger. Whatever the target might be it is clear that errors of 5–8 kcal/mol point to unacceptable inaccuracies in the FF.

A further important lesson from these data is that free energies, are consistently fit better than the component enthalpic and entropic contributions. This results from correlation of the errors in ΔH and TΔS resulting in cancellation of errors and misleading agreement with experimental ΔGs [141]. As such free energies are not the most trustworthy probes into the accuracy of FFs.

Best and Hummer [133] pointed out the same phenomenon in their optimization of backbone torsion parameters to fit helix-coil equilibria, as seen in the second and third sections of Table 1. They note:

> The thermodynamic fits of the helix-coil parameters indicate that while the torsional correction to ψ can approximately reproduce free energies at a given temperature, the enthalpic and entropic contributions to the helix-coil equilibrium are too small, each about half the experimental estimate.

They also suggest that this behavior reveals inherent deficiencies in the analytical form of the simple 12-6-1 fixed

charge FFs. Thus, they point out that the calculated hydrogen bond geometry distribution is not as narrow as seen in experiment or in QM, leading to a smaller entropy loss on H-bonding. They suggest that this may be due to a deficiency in the electrostatic representation, and indeed as we have seen quadrupole moments play a major role in determining H-bond angular dependence [142, 143]. In addition they note that a large component of the energy of hydrogen bonding has been found to result from electron redistribution on helix formation [144]. Accounting for this requires the inclusion of polarizability and/or charge flux neither of which is included in the 12-6-1 standard functional form. The inadequacy of the fixed charge model and need for including the physics of charge and polarizability flux in the FF is also supported by the results on hydrogen bonded systems by Dinur and Hagler [106], and Wallqvist [145].

Finally, we consider the thermodynamics of a third process crucial to the mission of biomolecular simulations, ligand binding. In the fourth section of Table 1 a selection of results [134] are presented that were obtained in conjunction with the SAMPL5 host–guest blinded prediction challenge for predicting binding affinities [146]. The thermodynamics of these systems reiterate the conclusions seen in the previous two systems showing that they are general, as one would expect them to be if the underlying cause is inadequacy of the FF in its ability to represent the underlying physics. Thus, once again we see that even when the ΔG of binding is reproduced as e.g. in the OAH-G5 complex calculated with the GAFF/TIP3P FF (-4.46 kcal/mol calculated vs. -4.5 kcal/mol exptl.), unacceptably large errors in ΔH (of 4.3 kcal/mol, 43%) and a corresponding error in $T\Delta S$ (4.3 kcal/mol or 79%) are concealed. Clearly if the enthalpic and entropic contributions had not been calculated, one would be misled in assessing the validity of the FF based on this result. Other results further reinforce the conclusions drawn from OAH-G5, as well as the helix-coil end protein folding systems. Thus, large deviations of 30–50% (~3–6 kcal/mol) are obtained for the components of the thermodynamics for these host–guest systems using GAFF with both water models, TIP3P [69] and OPC [138].

Another disturbing aspect of the results is the performance when the OPC water potential is invoked. The results with the latter are systematically worse than those obtained by the GAFF/TIP3P combination. Most dramatically the entropies of binding of the ligands are calculated to be of the wrong sign for all three host guest complexes given in Table 1 [134]. Given that OPC accounts for the properties of liquid water significantly better than TIP3P [138], one might expect it to yield better results for the properties of these aqueous complexes. There are many reasons this is not the case, including for example the use of flawed combining rules [130–132], among others. However, the simplest explanation is that the GAFF and TIP3P FFs have compensating deficiencies in the representation of the physics, and the combination conceals these deficiencies.

In agreement with the assessments of the studies cited and quoted above, in summarizing the results obtained in the SAMPL5 challenge Yin et al. conclude [146];

> Given that adequate conformational sampling can be achieved for such moderate- sized systems, and that the ionization states of these systems are relatively straightforward to ascertain at the experimental pH, the errors in predictions from carefully executed calculations presumably trace to limitations in the potential functions, or force fields, used in the simulations. It should be emphasized that, if current force fields yield errors of this magnitude on host–guest systems, one should not expect to achieve any better in blinded predictions of protein-small molecule binding free energies… The present results thus underscore the need for improvements in force field parameters and perhaps functional forms.

3.7.1 Summary: physics in current 12-6-1 fixed charge FFs is incapable of reliably accounting for peptide and protein properties

Consequently, based on these observations and the results emanating from the many validation studies covered here, the overwhelming preponderance of the evidence leads inalterably to the conclusion that the physics omitted by current FFs makes major, essential, contributions to the properties of these biomolecular systems. Force Fields with new enhanced analytical forms representing this physics, including for example some or all of: atomic multipoles; charge flux; polarizability; nonbond and polarizability flux; charge penetration; valence coupling; functionality of combining rules and out-of-plane distortions etc. must be investigated. Given the number of these factors and their documented significance discussed elsewhere in this perspective, it would be more surprising if the simple 12-6-1 quadratic function could account for the energy surfaces of organic systems than the fact that it doesn't.

3.8 Drude polarizable FF

MacKerell et al. initiated a concerted effort to implement polarizability, beginning in 2003 with the development of a polarizable water FF [147]. Rather than the induced dipole model favored by the AMBER [101] and AMOEBA [148] groups they exploited the classical Drude oscillator to simulate polarizability [49, 51, 53, 54]. The Drude oscillator consists of a virtual site carrying a negative charge, attached by a spring to the nucleus. The virtual charge is displaced by an electric field, the displacement being determined by the charge and spring constant, resulting in an induced dipole.

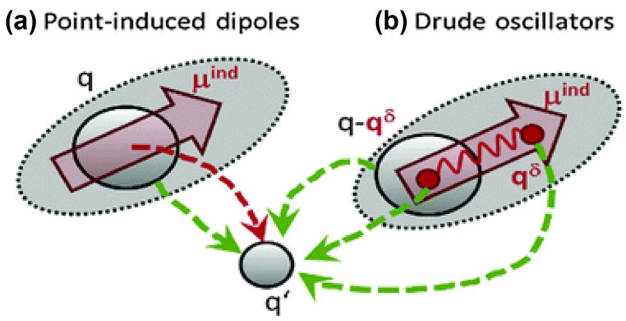

Fig. 3 Schematic of Induced dipole and Drude oscillator polarization models. Reproduced with permission Graphical abstract. Schmollngruber et al. [149]

This is depicted nicely in the schematic by Schmollngruber et al. [149] (Fig. 3).

A classical strategy was taken in the development of the CHARMM polarizable FF by these workers in that FFs for individual families of compounds containing functional groups found in biomolecules were developed, with the goal of transferring the parameters to proteins, nucleic acids etc [150]. As mentioned, the first step in this effort was the development of the "SWM4-DP" polarizable water model in 2003 [147]. This was followed by a reparametrization of the model in 2006, motivated primarily by the desire to replace the counterintuitive positive Drude particle invoked in SWM4-DP with a more physically reasonable negative charge. The resulting FF was labelled SWM4-NDP (simple water model with negative Drude polarization).

The SWM4-NDP water model is a four point rigid geometry model similar to the original Bernal-Fowler [151] model, also used for TIP4P [152] (Fig. 9a, previous paper [1]). In addition to the 3 atomic sites and the virtual charge site (m), the model also includes a negatively charged Drude particle attached to the oxygen by a harmonic spring with a force constant of 1000 kcal/mol/Å^2. The FF is defined by four parameters, ε_O, σ_O, r_{Om} and q_d, the van der Waals well depth, diameter of the oxygen, the distance between the oxygen nucleus and the virtual negative charge and the charge on the Drude particle respectively. These four parameters are determined by fitting to four properties of the neat liquid at room temperature and pressure, vaporization enthalpy, density, static dielectric constant and self-diffusion constant. The charge on the negative virtual site q_m, (and the partial charges on the protons which are $-1/2q_m$), are determined by the gas phase dipole moment. Since there are four parameters and four observables the parameters are solved for by a 4-dimensional grid search [153]. As might be expected, the training set observables are fit well. To test the model, several additional properties are considered. The radial distribution functions are reasonably well accounted for, though the second O···O peak, representing the degree of tetrahedral structure, is slightly smaller than observed, and the first neighbor O···H peak is significantly higher and shifted. Shear viscosity is somewhat smaller than experimental (0.7 vs. 0.89 cP) and the Debye relaxation time significantly larger (11.2 vs. 8.3 ps). Additionally, rotational relaxation times, surface tension and hydration free energy are compared to experiment with similar outcomes.

Overall a reasonable fit to experiment is achieved, though significant discrepancies remain. As pointed out by Wang et al. [147] none of the models tested can "simultaneously yield reliable diffusion coefficient, rotational relaxations, and dielectric constant", though it is a nice demonstration of the need for polarization to get proper dielectric behavior. This is shown even more dramatically with hydrocarbons, discussed below. Interestingly one of the models they tested was an induced dipole version of the SWM4-NDP model, which in some cases yielded better agreement than the Drude version. It would also be worthwhile to increase the relatively limited number of observables in the training and validation sets according to Lifson's paradigm [7, 8], as for example in the extensive series of studies carried out by Clementi and Corongiu [154] and references therein (and reviewed in the previous paper [1]).

3.8.1 A major concern—omission of flexible geometry and charge flux

Of more concern, in common with many common water potentials, are the use of rigid geometry and the omission of charge flux (i.e., geometry dependent charges). These factors, discussed in more detail below, have been reported to play a major role in the structural, energetic and dynamical properties of water [145, 155]. Thus, Wallqvist [145], in a rigorous MD simulation and analysis showed that when charge flux is accounted for, the increase in nuclear dipole moment induced by polarization, on going from gas to liquid, is only one-third of what is predicted using geometry independent charges. Thus, the flux opposes polarization. This implies that the polarizabilities derived by fitting liquid properties are "effective" parameters, much like the "effective charges" used in non-polarizable FFs which are meant to compensate for lack of polarizability.

The worry is, that as with effective charges, the dependence of the factors that are being compensated for differ drastically, with respect to configuration, distance and environment, just as effective charges are independent of environment; polarizability depends on intermolecular distance while charge flux is molecular geometry dependent—very different coordinate dependencies. Thus, just as effective charges can account for polarizability only over a limited domain, it is essentially inevitable that the "effective polarizabilies" will fail to account for the significant effect of charge flux in domains where the functionality fails. It may

be that the discrepancies already identified in these studies [64, 153] reflect the omission of these contributions.

Wallqvist also emphasizes that the effects of both nonbond and polarizability fluxes are non-negligible, and concludes:

> The coupling between intra- and intermolecular degrees of freedom has a large effect on liquid water properties such as structure and energetics. Even the small differences in intramolecular properties, introduced upon incorporating flexibility of bonds and angles, between the constant charge harmonic and anharmonic system have significant effects on the energetics

As noted below, it is likely that these effects are not restricted to water, and may well underlie the significant deficiencies remaining in polarizable FFs. For example there is clearly a significant coupling between inter and intramolecular energetics in amides, and by extension proteins, as reported on by the dramatic decrease in the amide C′–N bond length of ~0.07 Å, with a concomitant large increase of ~0.04 Å in the carbonyl bond, on going from gas phase to the crystal [156]. Similar behavior is seen in carboxylic acids [156].

3.8.2 Hydrocarbons

The hydrocarbons were the first family to be addressed in the derivation of the Drude polarizable FF [157]. Parametrization was carried out by fitting to the properties of five small alkanes–ethane, propane, butane, isobutane and pentane. The first step in the parametrization involved determination of the partial atomic charges and polarizabilities (charge on the Drude particle). These are obtained by fitting to the electrostatic potential of the model compounds, both in vacuo, and to parametrize the polarizability, as perturbed by a small external field.

3.8.3 Observation of consequences of omission of charge flux

A "problem" that arose early on was the observation that the partial atomic charges were dependent on conformation. For example, the charges on carbon in the *gg* and *gt* conformers of pentane are found to be 0.22 and 0.29e, and an even larger difference of 0.0.14e arose when CH_n group neutrality was imposed (i.e., $q_C = -nq_H$) where q_C was found to be −0.25 and −0.11 in the *gg* and *tt* structures respectively. This is another manifestation of charge flux, and is by no means inconsequential. For example, C–H···O interactions, characterized by C···O distances of 3.2 Å, and less, are found in crystals of small molecules as well as proteins [158, 159]. A difference of charge of .1e on a carbon interacting with an oxygen carrying a partial charge of ~0.5e at a distance of 3.2 Å correspond to an energy difference of 5 kcal. If the charge on the oxygen is centered on lone pairs [160], the distance could be shorter and the concomitant energy larger. Of course, this is mitigated by interactions with bonded atoms, but nevertheless this is a significant energy difference, and as noted, the effect is omitted in essentially all existing biomolecular FFs.

Validation of the atomic charges and polarizabilities was carried out by fitting experimental and QM molecular dipole moments and polarizabilities. The dipole moments of hydrocarbons are very small (~0.1D), but polarizabilities were accounted for reasonable well (within ~6%).

3.8.4 Internal parameters

The force constants for bond stretching and angle bending were obtained by fitting *QM* vibrational frequencies of ethane, propane, butane and isobutane, calculated at the MP2/6-31G(d) level, and structural data from both QM and crystal structures. The bond lengths and angles were in excellent agreement with experiment. The vibrational frequencies revealed significant discrepancies, in some cases approaching 100 cm^{-1}. Though these deviations are typical of diagonal quadratic FFs, they don't approach the accuracy of FFs which account for anharmonicity, and coupling between internal deformations (aka cross terms), such as MM4 [108], CFF93 [161] or SDFF [46]. The latter achieved essentially quantitative agreement with experimental frequencies (RMS ~ 10 cm^{-1}) [46]. It should also be noted that many more compounds, including congested and cyclic compounds were treated in the derivation and testing of these FFs.

Torsion force constants were parametrized against QM derived rotational barriers, and relative conformational energies of butane, pentane, hexane and heptane. Good agreement was achieved with deviations of a couple of tenths of a kcal in rotational barriers of 3–5 kcal/mol—the only exception being the C (T/G) barrier in butane which deviated by 0.84 kcal/mol. Fits to the conformational energy minima were even better. There is little difference in the accuracy achieved in accounting for these observables between the fixed charge and polarizable FFs.

A unique approach was taken in the optimization of nonbond parameters. In the first step, relative values of the LJ parameters are adjusted by fitting interactions between model compounds and He and Ne. The use of the rare gases allows calculations to be carried out with high levels of theory with the correlation required to treat dispersion interactions, in this case MP3/6-311++G(3d,3p). These relative

values were than refined by fitting the heats of vaporization and molar volumes of ethane, propane, butane, isobutane, heptane, and decane. Good agreement was found for all neat liquid properties with the Drude FF and it was noted that the quality of fit extended to the longer chains, though these were not included in the parametrization, and not fit well by the C27r CHARMM fixed charge FF [162].

It seems puzzling and unlikely that polarizability would have a significant effect and be responsible for correcting deficiencies in vaporization energy of alkanes: Certainly, not the 20–25% difference noted between the two FFs. As noted above the dipole moment of these nonpolar compounds is essentially zero and thus polarization energy is almost certainly inconsequential (this could be easily determined by examining the contribution to the total energy of the polarization contribution to ΔH_{vap}). On the other hand, differences in torsion energy, which are significantly different in the two FFs, will have a significant effect on the conformational equilibria, especially in the longer chains, affecting packing and having a major consequence on the heat of vaporization. Also, the relative vdW parameters may differ as they were determined with different basis sets. In any case, if the polarizability contribution is negligible the functional form of the two FFs is identical. Thus, it follows that C27r could account for ΔH_{vap} as well as the Drude FF. The difference most likely reflects incomplete optimization of the C27r FF, perhaps caused by a limited training set. This is in fact indicated by the authors who suggest limitations with the parameters in the C27r FF [157]. As pointed out above in regard to the induced-dipole AMBER FF [64, 99–101], in order to rigorously determine the effect of including polarizability in the FF, the additive and polarizable FFs need to be derived by fitting the identical training set, and assessed with the same validation set.

The Drude FF was tested by considering a variety of physical and dynamic properties, including isothermal compressibilities and self-diffusion constants of heptane and decane. Diffusion constants were slightly underestimated and the isothermal compressibility of heptane was ~25% too large. It was speculated that these discrepancies might be due to a limitation inherent in the use of spherical atoms in the FF (See below for discussion of anisotropic nonbond potentials).

The dielectric constant of five normal alkanes and isobutane, at several temperatures were also calculated and found to be in excellent agreement with experiment. Not surprisingly this is one property which is critically dependent on polarizability, as the response of the molecular electron distribution to an external field is the overwhelming dominant determining factor in nonpolar molecules (as opposed to reorientation of dipoles in highly polar systems). The dielectric of "fixed charge" alkane FFs is essentially 1, while the observed dielectric is ~2.

Finally, the Drude FF was tested by comparing experimental and calculated hydration free energies of ethane, propane, butane, and isobutane. The results were disappointing, and even trends were not reproduced. For example, while the experimental ΔG_{hyd} for ethane is less than that for butane, 1.77 versus 2.15 kcal/mol respectively, the calculated values reverse the trend (1.84 vs. 1.46 kcal/mol). Though this might indicate deficiencies in the FF, the authors point out that the convergence of the simulations is questionable. The free energies were calculated by FEP with samples collected from 10 40 ns windows of two trajectories (forward and reverse). For comparison, a later study of solvation free energy employed 12,600 ns windows, or an order of magnitude longer trajectory to achieve convergence [163]. Thus, it is likely that convergence may well have been an issue. Of interest is that the electrostatic contribution to the free energy is small, of the order of 10–15% of the nonbond contribution, again as one might expect for a nonpolar compound (it is not clear whether there is a difference in the valence energy due to conformational differences in the two phases).

In summary, it would appear that the effect of polarizability to properties of normal hydrocarbons is small to negligible, with the important exception of the dielectric constant. Here it plays the dominant role and is crucial.

3.8.5 Benzene

Having parametrized polarizable FFs for water and alkanes MacKerell, Lopes et al. went on to systematically parametrize the remaining functional groups found in biomolecules. Benzene was the next compound to be addressed with the Drude model [164]. Essentially the same protocol as used for the hydrocarbons was executed for benzene. In general excellent agreement with experiment was achieved with both additive, in this case the C22 FF [22], and polarizable FFs for properties such as diffusion constants, heat capacities at constant pressure, and isothermal compressibilities. The exception is the dielectric constant, where again dramatic differences arise between the two models. Again, the fixed charge model yields a dielectric close to one, while the polarizable FF, able to respond to an external field, yields a dielectric of 2.2, in close agreement to the observed value. A disappointing aspect of the parametrization, as the goal of including polarization is to be able to account for properties across environments, was the consequence of the need to scale the partial charges derived from the RESP fits (in vacuo) by a factor of 0.7. As pointed out by the authors, this led *to … some decreases in the ability of the model to reproduce gas-phase target data associated with the benzene dimer and benzene-rare gas interactions; however, the model with the scaled charges led to good agreement with a variety of condensed-phase data* [164].

Though condensed phase behavior was examined through simulation of liquid properties, it would be nice to see how the polarizable FF performs in reproducing the crystal structures and sublimation energies of benzene both at atmospheric and high pressure. This is a classic, and powerful system for testing aromatic FFs [85, 165–168]. It is high resolution data, as opposed to liquid data, and computationally less demanding than simulating liquids. *Crystal systems such as this are far more robust than the corresponding liquid simulations. They contain detailed structural information which itself is extremely valuable, and, in addition, ensures that calculated thermodynamics such as sublimation energy correspond to the correct lattice structure*. In contrast, liquid heats of vaporization, though fitting experimental data, may correspond to an erroneous configuration of molecules in the liquid phase (making the comparison moot). Given that crystal observables are high resolution, more information rich than liquid observables, and are less computationally demanding, it is perplexing to say the least, why they have been de-emphasized to the point of almost being discarded in the derivation of most biomolecular FFs.

Interestingly, the Drude FF for benzene later required extension, by the inclusion of a virtual vdW site at the center of the benzene ring, in order to account for interactions with cations [169]. This immediately raises the question as to whether the new model can still account for the properties used to develop the original Drude FF. This is critical as clearly one can't have two different benzene FFs depending on what the interaction is. Though the lack of testing against the original observables used in deriving a FF is unfortunately a common practice today, it is clearly less than optimal. It often leads to rapid discovery of inadequacies in subsequent applications requiring yet another reparametrization study, and so on. This might be compared to the more rigorous approach of the original developers such as Allinger's derivations of MM2 [21], MM3 [26] and MM4 [170] where backward compatibility is ensured. It would be interesting, to assess whether testing of the original potential against the energetics and structures of the crystalline forms of benzene (as well as other aromatics) would have suggested the need for such a modification, and whether the modified potential can account for the properties of these crystals.

3.8.6 Extension of Drude FF to additional functional groups and proteins

Following the derivation of the water, alkane, and benzene Drude FFs, work was continued to cover the full span of functional groups in proteins. The next families addressed were the ethers [171, 172], alcohols [173] and amides [160, 174]. In general, the same protocol was used for parameter development in these families, i.e. charges and Drude particle parameters derived from ESPs with and without an applied external field, valence parameters from vibrational frequencies of model compounds, torsional parameters derived from QM dihedral scans, and nonbond parameters determined by scaling relative values derived from QM to experimental liquid densities and ΔH_{vap}. These were followed by application to the remaining functional groups characterizing proteins and other biomolecules [150]. The results in these studies were similar to those for water, benzene and the alkanes reviewed above.

The amide Drude FF, as an example, was derived by fitting the properties of *N*-methyl acetamide (NMA), "the small molecule analog of the peptide linkage" [160]. *Since the derivation was based on a single molecule, there are more nonbond parameters than observables*. Thus, the solution was based on a grid search of the nonbond parameters, reduced by requiring that QM water–NMA dimer energies are acceptable, and then chosen by reproducing density and vaporization energy. The FF was assessed by comparing calculated ΔH_{vap}, density and dielectric constant of the neat liquid, ΔG_{hyd}, diffusion constant and Debye relaxation time, with the corresponding experimental data. In addition, the densities, vaporization energy and dielectric constants of acetamide and *N,N*-dimethyl acetamide, were evaluated. (The nonbond parameters of the amide nitrogens were not transferred to the latter compounds, but rather parametrized individually.)

The density, and heat of vaporization of NMA were almost perfectly fit, though agreement might be expected as there were more than enough nonbond parameters to achieve fit to these properties. In addition, ΔG_{hyd} was also well accounted for, though again, the selection of the polarizable model was based in part on its fit to QM NMA–Water dimer energies. Though this certainly is not as strong a determining factor as direct fitting of hydration energy, it does restrain the parameters to at least account for the individual water–NMA interaction. In addition, the experimental dielectric, diffusion constant and Debye relaxation time were all well accounted for by the FF. The results were compared with a fixed charge CHARMM FF and again a dramatic difference was found in the dielectric constant with the fixed charge model severely underestimating experiment. Clearly polarizability is crucial to reproduce this property. Another advantage of the Drude FF is the ability to account for the 50% increase in the dipole moment on going from gas to liquid [160]. It was also shown that it reproduces the cooperativity in the interaction energies in a chain of NMA molecules, an effect only achievable with polarizability.

Overall all six properties were reproduced better, to a greater or lesser extent, than with the CHARMM FF. However, this is again to expected, as the parameters were fit explicitly to these properties, and does not address the relative abilities of polarizable vs, fixed charge FFs The FF

derived here is an NMA FF, rather than being a transferable FF for the amide family. It contains more parameters than observables, which are free to be selected to provide an optimal fit to the former. This is further driven home by the fact that different nonbond parameters are used for acetamide and *N,N*-dimethyl acetamide. On the other hand, the CHARMM FF was derived by a fit to a whole set of different observables and validated by fitting a wide range of experimental quantities. To assess the relative performance of the two FFs the polarizable FF would have to be applied to the total body of data addressed by the CHARMM FF.

3.8.7 Danger of deriving a FF from one or two compounds

In addition to the inherent problems in the comparison of the NMA FF with the fixed charge FF, *it is not feasible to derive a transferable FF from the properties of one or two compounds*. A reasonable large set of analogs (10–15) and a diverse set of properties are required for rigorous validation [7, 8, 27]. To derive and assess the validity of an amide polarizable FF, an assessment against a large body of independent data for a reasonable set of compounds is necessary: For example an evaluation of ability to account for $\Delta H_{vap,}$, densities, and diffusion constants for a variety of amide liquids [106, 175, 176], crystal structures and sublimation energies of 10–15 amides and peptides [22, 24, 80, 91], relative conformational energies of tetra-alanine [177, 178], helix-coil equilibria, thermodynamics, and NMR parameters of Ala oligopeptides [58, 62, 65, 133] etc. Using smaller data sets will inevitably lead to discrepancies in applications to other systems.

3.8.8 A reparametrization of the amide FF

The insufficiency of parametrizing a FF for a functional group on the basis of a single molecule (or even a few molecules), was realized when the amide FF was applied to a Kirkwood–Buff analysis of a variety of solution properties of NMA and acetamide [174]. A new FF was derived to analyze these two compounds, but again with the limited data set its range of applicability was severely limited.

3.9 Drude-2013 protein force field

3.9.1 A third reparametrization of the amide FF

The Drude oscillator FFs resulting from this decade long initiative of small model compound parametrization were then incorporated into a Protein FF in 2013 [179]. Again, transferability became an immediate issue as J-coupling constants of penta-alanine, calculated with the Drude FF derived from NMA and acetamide, deviated significantly from observed values. Thus again, the parameters resulting from the two studies of NMA were not transferable [160, 174], in this case to the moiety in proteins [179]. To overcome this problem yet another reparametrization of this functional group, was carried out, using QM calculations of N-Ac, N′-Me-Ala, acetyl-$(Ala)_5$-amide (Ala_5), Ala_5–H_2O complexes, and several solution properties. A grid based approach, as used in the original NMA parametrization was invoked [160], to iteratively select out acceptable parameter sets. As with the fixed charge FF it was found necessary, even with polarizability included, to invoke the empirical grid-based CMAP corrections [38] to account for the backbone structures in proteins and peptides. As mentioned above, the lack of transferability is most likely a result of the small training sets used in deriving FFs for the model compounds. These are just not large enough to capture the domain of intra- and inter- molecular interactions that the FF needs to account for. We discuss this element of FF development in more detail below. In addition, it is not clear that the optimized peptide FF is still able to account for the properties of NMA and other amides used in the original parametrization.

3.9.2 Polarizability results in degradation of Fit?

The refined Drude-2013 protein FF was tested by carrying out ~ 100 ns simulations on a set of small proteins. The calculated RMSDs of the alpha carbon atom positions were compared with those obtained from simulations with the fixed charge C36 FF [122]. In a surprising and unexpected result the fit to the experimental structure resulting from C36 is degraded, sometimes significantly, with the Drude FF. Moreover, chemical shifts of Ubiquitin and Cold Shock Protein A. were also fit significantly better by C36, than by the Drude polarizable FF. This despite the fact that C36 has subsequently been found to be significantly flawed [65]. This result is analogous to that found with the condensed phase properties of the ethers [171], and as the authors there noted, is puzzling. Polarizability introduces a significant number of additional parameters, which should certainly allow a better accounting of experimental observables. In theory, it can't degrade the overall fit to experiment relative to a fixed charge potential, in the null case (all polarizabilities set to zero) one would simple get back the fixed charge fit. Thus it would appear that there is an artifact somewhere in the parametrization protocol, likely contributing is the limited observable sets used in optimization and validation.

3.10 Summary of Drude FF development for organic compounds and proteins. Polarizability does not lead to a general improvement of FF performance—often degrades fit

The extensive body of work represented by these studies represents a pioneering effort in the attempt to develop a

polarizable FF for proteins. Several themes emerge from the studies, which are both informative and can help in the design of future FF improvements. One of the clearest results to emerge from all studies is that polarizability is crucial to account for dielectric behavior. Beyond this the situation is murky. Comparison with CHARMM fixed charge FFs did not reveal a clear superiority of the polarizable FF for the polar systems. Some observables were accounted for better with the Drude FF while better agreement with experiment for others was achieved with the fixed charge FF. This is perhaps best exemplified by the comparisons made in the treatment of ethers where the additive FF actually outperformed the Drude FF in reproducing the properties of these systems. This led the authors of the ether study to comment [171]:

> "Somewhat disappointing is the inability of the polarizable model to yield overall improvements in condensed-phase properties as compared to the additive model. Given the extra degrees of freedom in the polarizable model it would be assumed that improved agreement should be achieved."

A similar sentiment was expressed by Guillot [115] in reviewing the over 40 water potentials that have been proposed:

> "…Much more astonishing and very frustrating is the fact that the explicit introduction of molecular polarizability does not lead to significant improvement (of the properties of water)."

Most dramatic was the degradation in fit of protein structure and chemical shifts with the Drude-2013 polarizable FF relative to the flawed fixed charge C36 FF. Clearly this is the result of some inadequacy in the parametrization protocol. Given that the inclusion of polarizability introduces additional adjustable parameters it can only improve the fit, or at worst produce an equivalent fit if all polarizability parameters are zero.

There is no debate that molecules are polarizable, and that this polarizability plays a role in structures and thermodynamics of molecular systems. Based on the overall collection of results in these studies and others, it would appear that the effects of polarizability on most systems of interest are small. Its inclusion has not led to significant improvement in accounting for the structural and energetic properties. Two exceptions to this are dielectric constant, which simply can't be accounted for by a fixed charge model, and ionic interactions such as those in ion-binding proteins [180]. Charge induce-induced dipole interactions are large and important, having major effects in these systems. Aside from these, it would appear from studies to date, that the deficiencies in fixed charge FFs go further than polarizability, and additional physics needs to be considered.

3.10.1 Inadequate training sets can lead to future failures and need for reparametrization

A characteristic of these initial polarizable FF derivations, is the use of extremely small training and test sets (in contrast to derivation of fixed charge CHARMM FFs [22, 65, 112]). They were typically comprised of three to four unstrained compounds, often homologs, with an additional two or three compounds in the test set. This is inadequate to derive a robust transferable FF which can be expected to predict properties of compounds outside the training set. Another recurring theme emerged as a consequence of these limited training sets. In many cases, it was found in short order, that a complete reparametrization was required of the functional groups. This resulted in basically a duplication of the work (e.g., alkanes, benzene, amides, and ethers). This would be obviated if comprehensive representative training sets comprised of linear, branched, strained and cyclic compounds were invoked, such as those used in the FF studies of Allinger [108], Ermer and Lifson [181], or Hagler et al. [182] among others, standardly involving an order of magnitude more compounds and observables.

An example of this is the derivation of the Drude hydrocarbon FF, where the compounds addressed are limited to three or four small linear alkanes in addition to isobutane. This can be compared to the CFF alkane force field [7, 86] which included, in addition to vibrational, energetic, and structural properties of small linear alkanes, among other observables, excess enthalpies of cycloalkanes C_5–C_{12}, conformation of chair cyclohexane, the lowest torsional frequency of cyclopentane, the amplitude of psuedorotation of cyclopentane, and vibrational frequencies of cyclopentane, cyclohexane and cyclodecane, unit-cell parameters, heat of sublimation, molecular and lattice vibrations, thermal expansion of the unit cell, for n-hexane and n-octane crystals. *Notably when problems in the calculated values of strained rings arose, even with this extensive training set, the observable set was augmented by experimental values of the bond angles of substituted cyclodecane, 116° and 119°.* The observable set for the MM4 FF for alkanes [108] was comprised of heats of formation, structures, and barriers, *from among 56 hydrocarbons*. These included the linear alkanes C_1–C_9, cycloalkanes C_5–C_{12} including 1,2,3,4,5,6-hexarnethylcyclohexane, diadamantyltetramethylbutane, 2,2,3,3-tetramethylbutane, and tri-t-butylmethane.

Clearly the training sets used in both CFF and MM4 are far more extensive than those used not only in the CHARMM polarizable FF but in many of the more recent FF derivations. It should be emphasized that although we are discussing alkanes here, the training sets used for derivation of other functional groups suffer from the similar comparisons. And though the polarizable FF training sets are an extreme, the use of limited observables in current FF

derivation is more the rule than an exception. Much of the accumulated wisdom of the earlier FF derivations seems to have been lost. This is a crucial issue. Transferability depends on accounting for the properties of a representative set of compounds. If only normal alkanes are used for example, one samples a basically unstrained limited configurational space. When these moieties are subject to strain, either through inclusion in rings, such as in proline, or in cyclohexyl moieties in prospective drugs, or induced by ligand binding, regions of configurational space are visited which just were not accounted for in the parametrization. This is demonstrated dramatically by the examples of CFF and MM4. In the former, even though the training set was extensive, errors arose which indicated the need to sample additional configurational space and substituted cyclodecane had to be added to data set. Discrepancies that arose from applications of MM3 which was also parametrized against a respectably large training set, called for additional physics to be incorporated into the FF and even larger training set to be used.

The use of small training sets, either due to a small set of compounds *or lack of a diverse set of observables*, result in inadequate sampling of the configurational space accessible through either intramolecular strain due to covalent structure or strain induced by intermolecular interactions. This will soon be exposed when the FF is applied in applications to systems of interest, especially when calculating properties such as energetics, not included in the observables addressed in the derivation. This will then require reparametrization and duplication of effort as we have seen. In current FF studies reparametrization often involves a different training sets, also limited and excluding even the original observables. They are often targeted to fix a particular discrepancy as Hornak pointed out [57], This becomes a vicious cycle which has led to the proliferation of FFs we have seen over the last decades.

3.11 CHARMM polarizable charge equilibration FF

Patel and Brooks also introduced polarizability into the CHARMM FF, employing the charge equilibration method (CHEQ) [110, 183]. In this formalism, polarization is accounted for by allowing the atomic charges to respond to an external field. The response to the field (or charge flow), is determined by the electronegativities and hardness, or resistance to electron flow, of the atoms [183–185]. (Rick and Stuart [184] have reviewed the different methods for accounting for polarizability including an excellent description of the Charge Equilibration formalism). CHEQ has the advantage that, since polarizability is accounted for through shifts in atomic charge, no new terms need be added to the FF. A disadvantage is that since the charge flow is determined by covalent connectivity the model can't account for out of plane polarization, as for example may be important in interactions involving a phenyl ring.

In the implementation of Patel and Brooks, the atomic hardness and electronegativities are determined by fitting electrostatic potentials of model compounds in the presence and absence of an external field designed to mimic the field produced by a water dipole. The authors noted that these parameters are not entirely transferable, as parameters for equivalent atoms in different residues may differ. This may be indicating the omission of the physics underlying charge flux, or other deficiencies in the analytical representation.

Van der Waals parameters are then optimized in an iterative procedure, first fitting QM gas phase energies and geometries of the set of 29 dimers of water-model compound complexes provided by Rablen et al. [186] These were calculated at the B3LYP/6–31+G(d(X+),p) level, and the TIP4P-FQ [187] potential was employed for water. In the second step the parameters were further refined to account for the heats of vaporization and densities of 14 organic liquids as well as sublimation energies and lattice constants of imidazole and indole. As noted above, inclusion of a large data set of crystal properties including sublimation energies provides more high resolution information rich data than liquid observables. Though two crystals were addressed here most of the compounds comprising the neat liquids included have crystalline counterparts which, like indole and imidazole, would provide more and higher quality observables than the corresponding liquids, though the latter are also useful and could profitably serve as an additional test set. As per Lifson's CFF paradigm [8] the most rigorous protocol would be to include both types of experimental data.

As 36 atom types are identified, this corresponds to 72 nonbond parameters. The QM dimers provide 87 observables including H-bond lengths and angles while the condensed phase properties provide another 37 observables for a total of 124 observables. This corresponds to an observable/parameter ratio of 1.7, which, though determinate, is significantly less than optimal (and would be greatly improved by inclusion of additional crystals).

3.11.1 Significant deviations remain, indicating flaws in CHEQ FF

The energies of the water complexes are fit moderately well although large deviations occur in several of the dimers including deviations of 1.3 kcal/mol (16%) and 2 kcal/mol (40%) for two acetic acid–water configurations, and 2.6 kcal/mol (38%) for an *N*-methyl formamide water dimer, among others. These fits, commensurate with the magnitudes of deviations obtained with the Drude CHARMM FF [179] don't seem to be conclusively better than similar results from fixed charge FFs [22], though again we are faced with the

pervasive problem of the use of different, custom sets of observables used in the derivation and validation of almost every FF, with little to no overlap.

A similar quality of fit is observed for the geometry of the dimers. Thus, the RMSD of the hydrogen bond lengths is 0.19 Å, which is larger than desirable, and larger than analogous deviations obtained with the CHARMM22 fixed charge FF [22]. In addition, as with all RMSD measures, it contains significantly larger individual deviations such as 0.3 and 0.5 Å in the same water-acetic acid dimers which displayed problematic energies, and 0.35 and 0.6 Å in formic acid–water dimers, as well as others. A similar quality of fit was observed for the hydrogen bond angles. A comparable pattern was observed with heats of vaporization, where large deviations of 1–2 kcal/mol (12–18%) in four of the 14 dimers occurred. These deviations seem to clearly point to remaining significant deficiencies/omissions in the physics represented by this functional form, even with the inclusion of polarizability.

All in all, as the authors observe, the fit is similar to that of the CHARMM non-polarizable FF. The authors point out that one could achieve a better fit by relaxing the constraint that only CHARMM atom types are used, and by increasing the number of atom-types, i.e. reducing transferability. However, this is obviously detrimental, and is also true of the fixed charge FF. The almost universal goal of introducing polarizability into FFs, is to correct for the omission of what was thought to be an important deficiency in accounting for a basic physical property of molecular interactions [100, 150]. This was expected to achieve a more accurate fit to experiment, and hopefully at the same time *reduce* the number of atom types which might have been needed to account for by the omission of this phenomenon.

3.11.2 CHEQ and other FFs (other than OPLS) have difficulty accounting for energetics of tetra-ala conformers

Following the derivation of the CHEQ polarizable protein FF it, was tested against a set of peptides and proteins [110]. The results mirrored the quality of fit to the training set. The alanine dipeptide map, considered as the basic model for the protein backbone, was the first system considered. Φ–Ψ maps calculated with the FF were compared to QM maps calculated at the LMP2/cc-pVQZ//MP2/6-31G* level, as a benchmark. The maps look extremely similar, though it is difficult to make quantitative conclusions from the contour maps. Nonbond parameters were not transferable from the original derivation, especially oxygen and nitrogen parameters, and had to be readjusted. In addition, the CMAP grid correction (at 15° intervals of Φ and Ψ) was applied to reconcile the differences between CHEQ FF and QM energies, so the maps should be virtually identical. More informative is the subsequent comparisons with the Beachy set of 10 Ala tetrapeptide configurations, calculated at the LMP2/cc-pVTZ(-f) level as well as with results on the same set resulting from CHARMM22, PFF146, OPLS-AA/L34, and AMBER PARM99(PFF) [110]. As with the training set fits described above, the relative energies of the tetrapeptide reveal deficiencies in the force field, with three of the 10 conformers deviating from the QM energies by 1.23–2.5 kcal/mol (32–90%).

Interestingly both the OPLS-AA/L fixed charge and OPLS polarizable FF (PFF) fit the data well, with the fixed charge OPLS-AA/L very slightly outperforming the polarizable version (RMSDs of 0.56 vs. 0.69 kcal/mol), a persistent theme in the comparison of fixed versus polarizable FFs.

3.11.3 Puzzling results—does the grid based correction factor, CMAP, improve accuracy?

These latter results are unexpected and puzzling. First, based on the OPLS results one might expect that accounting for the geometries and relative energies of the Ala dipeptide would lead to a corresponding fit to the Ala tetrapeptide conformational properties. In OPLS fitting only the dipeptide led to a good fit of the energetics of the tetrapeptide as well. Secondly one would expect that the CMAP empirical correction, constructed to account for peptide conformational energies—especially Ala from which they are determined, would ensure an accounting of the energetics of small Ala oligopeptides. The fact that it clearly doesn't would seem to be a clear indication that it has the wrong coordinate dependence, and this leads to non-transferability. For example, if the deficiency it was "correcting for" in the dipeptide was an error in the dispersion, the deviation would depend on the inverse 6th power of interatomic distances. It would distort the results of longer peptides, calculated with the CMAP correction, as the error introduced on distant atoms coming in contact, does not vary with the sum of the correction terms of the individual residues based on their torsions. A similar concern was voiced by Shi et al. in their derivation of the AMOEBA FF described below [148].

The FF was also tested by minimization and 1 ps simulations of 22 proteins in vacuo [110]. The average RMSD from the experimental structure for the heavy atoms of these proteins was 1.91 Å (1.53 Å for backbone atoms), with 7 of the 22 structures displaying RMSDs between 2 and 3 Å. Simulation with OPLS-AA on the same systems returned a similar, if not slightly better fit. Though quantitative results are not given, a "worsening of the structure" with respect to

CHARMM22 is alluded to, indicating that the situation may be analogous to the results with the Drude FF where the fit to experimental structures actually deteriorated, on accounting for polarizability. As the authors note these are extremely short simulations in vacuo, so it is difficult to draw definitive conclusions but the large deviations which arise, essentially immediately, suggest that inclusion of polarizability does not significantly improve accuracy for these systems, and significant flaws in the FF remain.

3.11.4 On abandoning combining rules for vdW interactions and introduction of phase dependent polarizabilities

Continuing development of the CHEQ FF was carried out in a Kirkwood–Buff analysis of aqueous alcohol solutions [188]. The authors note the deficiencies in the standard Lorentz-Berthold combining rules and hypothesize that these may be responsible for deficiencies in the previous CHEQ alcohol FF [189]. Although they cite the more accurate Waldmann–Hagler [130] and Halgren [190] combination rules they chose to abandon combination rules entirely, instead introducing pair-specific parameters. This is undesirable for the very reason that combination rules have been used all these years, namely pairwise specific parameters introduce many more parameters, and require major parametrization efforts whenever a new atom type is introduced. Thus, without combination rules one needs to parametrize all mixed interaction, requiring QM or experimental data from heterogeneous systems containing the new atom type with all other atom types in the FF. (With a combining rule, only the single new atom type needs to be parametrized requiring QM or experimental data only from systems containing that type). It would seem more desirable, and simpler to first attempt to implement one of the more accurate combining rules before abandoning them altogether [132, 191].

Discarding combination rules resulted in the addition of 16 new pairwise LJ parameters. These were optimized against 20 observables, comprised of hydration free energies of the four linear alcohols, methanol through butanol, 8 gas-phase alcohol–water dimerization energies, and 8 QM gas-phase alcohol–water hydrogen bond lengths (four with the alcohol as the donor and four as acceptor). The observable to parameter ration of 20/16 is minimal, and inadequate. It is made worse by the fact that the H-bond lengths are essentially the same within each set for all four compounds. Thus, the H-bond lengths may in fact yield only two independent observables, H-bonds with alcohol as acceptor and as a donor. This would result in an effective observable to parameter ratio of 14/16, an underdetermined system. Given this it is not surprising that the fit to these observable were dramatically improved over the original CHEQ FF [188].

The concern that the training set may be inadequate to accurately determine the 16 mixed LJ parameters is supported by both the comparison made to the parameters that would result with various combination rules and the results of the Kirkwood–Buff analysis. The pairwise specific LJ parameters deviate significantly from those calculated with both the Waldmann-Hagler [130] and Halgren [190] combining rules. The latter have been shown to be fairly accurate, and result in similar values for the interactions considered here. Thus, the large deviation from both is concerning.

Finally, as the authors state in summarizing the results of the Kirkwood–Buff analysis with the modified FF

> …despite capturing the solute-solute and solvent-solvent interaction energetics accurately (to the extent that the pure liquid properties of solute and solvent reproduce well a series of experimental pure liquid condensed-phase data), along with the solute-solvent interaction in the condensed phase as demonstrated by reasonably good agreement of hydration free energies of solute in solvent …, we are not able to quantitatively and broadly reproduce the necessary local microstructure and its concentration dependence underlying observed macroscopic thermodynamics

The large deviations found in the Kirkwood–Buff analysis of the same solutions of compounds fit so well in the training set strongly demonstrate that the latter was inadequate resulting in ill determined parameters, which are not transferable.

Recently several enhancements gave been explored in an attempt to improve polarizable FFs. Kumar et al. [192] added terms to account for the physics of charge penetration, induction, and charge transfer to describe water. Naserifar et al. [193] have attempted to improve the model by combining the Charge Equilibration and Drude oscillator models. An important aspect of this model is the description of the electron density as a Gaussian function, which is polarized, rather than by a point charge. An attractive consequence of this description is that singularities that accompany point charges are avoided [193].

Bauer and Patel [185] reviewed applications and development of CHEQ FFs as well as addressing the phase dependence of polarizability. Several workers have commented on the coupling between atomic polarizability and intermolecular interactions (see citations in [185]). More recently the dependence of atomic polarizabilities on hydrogen bonding interactions in amino acids has been investigated [194]. In addition Dinur and Hagler [155] showed the coupling of nonbond and charge flux to H-bond formation, which would also imply polarization flux dependence, and Palmo et al. [195] demonstrated the need for both charge flux and polarizability flux to accurately account for dipeptide energetics. Thus, these fluxes (geometry dependencies) may underlie the phase dependence of the atomic polarizabilies, both

through hydrogen bonding and conformational effects of nonbonded interactions.

Bauer and Patel represented this phase dependence by coupling hardness and electronegativities to the atomic charges. This is intuitively reasonable as the polarizability is related to the deformability of the atomic electron density, which is also related to the atomic charge. The model was incorporated into a modified TIP4P-FQ water model [187] and labelled the TIP4P-QDP model (Transferable Intermolecular Potential 4-Site with Charge-Dependent Polarizability) [185]. Agreement with 14 gas and liquid properties of water are improved somewhat over the TIP4P-FQ model, which might be expected due to the increased flexibility of the model, but is nevertheless encouraging.

3.11.5 Summary, CHEQ FF

The results of applications of the CHEQ FF are comparable to those obtained with the Drude FF. Improvement of fit to experimental or QM observables has yet to be achieved and noticeable problems remain. Perhaps most significant are the discrepancies in the conformational energetics of the Ala tetrapeptide, and the degradation in the fit to protein structures noted above. The inclusion of coupling between intermolecular interactions and polarizability is encouraging and hopefully presages inclusion of nonbond, charge and polarizability fluxes and coupling as well.

As mentioned above, there is no question that molecules are polarizable, though the magnitude and importance of this effect on structure and energetics of peptides, proteins and other biological systems remains in question. Thus, the deterioration in the ability to account for observed molecular properties is puzzling if for no other reason than the additional adjustable parameters available can only lead to improvement of the fit. We suspect that the root cause for this degradation of fit may be twofold: First small training sets lead to under-determined parameters which are not transferable; and secondly, polarizability may not play a major role in these properties with the exception of charged systems. The validity of these suppositions awaits further comprehensive and rigorous studies.

4 OPLS

4.1 OPLS2.0

There have been fewer revisions to the OPLS FF since the development of OPLS-AA/L [36], than for the AMBER and CHARMM FFs. In 2012 Shivakumar et al. [163] presented the development of OPLS2.0 which was the first in a series of enhancements designed to improve the representation of drug-like molecules. This initiative culminated in the development of OPLS3 [196] discussed below. The number of torsion parameters in OPLS2.0 was exponentially increased to fit some 11,000 QM rotational profiles. In addition the use of the Cramer–Truhlar CM1A charge model [197] with bond charge corrections (BCC) [198] was introduced to calculate atomic charges. The BCC terms were then optimized against a training set of 153 solvation free energies. The resulting FF was tested by calculating solvation free energies of 239 additional diverse compounds. Significant improvement in the fit was reported relative to OPLS_2005 FF (implemented in the Schrodinger suite 2008). Absolute unsigned errors (AUE) were, for the most part, under 1 kcal/mol with the exception of carboxylic acids, aliphatic amines and amides. As with previous studies the amides were the most problematic with an AUE of ~ 1.5 kcal/mol (~ 15%) [163].

4.2 OPLS-AA/M

In parallel with the developments of OPLS2.0–OPLS3.0, Robertson et al. [178], undertook another reparametrization of the basic OPLS-AA FF [32] As with the continuing efforts to address errors in the CHARMM and AMBER FFs discussed above, the approach taken was to reoptimized the torsion error functions for both backbone and sidechain rotational states. In common with these efforts, torsion functions were optimized against high-level QM energy scans (ωB97X-D23/6-311++G(d,p)-311++G(d,p) with single point calculations at the B2PLYP-D3BJ24/ aug-cc-pVTZ level) [178]. In a departure from the standard protocol, it was found that weighting low energy conformers in the optimization, by a Boltzmann factor corresponding to a temperature of 2000°K, significantly improved the fit.

The newly optimized parameters yielded a good fit to the Ala and Gly dipeptide maps, with RMSDs of 0.93 and 1.09 kcal/mol respectively. This was a significant improvement over the OPLS-AA. and OPLS-AA/L [36] FFs, based on these surfaces, though as noted with such comparisons in other FFs, this is to be expected as they were fit to different QM maps. Important minima on the Ala ϕ–ψ map were fit even better e.g. the RMSD in energy for the C7eq, C5, C7ax, α′, β_2 and α_L configurations was ~ 0.5 kcal/mol, though the β_2 and α_L conformers were not minimum energy structures on the OPLS-AA/M surface. (Similar fits for these conformers were found with both OPLS-AA and OPLS-AA/L). For Pro, two scans were carried out about ψ, with the proline ring fixed in trans and cis conformers. The fit to these scans yielded almost perfect agreement, 0.28 kcal. Given the results for Ala, and Gly, this is almost too good, suggesting that freezing the degrees of freedom in the Pro ring may simplify the surface to the point that it becomes almost solely a function of ψ. This could be tested by relaxing the Pro ring at each value of ψ.

4.2.1 Ala tetrapeptide and NMR properties

To further test the FF, the 27 conformers of the blocked alanine tetrapeptide (Ace-Ala-Ala-Ala-NMe) identified by DiStasio et al. [199] were investigated. Because there was concern that the geometries may not be accurate, the conformers were reoptimized at the at the ωB97X-D/6-311++G(d,p) and M06-2×31/6-31+G(d) levels of theory. Four conformers were found to have significantly different geometries with the two functionals and were omitted from further considerations. Single point calculations were then carried out with aug-cc-pVTZ and jun-cc-pVQZ32 basis sets to assess basis set dependence [178]. (it is not clear why there has been such an emphasis in the literature on fitting minimum energy structures). Clearly some are desirable, but the structure optimized in one basis set will probably not be the minimum energy structure in the larger basis set used for the more accurate single point calculations in any case. For a given structure (set of coordinates) the FF should reproduce the QM energy whether it is a minimum or not. It's unlikely that structures optimized, even with slightly smaller basis set will have extremely high energy clashes, which might be problematic in a fit. Furthermore, the configurations sampled in MD simulations and ligand binding will be strained, and significantly displaced from the minima of the isolated residues. In any case the FF did a good job of accounting for the 23 tetrapeptide conformers, with RMSDs ranging from 0.8 to 1.3 kcal/mol versus the two basis sets used here and the RIMP2(CBS)//HF/6-31G** calculations of DiStasio et al. [199].

As has become the practice in the literature the FFs are assessed by their ability to account for NMR solution properties. To this end simulated J-coupling constants for Ala_5 and Gly_3 were compared to the experimental results of Graf et al. [200] χ^2 values (agreement between experimental J-couplings and those calculated from the trajectories) were calculated using the three sets of Karplus parameters for calculating J couplings from Best et al. [62] The values of χ^2 ranged from 1.2 to 2.6 for Ala with the three Karplus models, and 3.1–4.0 for Gly. Though an improvement over previous FFs, the level of agreement, especially for Gly suggest remaining deficiencies in the FF. The distribution of secondary structure in Ala_5 also differs significantly from that reported by Graf et al. [200] who found 14% β and 86% poly-L-proline II helix type structure (PP_{II}) and no α-helix, as opposed to the 12% α-helix, 33% β, and 55% PP_{II} obtained with the OPLS-AA/M FF [178]. Graf et al. also reported a systematic trend of increasing J-coupling along the peptide going from the N to C-terminus, as well as temperature dependence of the coupling constants, results for a variety of other chain lengths, as well as coupling constants for two peptides extracted from lysozyme containing Ala_3 [200]. These would provide a useful set of observables to more rigorously evaluate the FF, especially given the apparent discrepancies.

Side chain χ_1 torsion functions were parameterized against QM scans in a similar way to the backbone functions. The transferability of torsion parameters invoked in OPLS-AA was relaxed in order to get a better fit, though not as many χ_1 torsion types as OPLS-AA/L were used. Though weighted deviations from the QM energies ranged from ~0.4 to 0.8 kcal/mol, several problematic systems were revealed. Thus, in order to account for the rotational energies of Leu, Ile, and Val different torsion error functions were needed. This emphasizes the nature of these torsion correction factors. These side chains are essentially hydrocarbons, and the chemical nature of the χ_1 torsion in these compounds is almost identical. The difference in the intrinsic χ_1 torsion potential in these residues is insignificant. Clearly the need for separate torsion functions is to compensate for likely errors in the nonbond interactions in the strained branched sidechains, or the lack of coupling between the torsion and angle coordinates, the latter likely distorted by the strain in the branched hydrophobic side chains.

Consideration of rotamer populations of polar amino acids (Ser, Cys, Asp, Glu and Trp) revealed a likely problem with the balance between inter and intramolecular forces. Thus, the sidechain torsions derived from the high-level QM scans failed to reproduce experimental rotamer populations. It is likely, given the polar nature of these residues, that this discrepancy is probing errors in the inter or intramolecular nonbond interactions, as, if these were "correct", the intermolecular interactions ought to recapitulate the perturbation of the intramolecular rotamer distribution. This is also consistent with the need for continuing reparametrization of these interactions [201].

As a final evaluation ^3J couplings of the small proteins ubiquitin and GB3 were calculated. Overall good agreement was obtained with the overall RMSD in simulated couplings from experiment being 1.12 and 0.91 Hz for ubiquitin and GB3 respectively. There were however larger deviations in the $^3J(H_\alpha,H_\beta)$ coupling of 1.88 and 1.52 Hz respectively, the origin of which is unclear. Furthermore, these data have relatively low information content, as described above. The structures of these proteins are known to atomic resolution and it is more useful to assess in depth, how well these structures are reproduced by the FF.

4.2.2 Limited size and information content of observables considered

The results of the comparisons as a whole indicate reasonable agreement with the data considered. As discussed elsewhere in this perspective an issue is the size and

diversity of the training and validation sets. The data set used here is small, when compared for example to those used by Huang et al. [65] in their reparametrization of CHARMM, or by Lindorf-Larssen et al. [76, 128] in their comparison of different FFs. More importantly these additional observables revealed important deficiencies in the FFs, which otherwise would have gone undetected until revealed in subsequent applications. For example, though ubiquitin was found to be moderately stable over the course of a 1 ns trajectory (RMSD 2 Å) as were many other protein systems, simulations of intestinal calcium-binding protein (3icb), and the C-terminal domain of human transcription factor IIF (1i27), revealed severe inadequacies with RMSDs approaching ~4 Å each (Fig. 2) .This was only found because a relatively large and diverse set of 15 crystal structures (probably a minimal protein stability validation set), were tested, in addition to a large set of other properties.

Further, as noted above, an issue with the NMR measures used here as well as elsewhere, is the low-resolution information content in these observables. Thus as an accessory to more informative data on structure and energetics, they can provide valuable information on FF deficiencies, such as over prediction of helices [62] or other problems in local structural properties in solution [74, 128]. However, these observables are not sufficient to evaluate FF accuracy as evidenced by the observation that significantly flawed FFs can reproduce these NMR observables well, but result in erroneous thermodynamics [76, 133] (Table 1). Deviations in NMR parameters can give an overview, but can't be easily interpreted in terms of structural and energetic deviations, such as how well are carbonyl–carbonyl interactions [202] reproduced, or how faithful to experiment is calculated H-bond geometry, or how well are the energetics of amide–amide, or salt-bridge interactions reproduced. These are the fundamental quantities being sought in most applications of MD simulations, and to assess the validity of FFs to calculate these we need to reproduce observables such as crystal structure and sublimation energies, heats of vaporization etc.

In summary, based on the available results it is likely that this FF is comparable to the latest CHARMM and AMBER FFs, though without a comparison of the FFs on a common, large, diverse validation set of observables it is impossible to make an unambiguous conclusion.

4.3 OPLS2.1 and 3: a hybrid physics based—free energy function

More recently further optimization of the OPLS FF, was carried out [196, 203]. The primary objective of these studies was to achieve a useful tool for the calculation of relative free energies of binding in the lead optimization step of the drug discovery process. The derivation followed standard methodology, with the exception of the introduction of thousands of torsion error functions to account for medicinal chemistry space, and the exploitation of off center charges for aryl nitrogens and halogens [196].

Bond stretching and angle bending parameters were obtained by equating force constants to QM, B3LYP/6-31G* level second derivatives at the minimum energy conformation, while reference values were taken from the equilibrium geometries as well as crystal data where available. It was noted that the bond angle potentials are critical for obtaining accurate torsional energetics [196]. *Another way of stating this is that angle deformations and torsions are coupled*. This has been known for decades by spectroscopists and the importance of representing this behavior by coupling or cross-terms to account for molecular energy surfaces over accessible configurations has been quantified [28, 204, 205]. It is the underlying phenomena that led Warshel and Lifson to introduce the so-called "θθϕ" coupling term in 1969 to correct deficiencies observed in their alkane FF [23] as noted above. The omission of this coupling, among other interactions, is manifested by the immense number of context dependent torsion function correction factors required to represent these compounds.

The torsion error function parameters were obtained from restrained minimum energy structures obtained from torsion scans with the B3LYP/6-31G* basis set at 30° increments. The torsion parameters were then fit to the energies of these structures calculated at the LMP2/cc-pVTZ(-f) level of theory. In all 48,142 torsion error functions were derived by fitting the energy profiles of 11,845 model compounds. A major difference of OPLS3 from OPLS2.0 [163] and 2.1 [203] is that 1–4 nonbond parameters were scaled by 0.5 rather than by the factor of 0.833. This will of course have a significant effect on the resulting torsion constants. The resulting RMSD error in conformational energies of compounds in the training set was 0.9 kcal/mol, while test compounds containing the parametrized torsion exhibited an RMSD of 1.2 kcal/mol.

This coverage is obviously extensive covering an estimated 66% of all compounds likely to be encountered in a drug discovery program [196]. An automated protocol was developed to address compounds containing unparametrized torsions. This is almost equivalent to deriving a unique FF for the individual molecule of interest. Though clearly not based on the fundamental physics of molecular energetics, as seen below, it is an extremely effective approach to predicting ΔΔGs of binding.

Protein torsion parameters were also reparametrized by fitting to 324 configurations from the ϕ–ψ map of the Ala dipeptide sampled at 20° increments. This was supplemented with 2067 structures taken from a high temperature MD simulation of alanine dipeptide in water. As above,

all structures were minimized at the B3LYP/6-31G* level (with ϕ–ψ constrained) and the energy of each structure calculated at the LMP2/cc-pVTZ(-f) level. Analogous calculations were carried out for Gly and Pro. Side chain torsion error functions were fit to similar χ_1 and χ_2 torsion scans with the backbone either in the α or β conformation. The parameters for charged residues were then "tuned" to account for conformational propensities in proteins. The RMSD errors in energies of the Ala dipeptide in the training set was 1 kcal/mol. The RMSD of energies of 1700 Ala tetrapeptide structures not included in the training set was larger, 1.8 kcal/mol.

Van der Waals parameters were transferred from previous versions of OPLS [196], where they were derived primarily from fits to liquid densities and heats of vaporization [32]. As with previous OPLS FFs [163, 203] the CM1A-BCC charges based on the Cramer–Truhlar method [197] modified by bond charge correction terms [198] (BCC) were employed. Here the BCCs were parameterized against 6-31G* electrostatic potentials of ~300 aromatic rings and 11,800 model compounds used for torsion parametrization. They were then further refined by fits to ~150 solvation free energies. The RMSD error in solvation free energies with these charges is ~0.9 kcal/mol [203].

A significant enhancement in OPLS3 over previous OPLS versions is the introduction of off centered charges for aryl halogens other than fluorine and aromatic nitrogens [196]. This addresses nitrogen lone pair density and the lack of representation of the "σ-hole" in halogens resulting in a counterintuitive positive electrostatic potential at the tip of the halogen [206]. These charges are fit to 6-31G* electrostatic potentials, and were shown to significantly improve hydration free energies of compounds containing these moieties. Protein partial charges and vdW parameters were adopted from the 2001 OPLS-AA/L FF [36].

4.3.1 Secondary structure propensities of three peptides—low resolution observables

The protein FF was tested against a small set of observables. As has become standard recently [62, 63, 65, 127, 128], secondary structure propensities of oligopeptides were tested. In this case the propensities of two α-helical peptides, K19 [207] and $(AAQAA)_3$ [208], and a β-hairpin peptide, CLN025 [72] were investigated. Propensities were determined from simulations of ~1 μs, which, as we seen from other studies where 4–10 μs realizations were carried out, may not be sufficient for convergence [58, 65, 128]. Of the two helical peptides the helix content of (AAQAA) was reproduced well, but the simulated helix content of K19 was significantly higher than the observed value (74 vs. 50% respectively). The fraction of folded structure of CLN025 was recapitulated by the simulation.

4.3.2 Crystal structure, a more rigorous test

As emphasized above, in addition to determining the fraction of the CLN025 peptide folded in solution, Honda et al. [72] determined the crystal structure of this peptide. We emphasize again that the simulation of this structure would be a far more stringent test of the potential, and yield additional valuable information including for example configurations of individual amino acids and their side chains, and the ability to reproduce H-bond geometries, while also requiring less computational resources. It is not clear why this system has not been incorporated into the assessment of not only this FF, but the others cited above which also study the solution properties of this popular peptide model.

4.3.3 Information available from secondary structure propensities—necessary but not sufficient

The significance of the almost 50% deviation in the calculated α-helical propensity of K19 with OPLS is not easy to interpret. Clearly it reflects some deficiency, most likely in the FF, but which term or interaction? It also might reflect a deficiency in the water potential, or perhaps in sampling. This difficulty in tracing errors back to the FF, and thus provide direct information to improve the FF, is an intrinsic liability of these observables.

Furthermore, as discussed above in the "OPLS-AA/M" section, and shown elegantly by Best and Hummer [62], and confirmed in the studies of Piana et al. [76], secondary structure propensities (and other NMR observables of disordered peptides), can be fit extremely well by fatally flawed FFs. Thus, as seen in Table 1, FFs which fit NMR properties well, result in disqualifying discrepancies: 50% in the energy and entropy of helix initiation and extension [62] and an 8 kcal/mol deviation in the enthalpy of folding of a villin variant with C22*, a FF which has been assigned a "perfect score" based on NMR observables of peptides in solution and protein stability [128]. It follows that secondary structure propensities can reveal significant failures of FFs, as for example when significant populations of left handed helices arise, but they are not able to bear witness to the validity of a FF.

4.3.4 Energetic and structural observables

Again it is clear that enthalpies, and entropies where possible, must be included in any evaluation of FF accuracy. High resolution structural data is also a requisite. This is why the availability of the crystal structure of CLN025 provides such an opportunity. Protein structures may also be of use here, though they result from the interplay of so many

disparate interactions that deviations of individual structural elements which might shed light on particular FF term, such as particular H-bonds, Phe stacking, or CH···O interactions are hard to isolate. This is why the exploitation of small organic compounds and peptide crystals offers a powerful assessment tool for FFs [22, 77, 85, 88, 91, 93, 209–211], especially when sublimation energies are available as well.

4.3.5 Protein stability

The second set of data used to assess the FFs was the stability of seven proteins assessed over 200 ns of MD. The trajectories were run in triplicate, and the results from the final 100 ns averaged. It is difficult to assess FFs based on protein stability since it is so critically dependent on the length of the simulation. In addition, the intrinsic stability of the different proteins, their size, and number of disulfide bonds they contain introduce additional variables. Nevertheless, as shown by Huang et al. [65] if long enough trajectories of a large cohort of systems is employed (in their case 15 crystals), they can begin to reveal deficiencies in the FF. However, as with solution NMR properties and 2° structures discussed above, they only probe deficiencies, at the current state-of-the-art they cannot validate the accuracy of a FF, due to the limited trajectory length.

The results obtained here showed small RMSDs, ~ 1 Å, raising no red flags, and improving on several previous versions of OPLS. However, when compared to the similar simulations carried out using C36m, the results may well be misleading if interpreted as validating the FF. First as noted, the trajectories are significantly shorter than the 1 μs realizations employed for similar systems by Huang et al. [65] or the 10 μs trajectories of Debiec et al. [58] (Fig. 1). Several of these trajectories indicated structures might still be diverging, even after 1μ s, as seen in the trajectories of lysozyme and dethiobiotin synthetase shown in Fig. 2. This is especially relevant since the C36m FF is very similar to the C22* FF. In the short simulations carried out here, C22* and OPLS3 give comparable results. For lysozyme C22* is even slightly better, RMSD 1.1 versus 1.3 Å, yet, as seen in Fig. 2 the deviation for the Cαs with the corresponding C36m FF is twice as large, ~ 2.2–2.4 Å over the last 200 ns, and rising. Furthermore, these are not the most problematic systems obtained with C36m, emphasizing the need for a large test set (15–20 protein crystals or more). Thus, as noted above the RMSDs of the Cα atoms of bovine ICaBP (3icb).and the C-terminal domain of TFIIF (1i27), approached 4–5 Å, clearly indicating significant problems. Given the similarities of these FFs it is not only possible, but likely that if 15–20 proteins, including these systems were simulated for ~ 1–10 μs or more, similar deviations would be observed. It is likely that, as the authors suggest, the accuracy of OPLS3 is similar to contemporaneous CHARMM and AMBER FFs, such as C22* [76], C36m [65] and Fff99SB*-ILDN [62], with the corresponding flaws documented above, inherent in the common functional form.

4.3.6 A relative free energy perturbation tool for lead optimization

To a large extent the accuracy of the FF in fitting the typical energetic and structural properties of biomolecular systems is subordinate, in this case, to the main goal of the study. That is, rather than the derivation of a rigorous force field based on the physics of inter- and intra- molecular interactions, a primary goal of the work is to derive a tool to enhance the predictability of protein–ligand affinity by FEP in lead optimization [196, 203]. To this end OPLS along with the FEP protocol was tested by calculating the relative binding energy (ΔΔG) of a diverse set of ligands to eight pharmaceutically relevant targets. It was found that the modifications introduced into the OPLS3 FF resulted in an overall decrease in the RMSD of the calculated ΔΔGs from 1.11 kcal/mol with OPLS2.1 to 0.95, with OPLS3 (~ 25%). Most importantly it was found that compounds predicted to be potent by these methods are more likely to be active than those predicted by other theoretical or medicinal chemistry methods [203]. This is of great practical importance for lead optimization in pharmaceutical discovery.

4.3.7 A prospective study—FEP is a valuable tool for lead optimization

These preliminary results have been further supported by an exercise mimicking a lead optimization program in which a prospective evaluation of the FEP method was carried out [212]. In this study the binding affinity of cathepsin L inhibitors were optimized by prioritizing building blocks targeted to the S2 pocket. Three thousand, three hundred and twenty five (3325) amine building blocks were assembled and the challenge was to select ten, that when combined with the fluoropyrimidine nitrile scaffold, would result in more potent derivatives. Four design approaches were compared: Selection by a medicinal chemist with knowledge of the protein structure; manual selection by experts who visually assessed minimized ligand binding modes; manual selection by experts who visually assessed binding modes resulting from docking and filtered by strain energy evaluation; and FEP prioritization of 93 compounds resulting from Glide docking with MM-GB/SA scoring. The results were impressive; eight of the ten compounds selected by FEP had improved affinity as compared to one out of ten for the other methods. The authors concluded:

> From these results, we conclude that FEP is an attractive approach to prioritize compounds for synthesis, though our observation is based on this one single

system. It should also be noted that the S2 binding pocket of hCatL has a strong lipophilic character and that additional studies are required to further substantiate if the type of results obtained here is also observed for more polar active sites.

These results indicate that the protocol developed in these studies will likely become an important tool for future lead optimization studies.

4.3.8 Cancellation of errors makes free energy a poor criterion for FF validity

This is indubitably a significant advance in the application of computer simulation to lead optimization and, as noted by the authors, an extremely attractive approach, that is likely to become standard in the drug industry. Though a major advance having exceptionally important practical consequences, its implications for the validation of OPLS3 (or any other FF) should not be over interpreted. As stated in the OPLS3 study [196]:

> Ultimately, explicit inclusion of polarization effects will be required to achieve the best fidelity with the actual underlying physics of the system…

To this we would add charge flux, atomic multipoles, valence coupling, etc., discussed extensively below.

In addition, as pointed out by the authors, the performance relies on the introduction of literally tens of thousands or error functions and cancellation of errors. For example, systematic errors in the free energies of ligand-solvent and ligand protein interactions are likely to cancel leading to more accuracy in binding affinities than in either component. In addition, as noted above, and seen in Table 1, errors of 50% or more in enthalpy and entropy can result in relatively accurate free energies due to enthalpy–entropy compensation.

That cancellation of errors plays a crucial role in the ability to fit free energies can also be seen through consideration of the errors of individual components. Thus, the errors in the ligand torsion profiles alone are ~ 1 kcal/mol [206], and errors in the conformational energetics of the protein ~ 2 kcal/mol or more (based on Ala_4). These are likely lower bounds as the former relates to the training set, and though the latter is a test, the potentials were based on the training against the Ala dipeptide. Errors in the Coulomb interaction as reflected in solvation free energies from which they were parametrized are ~ 0.9 kcal/mol. Clearly the valence and nonbond components will also contain errors, likely of similar magnitudes. Simply summing these errors leads to a total deviation of > 4 kcal/mol, yet the relative free energies are fit to an order of a kcal/mol, significantly smaller than the errors in the FF.

Finally, we note that in retrospective studies of 28 ligands carried out to validate the use of FEP with cathepsin L, the RMSD error in ΔG itself was 1.5 kcal/mol or ~ 15%. Several deviations ranging from 1.5 to 2.8 kcal/mol or as much as 33% were observed (an outlier having a deviation of 5.5 kcal/mol which defied explanation was also observed). In addition, when structure of one of the active complexes found by FEP was solved and compared with the simulation it was found that the orientation of the piperonyl ring system was flipped resulting in differences in interactions with the protein. The correct orientation was also visited in the trajectory, though to a lesser extent.

Given these considerations, though an extremely valuable practical tool, analysis of the results reveals, not surprisingly, substantial remaining errors in the underlying FF, similar to the contemporary CHARMM and AMBER FFs to which it was compared.

4.4 Summary of quadratic diagonal fixed charge FFs. The end of the road?

These FFs have played a major role in the history of computer simulations of molecular properties. They have demonstrated their utility in modeling and hypothesis generation [213], hit generation through docking, in some cases, as well as most recently in lead optimization through FEP calculations. A similar qualitative insight was obtained by Robinson et al. [214], who were able to explain the reason a modification which didn't interact with any residues in PI3Kβ or δ, nevertheless conferred specificity for β. They showed that the selectivity was due to differences in the free energy of the water in the ligand binding site on binding of the analog, rather than any difference in protein ligand interactions. This, analogous to FEP lead optimization technique, is an extremely valuable insight and of practical importance. It is doubtful one could understand the selectivity without the simulation. Though clearly of extreme practical utility, it is likely that the accuracy achieved is due to cancellation of errors as in the FEP ligand binding method.

Notwithstanding the utility of these free energy techniques, it would appear from the fifty or more-fixed charge FFs which have been developed over the years, that the accuracy achievable from this functional form has been attained, and the deviations resulting from its application thoroughly documented. Unacceptable deviations in thermodynamic, and structural properties remain as seen in the discussion above (e.g., the data in Table 1; Figs. 1, 2, as well as in the primary literature). As noted above, at this point it seems that trying to wring improvements in accuracy from this functional form is analogous to a game of whack-a-mole: optimizing parameters to address a particular deficiency introduces unacceptable discrepancies

in other properties. Based on these results and an extensive literature on the effect of physics not accounted for in this functional form, it would seem the time has come to incorporate the known physics of inter and intramolecular interactions omitted.

5 Expanding the physics represented in force fields: charge, nonbond and polarizability fluxes and anisotropic nonbond interactions

5.1 CFF

In the late 1980s Dinur and Hagler began a series of investigations to describe the physics omitted in FF representations of inter and intramolecular interactions [215–217]. The key observation made by these workers was that the physics governing these interactions, including charge distribution (atomic multipoles), charge flux, nonbond interactions and their anisotropy, nonbond and polarizability flux, etc. were directly reported on, and could be extracted directly, from first and second derivatives of the energy of monomers and dimers available from QM. They went on to characterize these interactions, develop analytical forms which could be incorporated into the FF, often at trivial computational cost, and assess their significance.

5.1.1 Charge flux—geometry dependent charges

That charges are not invariant with respect to molecular geometry has long been known especially in the field of infrared spectroscopy where it underlies the IR intensity. This coordinate dependence of atomic charge was referred to as charge flux [218–221]. The significant conformational dependence of atomic charge was also noted early on by the biophysical community, primarily through QM studies [217, 222–225]. For example Cieplak and Kollman commented [223]

> "One of the fundamental assumptions in most molecular mechanical models is the conformational independence of the electrostatic charges. This assumption cannot be correct, but it is important to assess the magnitude of the error made by this assumption" … "using trans-NMA charges lets one assess the errors inherent in assuming a single set of charges and that error turns out to be ca. 0.9 kcal/mol" (in the cis trans free energy difference).

Despite these observations, the contribution of charge flux has not been accounted for in the standard biomolecular FFs to date, though its inclusion can be implemented in a straightforward, and computationally inexpensive manner [217].

It should be noted that charge flux and polarizability are distinct phenomena describing different physical processes. Charge flux describes the redistribution of charge accompanying variation in valence coordinates such as bond lengths and angles—through bond interactions (see discussion below and Eqs. 3, 4)—while polarizability describes the rearrangement of the molecular charge density induced by an external electric field, or through space interactions. It is of interest to assess the relative contributions of these effects. This was studied by Dinur and Hagler for a series of alkanes, aldehydes, ketones, and amides, where it was found that inclusion of charge flux could not only significantly improve the fit of dipole moments for different configurations of these compounds, but, perhaps more importantly also improve molecular electrostatic potentials (MEP) and electrostatic forces on nuclei over those calculated with invariant charges, even those calculated by fitting the MEP [217].

5.1.2 Analytical representation of charge flux—a significant improvement without computational cost

Dinur and Hagler formulated an analytical representation of the charge flux, or geometry dependence of the charge, in terms of bond increments as:

$$dq = dq_0 + J_b(b - b_0) + \sum_{b'} J_{b'}(b' - b'_0) + \sum_{\theta} J_{\theta}(\theta - \theta_0) + \sum_{\theta} J_{\phi}(1 \pm \cos(n\phi)) \quad (1)$$

where dq is the bond increment of the bond being discussed b [91], b' is any bond connected to b, θ is any valence angle that contains the bond, *and* ϕ is any torsion angle that contains the bond, b. b_0, and θ_0, are reference values, and the sign in front of the cosine term depends on the periodicity n. The constant dq_0, is the intrinsic or equilibrium bond increment for that bond, J_b is the charge flux constant for distortions along that bond, $J_{b'}$, J_θ and J_ϕ are the corresponding constants for the flux along bond b due to distortions of the adjacent bonds, angles and torsions.

As described in the previous paper, the charge on atom i, q_i, is obtained from the bond increments as in Eq. 2 [91]

$$q_i = q_{i0} + \sum_j dq_{iJ} \quad (2)$$

where q_{i0} is a reference charge on atom i and the sum is over all bonds, j, containing atom i. The flux constants J, were obtained by fitting the Cartesian derivatives of the *molecular* dipole for different conformers of a set of compounds [217]. That is, the total molecular dipole moment, μ as formed from the atomic point charges q_i is given by,

$$\mu = \sum q_i x_i \quad (3)$$

The derivative of the molecular dipole moment with respect to the Cartesian coordinate of an atom j is then given by

$$\partial\mu/\partial x_j = \partial \sum q_i x_i/\partial x_j = q_j + \sum x_i \partial q_i/\partial x_j, \quad (4)$$

where the second term, the change in the charge with respect to atomic coordinates, is the charge flux. This encapsulates the geometry dependence of the charge, Obviously, in the fixed charge model this is assumed to be zero.

Dinur and Hagler found that the dependence of the atomic charge on geometry was localized, and could be described by its dependence solely on the bonds, angles and torsions it was contained in [217] and furthermore can be formulated, to a good approximation, as a simple linear expression of the bond and angle deformations along with a cosine dependence on the torsions as in Eq. (1). They determined the flux constants J by minimizing a target function which is the weighted sum of squared deviations between QM and analytical calculations of molecular dipoles and dipole derivatives. The latter calculated by substituting the expression for the charge given by Eqs. (1) and (2) into (4).

$$\sigma^2 = \sum w\left(\mu_{QM} - \mu_{calc}\right)^2 + \left(\partial\mu_{QM}/\partial x_i - \partial\mu_{model}/\partial x_i\right)^2.$$

where w is a weighting factor, and the sum is taken over a large number of distorted configurations (~ 15–30 per compound) of a family of model compounds.

An analogous procedure can be used to obtain dipole fluxes from quadrupole derivatives [215]. Flux terms including charge, nonbond and polarizability fluxes are elaborated on below.

The dramatic error introduced in forces by omission of the geometric dependence of atomic charge, or charge flux, is shown in Fig. 4. Here a point charge of 0.1e was placed on a line connecting the two carbon atoms in *N*-formylformamide as depicted in the figure [217]. The forces on the N, O and C nuclei were calculated by QM at the 6-31G* level (though this is a rather small basis set yielding dipole moments ~ 15% too high, and one would expect absolute values of forces to change with more complete basis sets, it serves to demonstrate the qualitative importance of charge flux in determining forces on atoms in MM and MD.) The force on the nitrogen calculated with QM and with both fixed and geometric dependent charges ($-\partial E/\partial x_N$) are given in Fig. 4 as a function of the distance between the probe charge and the leftmost carbon atom [217]. We note that the calculation was done with *N*-formylformamide at its equilibrium conformation so only the coulomb interaction contributed to the force on the atoms. Similar behavior was observed for forces on the other atoms [217].

The force on the nitrogen atom, exerted by the point charge, P, of +0.1, as calculated directly from QM, is given by the filled circles in Fig. 4. The forces are compared to those derived from the derivatives of the coulomb energy with charges including the effect of flux (open squares) determined by Eq. 1, and from fixed charges calculated by fitting the electrostatic potential (open diamonds). The charges and flux constants in Eq. 1 were obtained by fitting dipoles and dipole derivatives of 200 configurations of 12 alkanes, aldehydes, ketones and amides [217].

As can be seen by these results, the commonly used potential derived charges result in extremely large errors in the force (~ 80%) at 4 Å, while the charges accounting for flux, using Eq. 1, reproduce the forces extremely well. This is especially significant since the PD charges were optimized for *N*-formylformamide itself, while the constants in Eq. 1 were transferred from the fit to the diverse training set compounds alluded to above [217].

Furthermore, as seen from the simple form of the expression, once the flux constants are determined, the geometry dependent charges *can be accounted for at essentially no computational cost*. The quantities in Eq. (1) are all available from the calculation of the energy.

Similar deficiencies in the ability of fixed charges to be able to account for the forces arising from intermolecular interactions in a different system, the interaction of a point charge with a water molecule, were also demonstrated by Dinur [226]. He showed that the geometric dependence of atomic charges leads to a strong coupling between the inter and intramolecular forces, modifying the electrostatic forces on the nuclei in the water dimer *by as much as 80%*. It was further demonstrated that the contribution of atomic dipoles and polarizability to the electrostatic forces were comparable in the water dimer system.

5.1.3 Anisotropy of nonbond parameters: extracting parameters and functionality of pairwise nonbond interaction terms in FF from ab initio energy second derivatives

Dinur and Hagler demonstrated that individual Hessian elements (second derivatives of the energy with respect to the coordinates) of a complex, extracted pairwise atom–atom interactions [66, 215, 227]. They went on to determine the nonbond parameters for individual pairwise interactions directly by fitting these second derivatives of the dimer energy taken at a set of configurations of the dimers. Rather than, as standardly done using the energy itself at different configurations, which yields the sum of all atom–atom interactions, this analysis allows for detailed examination of the distance and orientation dependence of the discrete atom–atom pairwise parameters without the contamination of correlation with other interactions. The second derivatives effectively partition the energy into individual contributions, and thus can be used to determine the force constants, and functional form, as well as other characteristics directly, as shown below.

Dinur and Hagler demonstrated this in a study of homo and hetero dimers of water, formaldehyde and formamide [217]. An example of the methodology used is given by their consideration of the water dimers in Fig. 5.

The energy of the head to head dimer in the left panel of Fig. 5, E_{AB}, given by classical FFs is:

$$\begin{aligned} E_{AB} = {} & E_{Intra}(A) + E_{Intra}(B) + E_{Inter}\left(H_{A1,2} - H_{B1,2}\right) \\ & + E_{Inter}\left(O_A - O_B\right) + E_{Inter}\left(O_A - H_{B1}\right) \\ & + E_{Inter}\left(O_A - H_{B2}\right) + E_{Inter}\left(O_B - H_{A1}\right) \\ & + E_{Inter}\left(O_B - H_{A1}\right) \end{aligned} \tag{5}$$

where, E_{AB} is the total dimer energy, E_{Intra} (A) is the valence energy of water A, and likewise for E_{Intra} (B), $E_{Inter}(H_{A1,2} - H_{B1,2})$ represents the four pairwise nonbond energies between the protons in the different water molecules, $E_{Inter}(O_A - O_B)$ is the pairwise nonbond energy between the oxygens of molecules A and B, and likewise the term $E_{Inter}(O_i - H_j)$, for O–H nonbond interactions.

When the first derivative of the dimer energy given in Eq. 5, is taken with respect to a coordinate of the Oxygen in molecule "A" the result is:

$$\begin{aligned} \partial E_{AB}/\partial x_{OA} = {} & \partial E_{Intra}(A)/\partial x_{OA} + \partial E_{Inter}\left(O_A - O_B\right)/ \\ & \partial x_{OA} + \partial E_{Inter}\left(O_A - H_{B1}\right)/\partial x_{OA} \\ & + \partial E_{Inter}\left(O_A - H_{B2}\right)/\partial x_{OA} \end{aligned} \tag{6}$$

where for example $\partial E_{AB}/\partial x_{OA}$ is the derivative of E_{AB} with respect to the x coordinate of atom O_A, and similarly for the other terms in Eq. 6. As we see the intramolecular energy terms of molecule B have disappeared along with the nonbond interactions between the hydrogens in A and B, and the interactions of the hydrogens in A with O_B, as none of these depend on the coordinates of O_A.

5.1.4 Annihilating all terms but the single O–O pairwise interaction in the dimer

Finally, taking the second derivative of the energy with respect to a coordinate on O_B, results in:

$$\begin{aligned} \partial\left(\partial E_{AB}/\partial x_{OA}\right)/\partial x_{OB} &= \partial^2 E_{AB}/\partial x_{OA}\partial x_{OB} \\ &= \partial^2 E_{Inter}\left(O_A - O_B\right)/\partial x_{OA}\partial x_{OB} \end{aligned} \tag{7}$$

This derivative removes the remaining intramolecular energy terms of molecule A along with the nonbond interactions between the hydrogens in B with O_A, as none of these depend on the coordinates of O_B. *That is all interactions other than the O_A–O_B interaction have been annihilated*, because they don't depend on the coordinates of both O_A and O_B.

Thus, by taking the second derivatives with respect to the two water oxygens, *the pairwise O···O interatomic interaction is extracted from the total dimer interaction energy*. By fitting these derivatives for a variety of dimer geometries, with those calculated from the classical expression in the given FF, the potential constants and functional form of this individual atom–atom interaction can be determined. This is analogous to the parametrization of all nonbond parameters simultaneously by fitting the total dimer energy of many configurations. The advantage to fitting the second derivatives is obviously that one removes the correlation and uncertainty in fitting all interatomic interactions at once to total energies, and, as seen from the results, phenomena which are obscured by fitting total energies, such as anisotropy and flux become evident in fitting second derivatives of diverse dimer configurations.

5.1.5 Flux terms revealed by Hessian elements

As a second example, the authors considered the standard diagonal 12-6-1 FF representation of the energy to apply to

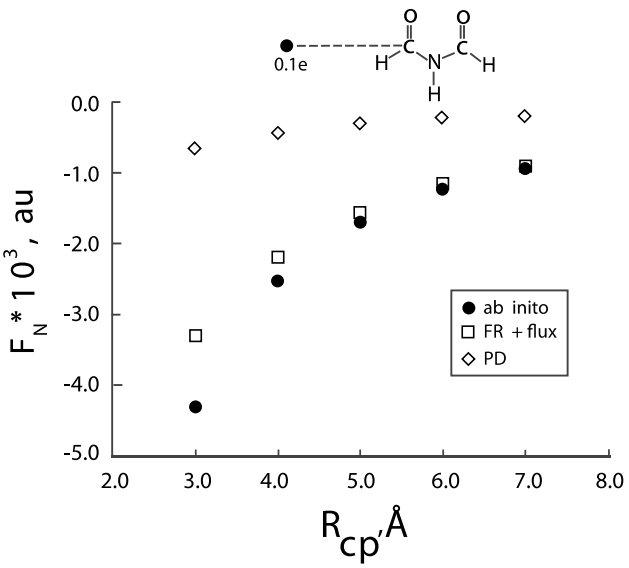

Fig. 4 Effect of charge flux (geometry dependence of atomic charges) on the calculated *forces* on individual atoms in a molecule. Here the force exerted by an external point charge on the nitrogen atom in *N*-formyl formamide as calculated by QM is compared with the classical coulomb force including and excluding charge flux terms. R_{CP} is the distance between the point charge and the carbon atom and F_N is the force on the nitrogen atom. Filled circles are the ab initio forces while squares are the forces calculated by substituting geometry dependent charges (calculated by Eq. 1) into the Coulomb term and diamonds are the forces calculated by using potential derived charges in the Coulomb term [217]. All calculations were done at the same level of theory. The large deviation between the QM forces and those calculated from the potential derived charges demonstrates the major contribution made to the force by charge flux

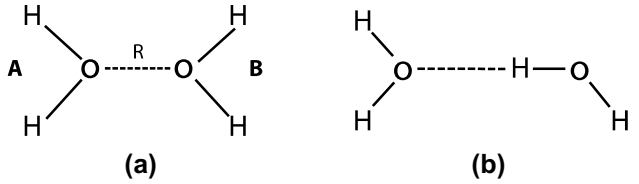

Fig. 5 **a** Head to Head and **b** hydrogen bonded water dimers. Pairwise nonbond energy can be extracted from Hessian elements. The Lennard-Jones O···O repulsion as derived from the second derivative of interaction energies displays a huge anisotropy with the O···O repulsion in the H-bonded dimer being four times as large as in the Head to Head configuration. It was suggested that this could be due to an inherent anisotropy in the atoms electron distribution or to polarization arising from the H-bond interaction (or both)

the water dimers in Fig. 5 as well as the other water, formaldehyde, and formamide complexes given in Table 2 below.

$$\text{i.e.} V_{NB} = A/r^{12} - C/r^{6} + q_i q_j / r.$$

All of the dimers were in the "head to head" configuration except the H-bonded water dimer in Fig. 5b. For each dimer second derivatives were calculated as a function of O···O distance.

One of the most important observations that emerged from these studies was that very different values of the parameters are obtained from fitting the second derivatives of the dimers in different directions, i.e. $\partial^2 E/\partial x^2$, $\partial^2 E/\partial y^2$, and $\partial^2 E/\partial z^2$. This is similar to the behavior observed where very different atomic charges resulted from derivatives of the energy of interaction of a point charge with an atom taken in different directions [215, 217, 227]. *This cannot occur if the assumptions in current FFs hold, if the repulsive parameter, and charges are independent of coordinate (i.e. a constant), fitting the derivatives will result in the same parameter, independent of direction!* The results are clear indications of nonbond and charge flux.

The problem can be overcome in planar molecules, by taking the derivative of the energy in the direction perpendicular to the plane. In this case the flux is zero by symmetry [215, 217]. Thus Dinur and Hager fit the second derivatives perpendicular to the dimer plane for these dimers, as a function of the distance between the dimers [227]. The charge product can be obtained from the limiting behavior at large distances, while the repulsive parameter can be obtained by fitting the Hessian at small O–O distances. As noted, for these purposes the 12-6-1 Lennard-Jones Coulomb law was assumed, and since the QM calculations were carried out at the HF 6-31G* level, dispersion was not accounted for in the QM derivatives, so only the repulsive constants and the charges (as a charge product), were fit [227]. (Of course, the method is independent of basis set or QM method, and more recent high level correlated methods could be invoked.) The results obtained for these constants are given in Table 2 [227].

5.1.6 Anisotropy of nonbond repulsion

Aside from the parameters themselves, the most dramatic result is the difference in the repulsive parameter of the water oxygen, A_{OO} in the head to head and the hydrogen bonded dimers. As seen from the first and last entries in Table 2, the value of the repulsive constant, A, is almost 4 times the value found for the head-to-head orientation! This is a huge anisotropy and could have significant implications for molecular simulations. The authors speculate that the anisotropy could be due to an inherent anisotropy in the atoms' electron distribution or to polarization induced by the hydrogen-bond interaction. The latter might draw electrons into the H-bonded oxygen, thus making it larger and more repulsive, while in the head to head configuration the opposite occurs [227]. It was suggested that further calculations including those of a stacked dimer could shed further light on this effect.

Another interesting observation made in this work can also be observed in Table 2. As can be seen by comparing the repulsive constants, the repulsive parameter for the carbonyl oxygen is larger than the corresponding parameter for the water oxygen, in the head to head orientation. This conflicts with the relative value found in OPLS for example where the opposite trend is observed [20]. Of course two caveats must be noted: first, these calculations were carried out with a relatively small, uncorrelated basis set and more rigorous QM should be carried out to confirm the relative values; and secondly, the experimentally derived values relate primarily to the H-bonded orientation, which will be the dominant configuration in liquids, where, as seen, the

Table 2 Charge (squared) and nonbond repulsion constant (A/r^{12}) for O···O interatomic interactions as obtained from second derivative of ab-initio energy

Dimer	Q^2	A_{O-O}
$H_2O\cdots O_2H$	0.42	**61,552**
$CH_2O\cdots OCH_2$	0.25	128,683
$CH_2O\cdots O_2H$	0.31	85,674
$NH_2CHO\cdots OH_2$	0.33	73,230
$NH_2CHO\cdots OH_2$	0.26	107,584
$H_2O\cdots HOH$	0.42	**220,000**

Note large difference in nonbond parameter (anisotropy) between head to head and hydrogen bonded water configurations (values in bold)

constant is much larger, and where it is possible that the trend is reversed.

Thus, as seen from these examples, fitting of the QM second derivatives allows pairwise interactions to be extracted, and yields information on the physics of these interactions as well as values of the component parameters, uncontaminated by correlation with all other dimer interactions. As stated by the authors [227]:

> The key to exploring the properties of the O-O interaction" (or any other) …" "including partial charges, transferability, anisotropy, etc., is to fit the ab initio second derivatives with an analytical representation of the nonbonding interaction and assess the ability of this analytic representation to describe the energy surface as reflected in (the fit to) those derivatives.

5.2 Nonbond and polarizability flux

Dinur and Hagler went on to exploit QM Hessian elements to explore the role of charge flux and nonbond flux in hydrogen bonding, again investigating water–water, water–formaldehyde, and water–formamide dimers [155]. The nonbond flux reflects the fact that concomitant with the redistribution of charge around atoms with change in molecular geometry, there are also changes in van der Waals properties and polarizability determined by this modified electron density [155]. For example by examining QM energy second derivatives it was found that *charge flux* introduced a (nonbond) repulsion between the donor hydrogen and acceptor oxygen not present in the rigid dimer interaction [155].

Basically, the attraction of the hydrogen bonded hydrogen to the acceptor stretches the donor's H–O bond. The stretch of the O–H bond is accompanied by a charge flux from the oxygen to the hydrogen such that the hydrogen partially regains electrons. As the hydrogen's electronic charge increases (its positive charge decreases), the exchange repulsion with the acceptor oxygen increases as well. Thus, the repulsive parameter, like the atomic charge, is geometry dependent or stated equivalently we observe a *nonbond flux*. The repulsive potential in this case may be expressed by the form [155]:

$$E_{Rep} = \left[A^0_{OH} + F_{OH}(r_{OH} - r_0)\right]/R^n_{OH} \quad (8)$$

where A^0_{OH} is the repulsive constant at the reference geometry, and F_{OH} is the nonbond flux constant for distortions along the O–H bond, (analogous to the charge flux constants, J, in Eq. 1), and r_{OH} and r_o are the internal OH bond length in the monomer and its equilibrium value, respectively. More generally, as with charge flux, we might expect the nonbond potential to depend on valence angles and torsions as well. In the case of the water dimer it was suggested that the contribution to the energy might be small, due to small change in bond length caused by H-bonding, but the contribution to the force (first derivative of energy) can be significant [155].

Wallqvist also investigated the effects of accounting for fluxes in water potentials [145]. He compared a number of models, including rigid geometry, harmonic and anharmonic fixed charge models as well as potentials incorporating geometry dependent atomic charge, polarizability, and dispersion in simulations of liquid water [145]. Profound effects on the liquid properties were noted on introduction of charge flux. *For example, introduction of charge flux reduces the increase in the gas phase water dipole moment by polarization on going to the liquid by 66%, compared to that predicted using constant charges*. This significantly affects the structural properties resulting in a loss in the tetrahedral structure of the liquid, and a concomitant reduction in the cohesive energy. This is compensated to some extent by the introduction of geometry dependent polarizabilities and dispersion coefficients, which improve the predicted properties.

In another study that further demonstrated the importance of charge flux, Palmo et al. [195] explored its effects on the physical properties of water, and peptides. In agreement with previous studies [155, 226, 228], it was shown that charge flux contributes both to the geometry of the water molecule in different phases, and, more importantly to the properties of the liquid. They also examined the role of charge flux as a function of the important ϕ,ψ potential in peptides. Analysis of atomic CHELPG charges [229] in a set of model amides recapitulated the now well accepted conformational dependence of the charges [195] Further, more rigorous QM calculations of the ϕ,ψ torsion potentials crucially corroborated the conclusions of Hagler et al. [230] from crystal lattice energy and QM studies, discussed in the previous paper [1], that the intrinsic barrier about ψ is roughly zero, and that about φ is a few tenths of a kcal. These conclusions were then tested and confirmed by assessing the ability of the SDFF including these effects to reproduce critical behaviors of the ϕ,ψ QM trajectory (BP/DZVP) of an alanine dipeptide analog [231] not observed in corresponding trajectories from the standard fixed charge FFs [195, 231].

Given these results, and those of others in the literature, it is clear that if we seek an analytical expression to reproduce inter and intramolecular forces (a FF) and reliably predict structure, energetics and dynamics of biomolecular systems, effects such as charge, nonbond and polarizability flux, anisotropy of electron distributions and resultant nonbond and electrostatic anisotropy, need to be represented in FFs.

5.3 SDFF: the most complete formulation of a FF to date, in terms of capturing the physics of inter and intramolecular interactions

There are two noteworthy aspects of the SDFF formalism developed beginning in the early 1990s by Krimm and coworkers [46, 205, 232]. The first is the functional form which captures more of the physics than any of the standard FFs employed to date, and the second is the protocol invoked to derive the FFs.

Krimm et al. introduce a novel transformation to directly produce quadratic force constants *and reference values*, including force constants for all possible quadratic coupling terms. The method is a derivative of the standard spectroscopic FF method where the potential energy is expanded to second order around an assumed equilibrium geometry [68, 233]. The key step is subtracting the second derivatives of an initial, nonbond energy, from the corresponding elements of the QM derived Hessian matrix [46, 233, 234]. (In this step the cosine representation of the torsion potential is approximated by a quadratic). Transforming the resultant matrix to internal coordinates, yields a complete quadratic valence FF including force constants for all quadratic coupling terms [46, 234]. This procedure also yields the corresponding reference vales (b_0 and θ_0), most often derived by manual fitting, by solving a simple set of linear equations. An attractive property of this procedure is that when the complete Hessian is then calculated from the resulting quadratic FF, augmented by the original nonbond potential, the same structure and vibrational frequencies as obtained from the original ab initio calculation are returned [46, 234].

This procedure was first carried out for stationary state configurations of a training set of *n*-alkanes [46]. The 6–9 LJ potential parameters of Ermer and Lifson were chosen as the initial guess [181]. Since the true energy surface is anharmonic, i.e. contains higher order terms, the force constants for the different alkane compounds and configurations differ. However, the results provide a good starting point for further optimization. Simple inspection of the magnitude of the coupling force constants obtained in this preliminary step gives an immediate indication of those that are essential to reproducing the molecular energy surface and those that are inconsequential and can be omitted from the final functional form. Furthermore the conformational dependence of the force constants gives insight into the higher order coupling present in the potential energy surface [46]. Thus for example it was found that the interaction between a bond and an angle, where the bond shares one of the angle's end atoms but not the apex atom, is modulated by the torsion angle containing them [46], described by $K_{bq} = K^0_{bq} \cos f$.

At this stage the nonbond parameters were optimized to fit crystal structure and sublimation energies of ethane and pentane using the CFF procedure [15, 235], with a common set of valence parameters for all conformers. Finally, cross terms that are negligible are removed and the valence constants are reoptimized to achieve an overall best fit to the structures, vibrational frequencies and energies of all compounds.

The methodology was extended to calculation of the structures, relative energies, and vibrational frequencies of a large set of branched saturated hydrocarbons [232]. Training of the FF was done against QM properties of 14 stable conformers of *n*-pentane and *n*-hexane, and 7 stable conformers of isopentane, 3-methylpentane, and neopentane, as well as additional calculations on 2,2-dimethylbutane, 2,2,4,4-tetramethylpentane, 2,3,3,4-tetramethylpentane, 2,2,3,4,4-pentamethylpentane, 2,2,3,3-tetramethyl-hexane, and 2,2,3,4-tetramethylhexane [232]. The FF was further assessed by addressing a challenging set of test compounds including cyclobutane, cyclohexane, isobutane, tri-*tert*-butylmethane (TTBM), and tetra-*tert*-butylmethane. Excellent agreement with experiment and QM and the need for different coupling terms was demonstrated. Vibrational frequencies are calculated to within an RMSD of ~ 6 cm^{-1} for most of the compounds, which is an order of magnitude more accurate than obtained with current FFs. The authors point out larger discrepancies in TTBM, which they speculate may arise from errors in the nonbond interactions in this crowded molecule, thus providing a system to test improved representations of exchange repulsion.

5.3.1 Multipoles, polarizability and charge flux in SDFF

Over the years the SDFF protocol evolved with significant elaboration of the physical description of the molecular energetics [195, 205, 236]. It was determined that for polar molecules, in addition to fixed partial charges, atomic dipoles, charge (and dipole) flux as well as polarizability were required to accurately describe the electrostatics [195, 237]. As with other FFs the order of parametrization is important. The electrostatic parameters, were determined first. The electrostatics are described through atomic charges (in terms of bond increments following Ewig et al. [91] Eq. 2), atomic dipoles, polarizability, and charge flux [205, 238]. Polarizability is accounted for as a combination of induced bond increments [238, 239] (equivalent to induced atomic charges) and induced atomic dipoles. The charges, multipoles and polarizability parameters are all determined by fitting to ab initio electrostatic potentials, generated with external electric fields covering a suitable range of magnitudes and directions [205, 238].

Though multipoles and polarizability are familiar concepts and have been incorporated into a variety of force fields [49, 50, 59, 240, 241], the same cannot be said of geometry dependent charges, and other flux terms [66, 155, 215]. Krimm et al. incorporated charge and dipole flux in the SDFF [205, 236] by adopting the Dinur-Hagler formalism [217]. The latter, as discussed above, found that the atomic charge, to a good approximation, varies linearly with the bond lengths, bond angles, and cosine of the torsion angles containing the atom of interest [217]. Dipole derivatives involving deformation of internals further removed from the atom of interest indicated that their effect on flux was negligible and could be ignored [217].

Following the determination of the electrostatic parameters from the ESPs, van der Waals parameters were derived. In the later development of the SDFF protocol, rather than determining the nonbond parameters from crystal data, they were obtained from a fit of QM potential energies as well as intermolecular gradients of a "multitude of different intermolecular configurations and intermonomer distances" of dimers of model compounds [205].

At this point the transformation of the modified QM Hessian described above was used to compute the valence parameters, other than torsions. Simultaneously with this the van der Waals parameters are fine-tuned as well, as part of a least squares optimization to achieve an overall best fit to the structures, vibrational frequencies and energies of all compounds [205].

Unfortunately this protocol was not extended to additional families, though it was applied to the water dimer [236]. In addition to the inclusion of charge flux and polarizability to account for the QM properties of hydrogen-bonded water, an additional interaction, an "overlap charge flux", associated with the O–H···LP–O interaction was suggested, where LP is the oxygen lone pair. In addition, further explorations into effects such as polarizability flux [145, 155, 242] and charge transfer in hydrogen-bonded systems [243–245] were carried out by this group [195, 246].

5.4 AMOEBA

The development of the Amoeba FF by Ponder, Ren and coworkers began in the early 2000's with the development of a FF for water [47, 247]. AMOEBA, an acronym for "atomic multipole optimized energetics for biomolecular applications" was motivated by the need to include a better representation of the electrostatics, through atomic multipoles and polarization [247–249]. The inclusion of these terms constitutes an important advance in the derivation of Force Fields to accurately simulate the properties of biomolecular systems. As discussed above and in the previous paper [1], the significance of both polarizability and atomic multipoles has long been known and in fact accounted for in many applications [66, 216] going back to the water potential described by Rowlinson in 1951 [250], the elegant work of Leiserowitz and Berkovitz-Yellin on crystal energies of amides and carboxylic acid in the early 1980s [87, 88, 251], the pioneering work of Stone and Price [252–254], and many others [53, 238, 255–257], but for the most part more realistic representations of electron density have been absent from the "standard" biomolecular FFs. As reported above, over the last 10 years, inclusion of polarizability in standard FFs has been attempted, unfortunately with little significant improvement in results. The choice of including polarization and not permanent atomic multipoles, is, on the surface, puzzling as the former is a third order effect compared to interaction of charge—(permanent) dipole, and second order with respect to charge—quadrupole interaction (e.g. charge—induced dipole interactions go as $1/r^4$ while the charge—permanent dipole interaction goes as $1/r^2$ and charge—quadrupole as $1/r^3$). Of course, the effects depend on the constants but along with the distance dependence the contribution of the atomic multipoles has been well documented (citations above), while the jury is still out on the magnitude of the contribution of polarizability except in ionic interactions with highly polarizable moieties. Having said this, it is clearly optimal to include both effects as done in AMOEBA.

The development of AMOEBA continued culminating in 2010–2011 with a FF covering an array of organic compounds including functional groups found in proteins [142, 191]. In this implementation the functional form and corresponding parameters used for valence terms, i.e. bond stretching, angle bending etc. were taken from MM3 [26], though the torsion–stretch and bend–bend interactions were not included. Allinger noted that the former term was required to account for bond stretching "when bonds are other than perfectly staggered". These effects might be significant in strain energy calculations as well as in generating the torsion potential. Of course, the omission of these interactions would also impact all the widely used standard diagonal quadratic FFs discussed here. An additional concern is that omission of these terms would result in different values of the parameters in MM3, resulting from the parameter refinement.

Thus, one can't assume that transferring a subset of the valence terms yields the same quality of fit to experiment as the complete MM3 FF. This was ameliorated in the later protein FF refinement [148] by modifying the parameters slightly to improve fit to MP2/6-31G* geometries and protein PDB structures. In addition, in a recent derivation of parameters for the phosphate group, bond–torsion and angle–torsion coupling were introduced to account for structural changes due to the anomeric effect [258].

The simple harmonic form was used to account for the out-of-plane deformation, with the Wilson Decius and Cross

definition invoked to describe the out-of-plane coordinate [28, 68] (Fig. 10 previous paper [1]). The functional form of the van der Waals contributions was taken as the buffered 14-7 potential proposed by Halgren [190], including the concomitant combination rules.

The major difference between AMOEBA and preceding force fields, and its major contribution is its treatment of electrostatics. Fixed partial charges were replaced by more realistic polarizable multipoles [87, 88, 238, 251–254] for the first time in a general protein FF.

5.4.1 AMOEBA parametrization

The methodology for parametrization of the AMOEBA FF involves a number of steps [142]. The atomic polarizabilities were taken from Tholes compilation [259] with the exception of aromatic carbon and hydrogens which were obtained by fitting molecular polarizabilies of benzene, napthalene, anthracene, and a carbon nanotube. Atomic multipoles are derived by carrying out distributed multipole analysis (DMA) [252] on small compounds (fewer than six heavy atoms). The effects of polarization are then extracted yielding "permanent atomic multipoles". (These then, when polarized return the atomic multipoles from the DMA). The atomic multipoles derived in this way are then further refined, with the charges (monopoles) kept constant, by optimizing them against the electrostatic potential on a grid in a 2 Å shell starting from 1 Å beyond the vdW surface. They are kept from straying far from the DMA values by carrying out only a partial optimization. Further adjustment was found necessary in some cases, for example to account for the proper geometry of the dimer structure of ammonia, the quadrupoles had to be scaled by 0.6, which was similar to what was found in the case of water [142].

Van der Waals parameters were obtained by fitting to ab initio (MP2 aug cc pVTZ) energies and geometries of six homo-dimers as well as the density and heats of vaporization of 37 neat liquids. The energies and geometries of the homodimers of methane, ethanol, propanol, hydrogen sulfide, methylamine, and formamide were exploited for optimization. There are 36 van der Waals parameters, so this yielded an observable to parameter ratio of a little over 2:1.

Finally, the parameters for the valence terms, are further optimized against geometries and frequencies calculated from high level ab inito data. Only after all these parameters are determined are the torsion parameters optimized, by fitting to high level ab initio conformational energy scans (it is here that coupling terms may play a key role).

Though the observable to parameter ratio in the optimization of vdW parameters is small a large variety of properties were then used to validate the parameters. The energies and geometries of mixed dimers as well as the dielectric constant and self-diffusion coefficients of twelve of the neat liquids, solvation free energies in water, and structures of five crystals were used in validation of the parameters. Overall good agreement with the experimental and ab-initio data was achieved [142]. For example, the rmsd of calculated dimer energies to the MP2/aug-cc-pVTZ values was 0.38 kcal/mol, with a maximum error in the methylamine water dimer energy (7.45 kcal/mol) of ~ 12% or 1 kcal/mol indicating some deficiencies in the representation of this system. Likewise, the heats of vaporization and liquid densities were fit well, with an rmsd of only 0.23 kcal/mol for the former for 37 liquids. The largest deviation obtained here was 0.9 kcal for the heat of vaporization of acetamide (13.3 kcal/mol) at 494 K. The authors comment that the improvement obtained over fixed atomic centered charge models in these properties is small, though they found, as did others [160] that accounting for polarizability is important for reproducing the dielectric and diffusive properties of liquids [142]. Several crystal structures were also minimized and the results compared with experimental structures. RMS deviations in coordinates of ~ 0.3 Å were seen, and deviations in cell constants were small as well. Unfortunately, sublimation energies were not reported, nor were the detailed structures. It would be interesting for example to see if the inclusion of atomic multipoles and polarizability reduced the opening of the H–O=C angle (from the observed 125° to ~ 140°) found with the fixed charge model [124] and as seen in Fig. 4 in the previous paper [1].

The results for hydration free energies were also good, though these were not accounted for quite as well as heats of vaporization. Thus, the rmsd in hydration free energies of 27 compounds calculated with AMOEBA was 0.69 kcal/mol. The largest deviation was 1.6 kcal/mol in the case of phenol (exptl. hydration free energy = 6.62 kcal/mol), with another four deviations greater than 1 kcal/mol. As the authors note, this points to remaining deficiencies in the model [142], and they suggest possible sources as the level of basis sets used in the parametrization, the 14-7 vdW potential, and the effect of combining rules on van der Waals interactions in different environments. In addition they cite charge flux [66, 205, 215, 217] (or coupling between the molecular charge distribution and molecular geometry) as an important omission in the force field. As discussed above, omission of flux is very likely to manifest itself in such interactions, especially in hydrogen bonded systems.

5.4.2 Valuable information in discrepancies

Further extensive validation was presented in a previous paper [191]. Notably, the solvation energies of an additional 30 drug-like and other small organic compounds from the 2009 SAMPL competition [260] were addressed [191]. The authors point out that AMOEBA did well for very soluble molecules such as sugars where fixed point charge FFs fail.

However, as they further note, the results also reveal large discrepancies with many being of the order of 20% or more and several of ~4 kcal/mol (e.g. the experimental hydration free energy of 4-nitroaniline is −9.45 kcal/mol while AMOEBA gives a value of −5.34 kcal/mol). These results also indicate that though improved, there are still major deficiencies in our representation of energy surfaces even when polarizability and atomic multipoles are accounted for (or perhaps problems with parametrization). As noted elsewhere in this Perspective, identification of systems which yield large deviations, such as those reported in these papers [142, 191] and others, are extremely valuable, much more so in our opinion, than the reported agreement, as they provide the foundation for testing further improvements in the process of FF advancement (while retaining the fit to "nonproblematic" observables). Also, as noted, the ideal situation would be if developers of FFs addressed these systems which present major deviations reported in the communities' work in a systematic way, much as Allinger did in his iterative development of the MMn series of FFs, but unfortunately this is no longer a standard practice.

5.4.3 The Ala tetrapeptide benchmark

Another noteworthy validation carried out was the assessment of the fit to the alanine tetrapeptide benchmark, the compilation of gas-phase conformational energies from high level quantum calculations of 27 conformers of $(Ala)_4$, introduced by Beachy et al. [109]. It had earlier been shown that basis set size could significantly affect the relative energies of the conformers in this benchmark—especially folded vs extended conformations, and a rigorous re-evaluation of the energetics was done with more complete basis sets [177, 199]. These Ala tetrapeptide energies, along with some additional calculations were used to evaluate the AMOEBA FF. Reasonable agreement was achieved though significant discrepancies remain. Thus, for these relative energies which range up to 7.9 kcal/mol, several conformers exhibit deviations of 1–2 kcal/mol. It is difficult to compare this result to the previously reported results using fixed charge monopole FFs, against this benchmark [36, 109, 261], though it would be interesting and important, since as noted the relative energies are significantly different. A more recent comparison of the energetics of these tetrapeptides was carried out in a study to improve the peptide torsional potentials in OPLS-AA [178]. The results indicated that the fit with this fixed charge FF was comparable to the fit of the Ala tetrapeptide conformational energetics with AMOEBA, though it didn't do as well in the prediction of stationary states [178]. These results are somewhat puzzling as one might expect/hope that the inclusion of multipoles and polarizability would significantly improve the ability to account for these conformational energies. We might postulate that there are significant contributions from valence strain to the conformational energy differences which might indicate that focus is needed on improving the representation of these deformations if "chemical accuracy" is to be achieved.

Several additional applications were carried out, including comparison of QM and AMOEBA energies for water–sulfate clusters, protein stability, and binding of ligands to Trypsin. The results for these studies parallel for the most part the comparisons described above. AMOEBA performs well on these systems, for example reproducing the ordering of energies of eight low energy water-sulfate clusters. On the other hand, as above, significant deviations remain (e.g., the relative energy of cluster "8" is calculated to be 2.27 kcal/mol with the FF, compared to the QM value of 3.62 kcal/mol [191]). In addition, short, 2–20 ns MD simulations of six small proteins ranging from 20 to 72 amino acids were carried out. The RMSD of the α-carbons from the experimental structures resulting from these simulations, were between 1.2 and 1.8 Å for six of the seven proteins simulated. As noted above these are extremely short simulations and based on the work of Debiec [58] and Huang [65] almost surely not converged. The relatively large RMSDs for α-carbons over these relatively short trajectories confirm the observations drawn from the properties discussed above, that even with the improved description of electrostatics, significant deficiencies in the FF representation remain.

5.4.4 Several studies point to the contribution of polarizability in ionic protein ligand interactions

Calculations carried out on ligand binding to Trypsin clarify systems in which polarizability may play a more important role than those noted above [191, 262]. For example, the binding free energies of six benzamidine-like ligands calculated with the AMOEBA FF were in good agreement with the experimental values (RMSD 0.4 kcal/mol). Analysis of the water–benzamidine interaction energy reveals that 10% of the hydration free energy is due to polarization (4.5 kcal/mol out of the total hydration energy of 45.8 kcal/mol). Furthermore it was found that the binding affinity though primarily determined by electrostatics was correlated to the molecular polarizabilities of the ligands rather than their dipole moments [191, 262]. In a study of the complexes of five pyrrolopyrimidine inhibitors with FAK kinase with SIBFA [255, 256, 263], de Courcy et al. [264] also found that inclusion of polarizability was critical to accounting for the correct ordering of the binding affinities of the congeneric series. Similar conclusions were reached by Zhang et al. [265] in a study of ligand binding to zinc containing matrix metalloproteinases. Here the inclusion of polarizability was found to be not only necessary to achieve the correct order of ligand binding affinities, but also to achieve

the correct coordination geometry about the zinc ion [265]. Studies of the energetics of binding of ions with 30 protein ion binding sites with QM and a Drude polarizable FF by Li et al. [180] demonstrated significant cooperativity in interaction energies. These are absent in an additive FF and thus accurate ion binding energies across a range of binding environments could only be achieved with the inclusion of polarizability [180].

5.4.5 Reparametrization of the AMOEBA protein FF

In 2013 a completely new AMOEBA protein FF was developed [148]. Van der Waals and valence interactions were transferred from the work described above [142, 191] modified to fit ab initio geometries and protein structures [148]. Electrostatics were derived analogous to the methodology described above (DMA multipoles optimized to fit MP2/aug-cc-pVTZ electrostatic potentials), though in this case these were obtained from calculations on several conformers of each of the blocked dipeptides (Ac-X-NMe). Torsion parameters were then obtained by fitting to QM energies (RI-TRIM MP2/CBS) of the Ala dipeptide. The difference between calculated and QM energies was attributed to the torsion potential and torsion constants were obtained by minimizing this deviation. These parameters were then refined by adjusting them to align a calculated potential of mean force (PMF) of $(Ala)_3$ in water with a statistically derived PMF from the PDB. For Gly a torsion–torsion spline term (CMAP grid) was needed in addition to the Fourier torsional terms for ϕ and ψ.

As the authors point out and noted above, the torsion term derived in this way is essentially an error function in classical force fields. Furthermore these "CMAP terms" [73] i.e. grid-based energy corrections to the ϕ–ψ 2D energy surface, analogous to the spline torsion–torsion coupling, *may also exacerbate unphysical features in the rest of the force field and therefore are not transferable* [148]. This is an important issue to overcome in deriving "physics-based" transferable FFs achieving accuracies approaching the sought for 0.5 kcal/mol [140].

The fit achieved to both the training set and properties used to test the FF were similar to those obtained by the previous AMOEBA FF [142, 191]. For example, though the calculated Ala tetrapeptide energies changed significantly from the 2010 values [191], they are still in reasonable agreement (RMSD of 1.15 kcal/mol), though as before there are some meaningful, probative discrepancies of 2–3 kcal/mol. Given the differences in tetrapeptide energies, and the authors' finding in the previous studies that further improvement was needed to account for solvation free energies of small molecules, it would have been nice to compare the hydration energies of the extensive sample described previously with those calculated with the new FF. Among other properties the structures of 10 proteins over the course of 10 ns of MD were compared to the experimental pdb structures. An overall RMSD of 1.33 Å was obtained, though as with other properties some pathological cases were observed with RMSDs of 2–3 Å. It was pointed out that this is often due to fraying at the termini, and may be a consequence of carrying out the MD in solution. (The uncertainty as to whether deviations are due to comparing solution to crystal structures could be obviated by simulating the protein crystal directly [266–268]). Again, the large RMSDs arising even from non-converged short trajectories, confirm remaining deficiencies in the FF, such as representation of flux, anisotropy and other aspects of the physics discussed above. In general, the FF provides a good fit to QM and experimental data, though not dramatically better than the standard fixed monopole FFs. It was concluded that, as we have emphasized throughout this Perspective, understanding the limitations of the FF, i.e., analyzing the interactions underlying well characterized, large structural and energetic deviations, are key to further FF improvements.

5.4.6 A puzzling outcome

As noted in the above discussion, for the most part the comparisons to experiment and QM observables indicate that the AMOEBA FF, though comparable to the best fixed charge FF is not demonstrably superior to these FFs. This is also borne out by recent studies on interactions of nucleic acid bases and small molecules [269] and on the binding free energies of host guest systems [270, 271]. In the nucleic acid study gas phase binding energies of 160 complexes calculated with CHARMM, AMBER, and AMOEBA are compared with B3LYP/6-311++g** energies. The three FFs perform similarly, though the quality of the basis set may compromise the significance of the results to some extent. The results of the SAMPL4 host–guest blind prediction challenge [270] are more unequivocal. The challenge revealed the need for continued improvement in FFs and methods with many of the predictions coming in worse than two "null" models (one with 0 kcal/mol for all guests and the other assigning 1.5 kcal/mol per heavy atom). In particular AMOEBA was employed to predict the binding free energies of 14 "guests" to the cucurbit[7]uril macrocycle [271]. The rmsd in predicted relative binding free energies of 2.2 kcal/mol was outperformed by a method based on the GAFF-AMBER potential with an rmsd of 1.9 kcal/mol [270].

The equivalence of the quality of the AMOEBA FF with these fixed monopole FFs is unexpected and puzzling. It is indisputable that the multipole representation is a better representation of the atomic charge distribution than an atom centered point charge [251, 272, 273]. Furthermore, there is no question that atoms are polarized in an electric field. Thus, it is hard to understand how including these effects would not lead to significant improvement in accounting

for molecular energetics. This begs for analysis. Several hypotheses occur to us. The use of a 14-7 van der Waals potential, as described above, at least in the case of the MMFF94 implementation [274] was reported to yield deviations of 30–40% in crystal lattice energies [275]. Although the van der Waals parameters have been reparametrized in AMOEBA, the use of a 14-7 potential as opposed to the usual 12-6 or 9-6 LJ potentials constitutes a significant difference. It may be that the 14-7 optimized to fit intermolecular interactions cannot simultaneously account for the intramolecular nonbonded interactions (which would be a problem shared with the 12-6-and 9-6-1 representations) [86]. Another possible explanation may lie in the derivation of torsion angles from the dipeptide ϕ, ψ energy map. Many strained conformations are represented in the Ramachandran map, and coupling terms, such as angle-torsion, and angle–angle torsion, which describe the dependence of the torsion barrier on bond angle may play a significant role in the energetics of the dipeptide [23, 182, 276]. Finally, as noted above, the omission of charge flux and nonbond anisotropy may also play a significant role. The absence of these terms will then be absorbed into the derived torsion terms distorting this potential leading to deviations that may well be common to both the AMOEBA and fixed point charge FFs. The absence of these terms also indubitably affects the energetics of the tetra-Ala QM energy benchmark calculations.

In our view the most likely culprits are the absence of torsion- angle coupling and/or charge flux. But, whatever the underlying cause it begs diagnosis. The representation of the electrostatic distribution by multipoles, and, perhaps to a lesser extent, polarizability, as implemented in AMOEBA, is clearly an important advance on the path to achieving quantitative accuracy in simulations. Hopefully understanding these results, and the source of discrepancies from experiment will help achieve that goal.

5.5 Optimization protocols—factors in the methodology that will affect the quality of the FF

Finally, as we have seen from the discussion of the various FFs both above and in the previous paper [1], the methodology used in their derivation varies greatly. It is worth noting some of the factors in the methodology that will affect the quality of the FF, and need to be considered carefully in their development (and application). These include:

- *The size and diversity of the data set used in derivation and testing* This should, in general, contain a large number of compounds per family (rule of thumb 10–20), and a variety of properties of these compounds such as gas phase structures, rotational barriers, conformational energies, vibrational spectra, crystal structure and sublimation energies, and liquid properties, such as density and ΔH_{vap}. Where possible experimental data should prevail, but high level QM is also required, especially for families where the former is sparse.
- *QM data in FF derivation* This is limited by the quality of the wave function. This is especially true with regard to the dispersion interaction, which is poorly modelled and is critical.
- *The mathematical method used in the derivation* Is a least squares or other optimization algorithm used, or are parameters derived manually. Are parameters optimized simultaneously for all terms or sequentially. (If the latter the last parameters optimized may be affected significantly by errors in others and become an "error function"). It would also be desirable to include statistical analysis such as standard deviations and correlation coefficients of parameters.
- *Focus on outliers vs averages* Assessment of the validity of FFs is carried out by comparing results with experiment or QM calculations. Though RMSD or other averages are important it is critical to look at, in fact focus on, outliers. Unless the experimental value is flawed or QM is carried out with an inadequate basis set, these outliers definitively demonstrate defects in the FF, often in the functional form. There is no guarantee that these defects won't affect applications on systems outside the training set.
- *Difficulty in comparison of FFs* Comparison of the accuracy of FFs is made extremely difficult, in that they are derived and tested against different datasets. This is even true of many versions of the same FF. A benchmark of data having the characteristics in the first bullet point would be a great benefit to the field. Until then, at least with successive versions of the same FF, it would be extremely beneficial to build a consistent benchmark by carrying forward all properties fit in previous versions of the FF.
- *Transferability assumptions* Assumptions that parameters are transferable to other similar atoms having similar or different connectivities may obviously affect the validity of a FF. This is also true of the assumption of combining rules to be invoked as discussed above (and more extensively in previous paper [1]).
- *Use of the same nonbond potentials' for intra and intermolecular interactions* The use of the same potentials for intra and intermolecular interactions has recently been questioned by Uzoh et al. [277] who fit separate exp-6 parameters for intramolecular interactions. They showed that this allowed them to account for both conformation and packing in crystal structure prediction. This was motivated in part by the fact that even when tailor-made molecule specific standard FFs are used one

can't account for both molecular structure and packing [97] This may well be due to the omission of the contributions discussed above, especially charge penetration, flux effects and valence coupling terms, notably angle-torsion coupling. Whatever the reason the conclusions being drawn by the crystal packing prediction community should be an alert for the biomolecular simulation field.

6 Summary and conclusions: reconciling the physics based force fields with the underlying physics

It is now some 55 years since the first molecular mechanics calculation carried out on a computer was published [4]. Advances over the intervening years in computational power and QM algorithms have been exponential and have allowed for computations inconceivable in those early days. Thus while the original calculations on small hydrocarbon rings was a tour de force at the time, today microsecond simulations of aqueous protein systems containing tens of thousands of atoms are commonplace [150, 278]. Where 50 years ago state of the art QM calculations were limited to semi-empirical methods, today rigorous large basis set post Hartree–Fock calculations are commonplace. Although these developments reflect the amazing progress that has been made in our ability to calculate the properties of complex molecular systems, to a large extent biomolecular force field technology has been left behind.

The advances in QM basis sets and methodology, allow us to envisage an approach to experimental accuracy and even "exact" solutions, while the development in force field simulations has focused on treating ever larger, relevant biological systems, over timescales that capture biologically meaningful events. Though of clear importance, by and large this has been accomplished at the expense of a devoted effort to improve the representation of inter and intramolecular interactions (the FF). Thus, while there has been a relatively concerted progression in the basis sets and methods in ab initio methods, the advances in classical FF rigor have lagged and diverged in approach. As done 50 years ago, current FFs continue to employ the discredited Lorentz–Berthelot combination rules and inaccurate improper torsions for out of plane deformations. In addition, for the most part valence-coupling, though accounted for in early FFs, has been omitted in most current biomolecular FFs. More advanced physics, such as more accurate representations of the electron density, flux terms, nonbond anisotropy, and charge transfer all remain unaccounted for. In fact, the most common current FFs remain identical in form to those of the earliest Hendrickson, Lifson, Allinger FFs of the 1960s and 1970s.

As we have discussed the reasons for this are most likely the focus on treating larger and larger systems. In the early years, systems treated were composed of several 10 s of atoms and energy minimization was carried out. Today, MD simulations of hundreds of thousands of atoms are typical. Thus, as described above, in the first several decades following Hendrickson's paper some groups focused their FF research into optimization of force constants in the simple Hooke's law—partial charge—Lennard-Jones approximation, and ability of this representation to account for larger and larger systems of biological relevance. Others, however, have sought to investigate the physics of inter and intramolecular forces, and improve the representation of this physics to achieve more accurate FFs.

6.1 Quadratic diagonal FFs

Among the former the Karplus (CHARMM), Kollman (AMBER) and Jorgensen (OPLS) groups abandoned the united atom approximation and carried out extensive optimization and assessment of the all-atom quadratic diagonal representation. This was achieved by fitting a variety of experimental data, supplemented by QM calculations. This research was presented in a series of papers described above, and culminated in the publications of the CHARMM22 FF [22], the PARAM99 FF [34] and the OPLS-AA/L FF [36] by the Karplus, Kollman and Jorgensen labs respectively. The Karplus group, in one of the most thorough and extensive studies adopted the Lifson philosophy of fitting a wide range of experimental (and ab initio) properties for a large set of compounds [22]. As noted above, this study, as the others, provide an important and powerful characterization of the limitations of this representation of the physics. In this sense, perhaps most important in these seminal studies were the several systems highlighted which were problematic and had unacceptably large deviations, such as the documented 3–6 kcal/mol deviations in select peptide conformational energies and significant deviations in peptide crystal structure characterized by MacKerell et al. [22]. Similar results were returned by OPLS and AMBER. Thus, as also concluded by Kaminski et al. [36] and others, the quadratic diagonal 12-6-1 representation of the physics, though capturing many of the physical characteristics of these systems, and providing a means to generate hypotheses and models to be tested, falls well short of capturing enough of the physics to yield quantitative accuracy.

6.2 Early attempts to better account for the physics: CFF and MM2/3

Some of the first studies in the field took the second approach, seeking to simultaneously optimize the FF and improve the representation of the underlying physics. Lifson early on articulated the consistent force field theory suggesting that a FF must simultaneously fit a wide range of

properties including energy, structure and vibrational frequencies, in both gas and condensed phase to ensure transferability [7, 8]. He started out with a Urey–Bradley representation of the physics, and soon after he and Warshel recognized the need to account for the physical coupling between the energetics of torsion about a bond and the constituent valence angles on either side of the bond [23]. He and Ermer [181] then further improved the representation of the molecular physics by including a larger set of cross terms to more completely represent known valence coupling energetics. Finally together with Hagler the physics underlying the hydrogen bond were investigated and it was found that the representations used at the time, implying covalent character, such as Lippincott–Schroeder [279, 280] etc. and even the 10–12 potential [281] which persisted for some time [18, 31], were not justified by the experimental data. Rather they found that a representation of the physics underlying the H-bond simply by the usual nonbond and electrostatic interactions while taking into account the withdrawal of electrons from the polar hydrogen by reducing its van der Waals repulsion to essentially zero, reproduced existing experimental observables as well or better than the explicit representations.

Allinger in his classic series of studies also took a systematic approach to optimization of the force constants and the representation of the physics. He carried out a thorough optimization of force constants for a given physics based representation, applied to a large set of compounds, with thorough studies carried out for numerous families of organic compounds. He gathered the inadequacies in fit found in his lab and others over the years, for each family, and used them to ferret out the flaws in the physics underlying these deviations. He then corrected these deficiencies by improving the physical representation, and repeated the process. This manifested itself in the MM2 [16], MM3 [26] and MM4 [108] force fields first published in 1977, 1989, and 1996 respectively. Examples of the improved physics in these iterations include, but are not limited to: the inclusion of 1 and twofold rotational barriers to better account for energetics in MM2; coupling between internals was accounted for through torsion-stretch and angle–angle energy terms, and bond dipoles were included to account for electrostatics in nonpolar hydrocarbons in MM3; additional coupling terms, as well as anharmonic coupling, an improper torsion angle, and a modified H-bond potential was introduced in MM4.

Somewhat later an elaborated approach to Lifson's CFF was undertaken by Hagler et al. in their effort to expand and improve the representation of the physics underlying the consistent force field [28, 282]. In their approach a method was developed to exploit QM energy surfaces (Quantum Derivative Fitting), to probe the underlying physics while optimizing the corresponding force constants [66]. Application of this method resulted in elucidation of deficiencies in the use of the standard improper torsion angle to describe the energetics of out-of-plane deformations, and the introduction of the more natural coordinate, the distance of the apex atom from the plane formed by the three atoms to which it's bonded (pyramid height), and the inclusion of a more comprehensive set of coupling terms including higher order coupling. In a separate study a more rigorous set of combination rules for nonbonded interactions was derived by graphical analysis of rare gas interactions [29] and further validated by simulation of crystal properties [91].

6.2.1 Second wave of development, an increasing divergence in approaches—the 2000's

This first wave of FF development culminated in 2000 plus or minus a few years. This also corresponded, loosely, with a new generation of investigators taking over the research and development of force fields, and the representation of the molecular physics they imply. If anything, the dichotomy in approach widened in the following years. The first approach involved a two-pronged strategy with emphasis on implementing algorithms that could be applied without delay, and could recapitulate protein structure through imposing empirical corrections, at the expense of being true to the physics, while, in parallel, implementing polarizability. The second school continued to seek to expand and improve the rigor of the representation of the underlying physics.

6.2.2 Path one: a shift from physics-based to empirical-based potentials, while implementing polarizability

Perhaps the best example of the former is the introduction of the CMAP correction, a 2D grid-based dihedral energy correction map in CHARMM in 2004 [38, 73]. MacKerell et al. further documented the inability of the diagonal quadratic representation of the physics to account for either the ϕ–ψ energy maps of blocked dipeptides, or protein structure without unacceptable discrepancies [38, 73]. To allow for immediate applications to simulation of protein structure and free energy calculations the strict adherence to physics-based force fields was abandoned and the purely empirical 2D grid correction was implemented by manual adjustment to reproduce the conformational distribution of amino acids in proteins. It was noted that the grid required for the latter differed from a similar grid built to fit the QM dipeptide energy maps and resulted in the degradation of the fit to these energies. The empirical approach has been incorporated into applications carried out in the intervening years

and in fact reoptimized to further correct deficiencies in the original implementation [122].

6.2.3 AMBER, OPLS, torsion parameter adjustment versus CMAP

AMBER and OPLS developers also recognized the deficiencies inherent in the force fields at this point and adopted a similar strategy of empirically adjusting the force field. Here however a less all-encompassing empirical correction was imposed. Basically differences between calculated and QM properties were incorporated into the backbone torsion potential, which essentially became an error function [57, 148, 283]. Perhaps not surprisingly the attempt to find a single set of torsion "error functions" which compensated for deficiencies in the representation of the physics by a simple quadratic harmonic has not proved successful, with, for example, roughly a dozen re-optimizations of these terms being carried out in AMBER [34, 57, 284]. Recently this has led to the introduction of the more global CMAP grid based corrections to AMBER [74, 75]. The torsion angles in OPLS, which had not undergone as many revisions, were similarly modified recently to account for observed deficiencies [178, 196].

In parallel with these efforts a huge investment has been made over the past 15–20 years in incorporating polarizability into all these FFs. Literally hundreds of papers have addressed this subject and tens of reviews have covered this literature [49, 53, 150, 285]. As discussed above essentially all the standard force fields have implemented a "polarizable" version [100, 150, 240, 286], though for the majority of applications the fixed charge representation continues to be used. Although there are notable exceptions as cited above, overall the inclusion of polarizability has produced mixed results, in most systems producing little or no improvement in reproducing experimental results. Another recent example of this, and the need to address remaining inadequacies in FFs, is the study of solvation free energies by Mohamed et al. [287].

6.3 Polarizability, necessary but not sufficient?

It is a fact that molecules are polarizable, and there is a need to address and represent this phenomenon in force fields. However, in our opinion there has been a disproportionate investment to this end. Disproportionate, in that it has largely been focused on to the exclusion of addressing other indisputable deficiencies in the analytical representation of molecular energetics, including: the crude representation of the spatial electron density by partial charges, coupling between valence coordinates, charge and nonbond flux, anisotropy of van der Waal interactions etc. Two factors make this concentration on polarizability inexplicable. First it is not clear that polarization is any more significant than these other contributions. In fact, there are reasons to speculate that some of these contributions—e.g. more accurate representations of electron density [288] and charge flux [155]—may be more important for many properties of systems of interest. Certainly, there has been no systematic study to delineate the relative importance of these contributions. The second factor is that many of these contributions, such as charge flux and valence coupling can be addressed by simple expressions, can be derived straightforwardly from quantum or experimental data, and have little to no impact on the computational cost, as opposed to polarizability which is extremely costly. Hopefully more effort will be devoted to inclusion of the developments which have elucidated these contributions in the future.

6.4 The second path: expanding the physics represented by the force field

Several groups have focused on a more rigorous representation of the molecular electronic distribution, its response to external fields and geometric deformations, and the energetics associated with these responses, i.e., the physics of molecular interactions. In a series of studies Dinur and Hagler demonstrated how various derivatives of the (quantum mechanical) energy and molecular multipoles reported on the charge, flux, and other inter and intramolecular interactions [66, 216]. In 1989 they demonstrated how any atomic multipole, from the charge (monopole) to atomic dipole, quadrupole etc., could be determined by the derivative of the next higher molecular multipole with respect to the atomic coordinates [215]. It was pointed out that an attractive feature of the method was its model independence, as opposed for example to all popular partition methods such as the appealing Hirschfeld "stockholder" partitioning [272], or the widely used DMA method of Stone [252]. Furthermore the unique charges and higher order atomic multipoles obtained in this way rigorously recapitulate the molecular moments and fit the electrostatic potential as well, or better than charges, (and multipoles) obtained by a direct fit of the latter [215].

6.5 CFF: charge, nonbond and polarizability fluxes: their time has come

Dinur and Hagler went on to investigate charge flux, or the geometric dependence of atomic charges, which is reported on simultaneously by these same quantum mechanical derivatives, (and also by the derivatives of the energy with respect to the coordinates) [66, 155, 215, 289]. These studies of charge flux showed that it was a major component of the interatomic forces (as much as 80% in the water dimer) and as such *cannot be ignored in calculation of forces for MD trajectories* [226]. They went on to derive an analytical representation for this geometry dependence, showing that the atomic charge flux could be represented by a linear relation

of local bond stretch and angle bend coordinates as well as a small dependence on torsions containing the atom [217]. This is important as it is a simple, computationally inexpensive, analytical form easily incorporated in MM/MD code.

The authors continued applying these principles to discover and characterize the physics underlying intermolecular interactions by investigating the role of flux terms in hydrogen bonding [155]. Here, in addition to charge flux, nonbond and polarization fluxes, represented analytically by allowing van der Waals constants and atomic polarizability to be coordinate dependent, were also investigated [155]. Again, these quantities were shown to be accessible from the appropriate QM energy second derivatives.

6.5.1 Second derivatives extract energetics of single atom–atom interactions and individual valence coordinate deformations from the total energy function

Dinur and Hagler also showed how fitting particular second derivatives annihilates all surrounding interactions, culling out direct information on individual valence and atom–atom nonbond interactions [66, 216]. This novel technique was applied to several complexes of water and simple amides, ketones and aldehydes. It was shown how interrogation of these derivatives of the QM energy yielded atomic properties including atomic charge, anisotropy of individual atom–atom repulsion and polarizability, as well as the constants that characterize these interactions and their transferability [227]. The method was also applied to obtain a rigorous decomposition of the total torsional potential into pairwise (dihedral) interactions, and characterize the intrinsic rotational barriers and functional form of these dihdrals [290]. Individual bond stretching and angle bending functional forms and constants were also investigated using these techniques [66, 216, 291].

6.6 SDFF

As noted previously Krimm and coworkers began the development of their Spectroscopically Determined Force Field for macromolecules in 1993 [46]. The name is somewhat of a misnomer as it is in all ways comparable to standard FFs, and the same wide variety of data was used in its parametrization and assessment. This includes inter and intramolecular energies and structures, vibrational frequencies, electrostatic potentials and quantum multipole derivatives [46, 236, 292].

What makes the SDFF unique, is that, unbound by legacy software or functional forms, Krimm and coworkers did a thorough examination of the physics and, for the most part, proceeded to incorporate analytical representations of the known inter and intramolecular interactions. Thus, the SDFF is an anharmonic force field containing a wide range of valence coupling terms. These are obtained by fitting the vibrational frequencies along with the above mentioned molecular geometries and conformational energies [46, 205]. Atomic dipoles were included to enhance representation of the electron density and polarizability was also accounted for. These were obtained from fits to electrostatic potentials (with and without applied external fields) [205, 238]. Van der Waals interactions were represented by a 9-6 LJ potential [7, 86], which was found superior to the 12-6 form. It was parametrized by fit to crystal properties [46] or QM dimer energies [236]. Following Dinur and Hagler's formalism [217] charge and dipole flux were also implemented [205]. In further work they investigated the importance of polarizability flux [195] and charge transfer [246].

The resulting FF comprises the most complete representation of the physics of inter and intramolecular interactions to date. It is unfortunate that, as noted above, the FF was not extended to the wide range of functional groups required to treat general biomacromolecules.

6.7 AMOEBA

Ponder et al. also sought to improve the representation of the underlying physics [47, 248, 249]. In their case they focused on the electrostatics and, introduced both polarizability, as did the other standard FFs, and atomic multipoles to better represent the spatial electron density [142, 148]. The resulting FF while a significant step forward, still required the CMAP correction in the earlier versions [148], though they recognized the liability of these "error functions" and removed them in the 2013 FF for all residues but Gly [148]. More recently an expanded set of intramolecular coupling terms have been included in the FF to account for the anomeric effect in dimethyl and trimethyl phosphate [258]. In addition, this group has also examined the physics of atoms in close contact where quantum effects due to charge penetration, or overlap of electron clouds occur. A correction, modifying the multipolar interactions to account for this penetration effect has been derived [293–295]. In addition they have also re-examined the representation for combining rules for van der Waals interactions [296].

7 The future—a recipe for a physics based potential achieving experimental accuracy?

A review of the research on intra- and intermolecular interactions, as we have seen, rapidly leads to the conclusion that the physics of many important phenomena are not accounted for in current standard force fields. This is consistent with the documented discrepancies remaining in fits to quantum and experimental data. It would seem clear that if we are

to reach the ultimate goal of quantitative accuracy, or at least achieving reliable prediction of binding energies and analogous properties to within 0.5 kcal/mol, we need to go beyond quadratic diagonal, partial atomic charge, 6–12 FFs even with polarizability. Known, well documented molecular behavior such as coupling between valence coordinates, geometry dependence of charges, and other force constants, etc. will need to be accounted for. Below we summarize these interactions.

7.1 Components of the physics currently unaccounted for in most "standard" FFs and likely required to achieve experimental accuracy in biomolecular force fields

(We note that most of these contributions have been discussed above with citations. Here we include a subset of references for each of these terms, which along with citations they contain, should provide a quick entry point to further investigation.)

- *Electron density-multipole moments*—improve description of molecular electron density by, for example, including atomic multipoles [251, 252, 297].
- *Out-of-plane angle*—replace "improper torsion" with more accurate out of plane coordinate such as the Wilson Decius and Cross or the distance of central atom to plane formed by 3 atoms to which it is bonded [28, 68].
- *Combination rules*—implement more rigorous combination rules for van der Waals interactions such as the Waldman-Hagler rules [29] or others [132, 296].
- *Polarizability*—include polarizability. As discussed, this has been extensively studied and included in versions of most standard FFs. Its impact in current implementations for uncharged systems remains uncertain, but it clearly contributes to the properties of ionic systems.
- *Charge flux*—include the geometric dependence of charge and higher order multipoles through simple, computationally inconsequential, relations such as the Dinur-Hagler analytical form [217, 298].
- *Nonbond and polarizability fluxes*—include the geometric dependence of nonbond constants and atomic polarizabilities (flux). Assess the extent to which they contribute to molecular interaction energies [155, 242].
- *Short range electrostatic penetration*—account for short range electron cloud overlap effects [293–295, 299].
- *Form of van der Waals potential*. An exponential repulsion is known to be a better representation of the steric interaction than the r^{-12}. In addition the r^{-6} dispersion is also an approximation omitting higher order terms, which may be important for close packed systems such as globular proteins [43, 44].
- *Anisotropic nonbond potentials*—include effects on nonbond potentials stemming from the fact that atoms are not spherical resulting in anisotropy of van der Waals parameters [66, 227, 253, 299, 300].
- *Charge transfer*—Account for the energetics associated with charge transfer occurring between compounds, as for example in H-bonded complexes [243–245].

There is no debate that these effects are all manifested in intra and inter-molecular interactions. They all contribute to the energetics of these interactions. It is not credible to assume that they are all negligible, nor that experimental accuracy or the goal of predicting binding affinities within 0.5 kcal can be achieved without accounting for these phenomena. It would seem that rigorous studies of these contributions in simulating the large set of experimental and QM data used over the years to validate the various FFs is called for. The initial studies described above indicate that these terms may well make significant contributions to such important interactions as H-bonding. It will be especially interesting to determine if inclusion of these terms correct the documented discrepancies in reproducing the experimental and QM properties with current FFs. Perhaps accounting for these effects will finally allow us to achieve the elusive goal of reliably predictive simulations of the energetics and dynamics of biomolecular systems.

Acknowledgements We would like to thank Drs. Mike Gilson, Sam Krimm, Alex MacKerell, Benoit Roux, Pengyu Ren, Jay Ponder, Ken Dill, Kim Palmo, Pnina Dauber-Osguthorpe, for reading parts of manuscript and helpful discussions and Dr. Ruth Sharon for reading and help with editing. We also thank Eitan Hagler for help with the figures, Martha Obermeier for help with proofing and referee 1 who made many helpful suggestions including the addition of the effect of methodology in FF derivation. Special thanks to the editor, Dr. Terry Stouch for his invitation to write this perspective, encouragement, and endless patience.

Note added in proof In a recent article Schmidt et al (J. Chem. Theory Comput., 2018, 14(2), pp 739–758) further demonstrated the need to account anisotropy of nonbonded interactions. They showed that inclusion of anisotropic exchange-repulsion, charge penetration, and dispersion effects, along with atomic multipoles yielded substantive improvement in accounting for 91,000 dimer energies of 13 small organic compounds as well as several experimental sytems.

References

1. Dauber P, Hagler AT (2018) On the evolution of force fields for molecular mechanics and dynamics studies of biomolecular systems and drug design: where have we been, where are we now, where do we need to go and how do we get there? J Comput Aided Mol Des. https://doi.org/10.1007/s10822-018-0111-4
2. Westheimer FH (1956) Steric effects in organic chemistry. Wiley, New Jersey
3. Allinger NL (1959) Conformational analysis. III application to some medium ring compounds. J Am Chem Soc 81:5727–5733

4. Hendrickson JB (1961) Molecular geometry I. Machine computation of the common rings. J Am Chem Soc 83:4537–4547
5. Wiberg KB (1965) A scheme for strain energy minimization. Application to the cycloalkanes. J Am Chem Soc 87:1070–1078
6. Bixon M, Lifson S (1967) Potential functions and conformations in cycloalkanes. Tetrahedron 23:769–784
7. Lifson S, Warshel A (1968) Consistent force field for calculations of conformations, vibrational spectra, and enthalpies of cycloalkane and n-alkane molecules. J Chem Phys 49:5116
8. Lifson S (1973) Recent developments in consistent force field calulations. In: G. Sadron (ed) Dynamic aspects of conformations change in biological macromolecules. Springer, Dordrecht pp 421–430
9. Allinger NL, Miller MA, Vancatledge FA, Hirsch JA (1967) Conformational analysis. LVII. The calculation of the conformational structures of hydrocarbons by the Westheimer–Hendrickson–Wiberg method. J Am Chem Soc 89:4345–4357
10. Allinger NL, Tribble MT, Miller MA, Wertz DH (1971) Conformational analysis. LXIX. An improved calculations of the structures and energies of hydrocarbons. J Am Chem Soc 93:1637–1648
11. Scott RA, Scheraga HA (1966) Conformational analysis of macromolecules. I. ethane, propane, n-butane, and n-pentane. Biopolymers 4:237–238
12. Scott RA, Scheraga HA (1966) Conformational analysis of macromolecules. III. Helical structures of polyglycine and poly-L-alanine. J Chem Phys 45:2091–2101
13. Allinger NL (1976) Calculation of molecular structure and energy by force-field methods. Adv Phys Org Chem 13:1–82
14. Weiner PK, Kollman PA, AMBER (1981) Assisted model building with energy refinement. A general program for modeling molecules and their interactions. J Comput Chem 2:287–303
15. Hagler ATT, Dauber P, Lifson S (1979) Consistent force field studies of intermolecular forces in hydrogen-bonded crystals. 3. The C=O···H–O hydrogen bond and the analysis of the energetics and packing of carboxylic acids. J Am Chem Soc 101:5131–5141
16. Hagler AT, Huler E, Lifson S (1974) Energy functions for peptides and proteins. I. derivation of a consistent force field including the hydrogen bond from amide crystals. JAm Chem Soc 96:5319–5327
17. Dauber P, Osguthorpe DJ, Hagler AT, Structure (1982) Energetics and dynamics of ligand binding to dihydrofolate-reductase. Biochem 10:312–318
18. Brooks BR et al (1983) CHARMM: A program for macromolecular energy, minimization, and dynamics calculations. J Comput Chem 4:187–217
19. van Gunsteren WF, Berendsen HJC (1987) GROningen MOlecular simulation (GROMOS) library manual. BIOMOS, Nijenborgh. pp 1–229
20. Jorgensen WL, Tirado-Rives J (1988) The OPLS potential functions for proteins. Energy minimizations for crystals of cyclic peptides and crambin. J Am Chem Soc 110:1657–1666
21. Allinger NL (1977) Conformational analysis. 130. MM2. A hydrocarbon force field utilizing V1 and V2 torsional terms. J Am Chem Soc 99:8127–8134
22. MacKerell AD et al (1998) All-atom empirical potential for molecular modeling and dynamics studies of proteins. J Phys Chem B 102:3586–3616
23. Warshel A, Lifson S (1969) An empirical function for second neighbor interactions and its effect on vibrational modes and other properties of cyclo- and n-alkanes. Chem Phys Lett 4:255–256
24. Hagler AT, Lifson S, Dauber P (1979) Consistent force field studies of intermolecular forces in hydrogen-bonded crystals. 2. a benchmark for the objective comparison of alternative force fields. J Am Chem Soc 101:5122–5130
25. Dauber P, Hagler AT, Crystal Packing (1980) Hydrogen bonding, and the effect of crystal forces on molecular conformation. Acct Chem Res 13:105–112
26. Allinger NL, Yuh YH, Jenn-Huei L (1989) Molecular mechanics. The MM3 force field for hydrocarbons. J Am Chem Soc 11:8551–8566
27. Allinger NL, Chen K, Lii J (1996) An improved force field (MM4) for saturated hydrocarbons. J Comp Chem 17:642–668
28. Maple JR, Dinur U, Hagler AT (1988) Derivation of force fields for molecular mechanics and dynamics from ab initio energy surfaces. Proc Nat Acad Sci USA 85:5350–5354
29. Waldman M, Hagler ATT (1993) New combining rules for rare-gas van der Waals parameters. J Comput Chem 14: 1077–1084
30. Lii J, Allinger NL (1991) The MM3 force field for amides, polypeptides and proteins. J Comput Chem 12:186–199
31. Weiner SJ, Kollman PA, Nguyen DT, Case DA (1986) An all atom force field for simulations of proteins and nucleic acids. J Comput Chem 7:230–252
32. Jorgensen WL, Maxwell DS, Tirado-Rives J (1996) Development and testing of the OPLS All-atom force field on conformational energetics and properties of organic liquids. J Am Chem Soc 118:11225–11236
33. Horta BAC et al (2016) A GROMOS-compatible force field for small organic molecules in the condensed phase: The 2016H66 parameter set. J Chem Theory Comput. https://doi.org/10.1021/acs.jctc.6b00187
34. Wang J, Cieplak P, Kollman PA (2000) How well does a restrained electrostatic potential (RESP) model perform in calculating conformational energies of organic and biological molecules? J Comput Chem 21:1049–1074
35. Wang JM, Wolf RM, Caldwell JW, Kollman PA, Case DA (2004) Development and testing of a general amber force field. J Comp Chem 25:1157–1174
36. Kaminski GA, Friesner RA, Tirado-rives J, Jorgensen WL (2001) Evaluation and reparametrization of the OPLS-AA force field for proteins via comparison with accurate quantum chemical calculations on peptides. J Phys Chem B 105:6474–6487
37. Cornell WD et al (1995) A second generation force field for the simulation of proteins, nucleic acids, and organic molecules. J Am Chem Soc 117:5179–5197
38. MacKerell AD, Feig M, Brooks CL (2004) Extending the treatment of backbone energetics in protein force fields: limitations of gas-phase quantum mechanics in reproducing protein conformational distributions in molecular dynamics simulations. J Comput Chem 25:1400–1415
39. Buck M, Bouguet-Bonnet S, Pastor RW, MacKerell AD (2006) Importance of the CMAP correction to the CHARMM22 protein force field: dynamics of hen lysozyme. Biophys J 90:L36–L38
40. Mu Y, Kosov DS, Stock G (2003) Conformational dynamics of trialanine in water. 2. comparison of AMBER, CHARMM, GROMOS, and OPLS force fields to NMR and infrared experiments. J Phys Chem B 107:5064–5073
41. Cardamone S, Hughes TJ, Popelier PL (2014) A. multipolar electrostatics. PhysChemChemPhys 16:10367–10387
42. Pierro M Di, Elber R (2013) Automated optimization of potential parameters. J Chem Theory Comput. https://doi.org/10.1021/ct400313n
43. Stone AJ (2013) The theory of intermolecular forces. Oxford University Press, Oxford
44. Hirschfelder JO, Curtiss CF, Bird RB (1954) Molecular theory of gases and liquids. Wiley, New Jersey
45. Halgren, T (1996) Merck molecular force field. J Comput Chem 17:490–519

46. Palmo K, Mirkin NG, Pietila: L, Krimm S (1993) Spectroscopically determined force fields for macromolecules. 1 n-alkane chains. Macromolecules 26:6831–6840
47. Ren PY, Ponder JW (2003) Polarizable atomic multipole water model for molecular mechanics simulation. J Phys Chem B 107:5933–5947
48. Lopes PEM, Roux B, MacKerell AD (2009) Molecular modeling and dynamics studies with explicit inclusion of electronic polarizability. Theory and applications. Theor Chem Acc 124:11–28
49. Khoruzhii O et al (2014) Protein modelling. Springer International Publishing, Basel pp 91–134. https://doi.org/10.1007/978-3-319-09976-7
50. Shi Y, Ren P, Schnieders M, Piquemal J (2015) Polarizable force fields for biomolecular modeling. In: Parrill AL, Lipkowitz KB (eds) Reviews in computational chemistry. Wiley, New Jersey pp 51–86
51. Baker CM (2015) Polarizable force fields for molecular dynamics simulations of biomolecules. Wiley Interdiscip Rev Comput Mol Sci 5:241–254
52. Cieplak P, Dupradeau F-Y, Duan Y, Wang J (2009) Polarization effects in molecular mechanical force fields. J Phys Condens Matter 21:333102
53. Cisneros GA, Karttunen M, Ren P, Sagui C (2014) Classical electrostatics for biomolecular simulations. Chem Rev 114:779–814
54. Ji C, Mei Y (2014) Some practical approaches to treating electrostatic polarization of proteins. Acct Chem Res 47:2796–2803
55. Wang L-P et al (2017) Building a more predictive protein force field: a systematic and reproducible route to AMBER-FB15. J Phys Chem B 121:4023–4039
56. Cerutti DS, Swope WC, Rice JE, Case DA (2014) ff 14ipq: a self-consistent force field for condensed-phase simulations of proteins. J Chem Theory Comput 10:4515–4534
57. Hornak V et al (2006) Comparison of multiple amber force fields and development of improved protein backbone parameters. Proteins Struct Funct Bioinf 65:712–725
58. Debiec KT et al (2016) Further along the road less traveled: AMBER ff15ipq, an original protein force field built on a self-consistent physical model. J Chem Theory Comput 12:3926–3947
59. Lopes PEM, Guvench O, MacKerell AD (2015) Current status of protein force fields for molecular dynamics simulations. In: Kukol A (ed) Molecular modeling of proteins, methods in molecular biology. Springer, New York, pp 47–71
60. Takemura K, Kitao A (2012) Water model tuning for improved reproduction of rotational diffusion and NMR spectral density. J Phys Chem B 8:6279–6287
61. Debiec KT, Gronenborn AM, Chong LT (2014) Evaluating the strength of salt bridges: a comparison of current biomolecular force fields. J Phys Chem B 118:6561–6569
62. Best RB, Buchete N-V, Hummer G (2008) Are current molecular dynamics force fields too helical? Biophys J 95:L07–L09
63. Song K, Stewart JM, Fesinmeyer RM, Andersen NH, Simmerling C (2008) Structural insights for designed alanine-rich helices: comparing NMR helicity measures and conformational ensembles from molecular dynamics simulation. Biopolymers 89:747–760
64. Wang J et al (2012) Development of polarizable models for molecular mechanical calculations. 3. polarizable water models conforming to thole polarization screening schemes. J Phys Chem B 116:7999–8008
65. Huang J et al (2017) Charmm36M: an improved force field for folded and intrinsically disordered proteins. Nat Methods 14:71–73
66. Hagler AT (2015) Quantum derivative fitting and biomolecular force fields—functional form, coupling terms, charge flux, nonbond anharmonicity and individual dihedral potentials. J Chem Theory Comput 11:5555–5572
67. Desgranges C, Delhommelle J (2014) Evaluation of the grand-canonical partition function using expanded Wang-Landau simulations. III. Impact of combining rules on mixtures properties. J Chem Phys 140:104109
68. Wilson EBJ, Decius JC, Cross PC (1955) Molecular vibrations: the theory of infrared and raman vibrational spectra. McGraw-Bill, New York
69. Jorgensen WL (1981) Transferable intermolecular potential functions for water, alcohols, and ethers. Application to liquid water. J Am Chem Soc 103:335–340
70. Wang L-P, Martinez TJ, Pande VS (2014) Building force fields: an automatic, systematic, and reproducible approach. J Phys Chem Lett 5:885–889
71. Horn HW et al (2004) Development of an improved four-site water model for biomolecular simulations: TIP4P-Ew. J Chem Phys 120:9665–9678
72. Honda S et al (2008) Crystal structure of a ten-amino acid protein. J Am Chem Soc 130:15327–15331
73. MacKerell AD, Feig M, Brooks CL (2004) Improved treatment of the protein backbone in empirical force fields. J Am Chem Soc 126:698–699
74. Wang W, Ye W, Jiang C, Luo R, Chen H (2014) New force field on modeling intrinsically disordered proteins. Chem Biol Drug Des 84:253–269
75. Perez A, MacCallum JL, Brini E, Simmerling C, Dill KA (2015) Grid-based backbone correction to the ff12SB protein force field for implicit-solvent simulations. J Chem Theory Comput 11:4770–4779
76. Piana S, Lindorff-Larsen K, Shaw DE (2011) How robust are protein folding simulations with respect to force field parameterization? Biophys J 100:L47–L49
77. Bernstein J, Hagler AT (1979) Polymorphism and isomorphism as tools to study the relationship between crystal forces and molecular-conformation. Mol Cryst Liq Cryst 50:223–233
78. Cruz-Cabeza AJ, Bernstein J (2014) Conformational polymorphism. Chem Rev 114:2170–2191
79. Hagler AT, Moult J, Osguthorpe DJ (1980) Monte-Carlo simulation of the solvent structure in crystals of a hydrated cyclic peptide. Biopolymers 19:395–418
80. Hall D, Pavitt N (1984) An appraisal of molecular force fields for the representation of polypeptides. J Comput Chem 5:441–450
81. Kitson DH, Hagler AT (1988) Theoretical-studies of the structure and molecular-dynamics of a peptide crystal. Biochemistry 27:5246–5257
82. Kitson DH, Hagler AT (1988) Catalysis of a rotational transition in a peptide by crystal forces. Biochemistry 27:7176–7180
83. Hall D, Pavitt N (1991) Molecular packing and conformational analysis of cyclo- hexaglycyl hemihydrate. J Crystallogr Spectrosc Res 21:241–245
84. Williams DE (2001) Improved intermolecular force field for molecules containing H, C, N, and O atoms, with application to nucleoside and peptide crystals. J Comp Chem 22:1154–1166
85. Williams DE (1966) Nonbonbonded potential parameters derived from crystalline aromatic hydrocarbons. J Chem Phys 45:3770–3778
86. Warshel A, Lifson S (1970) Consistent force field calculations. II. Crystal structures, sublimation energies, molecular and lattice vibrations, molecular conformations, and enthalpies of alkanes. J Chem Phys 53:582–594
87. Berkovitch-Yellin Z, Ariel S, Leiserowitz L (1983) The comparative roles of the proton-acceptor properties of amide and carboxyl groups in influencing crystal packing patterns: doubly vs. singly hydrogen-bonded systems in *N*-acyl amino acids and in other amide-acid crystals. J Am Chem Soc 103:765–767

88. Berkovitch-Yellin Z, Leiserowitz L (1984) The role played by C–H.O and C–H.N interactions in determining molecular packing and conformation. Acta Crystallogr B 40:159–165
89. Lii JH, Allinger NL, Molecular (1989) Mechanics. The MM3 force field for hydrocarbons. 3. The van der Waals' potentials and crystal data for aliphatic and aromatic hydrocarbons. J Am Chem Soc 111:8576–8582
90. Williams DE, Stouch TR (1993) Characterization of force fields for lipid molecules: Applications to crystal structures. J Comput Chem 14:1066–1076
91. Ewig CS, Thacher TS, Hagler AT (1999) Derivation of class II force fields. 7. Nonbonded force field parameters for organic compounds. J Phys Chem B 103:6998–7014
92. Donchev AG et al (2007) Assessment of performance of the general purpose polarizable force field QMPFF3 in condensed phase. J Comp Chem 29:1242–1249
93. Price SL (2014) Predicting crystal structures of organic compounds. Chem Soc Rev 43:2098–2111
94. Gavezzotti A (2012) Computational studies of crystal structure and bonding. Top Curr Chem 315:1–32
95. Gavezzotti A (2013) Equilibrium structure and dynamics of organic crystals by Monte Carlo simulation: critical assessment of force fields and comparison with static packing analysis. New J Chem 37:2110–2119
96. Nyman J, Sheehan Pundyke O, Day GM (2016) Accurate force fields and methods for modelling organic molecular crystals at finite temperatures. Phys Chem Chem Phys 18:15828–15837
97. Reilly AM et al (2016) Report on the sixth blind test of organic crystal structure prediction methods. Acta Cryst B 72:439–459
98. Cieplak P, Caldwell J, Kollman P (2001) Molecular mechanical models for organic and biological systems going beyond the atom centered two body additive approximation: aqueous solution free energies of methanol and *N*-methyl acetamide, nucleic acid base, and amide hydrogen bonding and Chloroform/water partition coefficients of the nucleic acid bases. J Comput Chem 22:1048–1057
99. Wang J et al (2011) Development of polarizable models for molecular mechanical calculations I: parameterization of atomic polarizability. J Phys Chem B 115:3091–3099
100. Wang J et al (2011) Development of polarizable models for molecular mechanical calculations II: induced dipole models significantly improve accuracy of intermolecular interaction energies. J Phys Chem B 115:3100–3111
101. Wang J et al (2012) Development of polarizable models for molecular mechanical calculations. 4. van der Waals parametrization. J Phys Chem B 116:7088–7101
102. Duan Y et al (2003) A point-charge force field for molecular mechanics simulations of proteins based on condensed-phase quantum mechanical calculations. J Comput Chem 24:1999–2012
103. Jämbeck JPM, Lyubartsev AP (2014) Update to the general amber force field for small solutes with an emphasis on free energies of hydration. J Phys Chem B 118:3793–3804
104. Sprenger KG, Jaeger VW, Pfaendtner J (2015) The general AMBER force field (GAFF) can accurately predict thermodynamic and transport properties of many ionic liquids. J Phys Chem B 119:5882–5895
105. Caldwell JW, Kollman PA (1995) Structure and properties of neat liquids using nonadditive molecular dynamics: water, methanol, and *N*-methylacetamide. J Phys Chem 99:6208–6219
106. Wang J, Hou T (2011) Application of molecular dynamics simulations in molecular property prediction. 1. Density and heat of vaporization. J Chem Theory Comput 7:2151–2165
107. Lifson S (1972) Protein–proptein interactions. Springer, New York pp 3–16
108. Allinger NL, Chen K, Lii J (1996) An improved force field (MM4) for saturated hydrocarbons. J Comput Chem 17:642–668
109. Beachy MD, Chasman D, Murphy RB, Halgren TA, Friesner RA (1997) Accurate ab initio quantum chemical determination of the relative energetics of peptide conformations and assessment of empirical force fields. J Am Chem Soc 119:5908–5920
110. Patel S, MacKerell AD, Brooks CL (2004) CHARMM fluctuating charge force field for proteins: II protein/solvent properties from molecular dynamics simulations using a nonadditive electrostatic model. J Comput Chem 25:1504–1514
111. Vanommeslaeghe K, MacKerell AD (2015) CHARMM additive and polarizable force fields for biophysics and computer-aided drug design. Biochim Biophys Acta 1850:861–871
112. Hatcher ER, Guvench O, MacKerell AD (2009) CHARMM additive all-atom force field for acyclic polyalcohols, acyclic carbohydrates, and inositol. J Chem Theory Comput 5:1315–1327
113. Guvench O et al (2008) Additive empirical force field for hexopyranose monosaccharides. J Comput Chem 29:2543–2564
114. Mijakovi M et al (2015) A comparison of force fields for ethanol–water mixtures. Mol Simul 699–712:699–712
115. Guillot B (2002) A reappraisal of what we have learnt during three decades of computer simulations on water. J Mol Liq 101:219–260
116. Ahlstrom LS, Vorontsov II, Shi J, Miyashita O (2017) Effect of the crystal environment on side-chain conformational dynamics in cyanovirin-N investigated through crystal and solution molecular dynamics simulations. PLoS ONE 12:e0170337
117. Barone G, Della Gatta G, Ferro D, Piacente V (1990) Enthalpies and entropies of sublimation, vaporization and fusion of nine polyhydric alcohols. J Chem Soc Faraday Trans 86:75–79
118. He X, Lopes PEM, MacKerell AD (2013) Polarizable empirical force field for acyclic polyalcohols based on the classical Drude oscillator. Biopolymers 99:724–738
119. Patel DS, He X, Mackerell AD (2015) Polarizable empirical force field for hexopyranose monosaccharides based on the classical Drude oscillator. J Phys Chem B 119:637–652
120. Clark GNI, Cappa CD, Smith JD, Saykally RJ, Head-Gordon T (2010) The structure of ambient water. Mol Phys 108: 1415–1433
121. Freddolino PL, Park S, Roux B, Schulten K (2009) Force field bias in protein folding simulations. Biophys J 96:3772–3780
122. Best RB et al (2012) Optimization of the additive CHARMM all-atom protein force field targeting improved sampling of the backbone ϕ, ψ and Side-Chain χ_1 and χ_2 dihedral angles. J Chem Theory Comput 8:3257–3273
123. Swaminathan S, Craven BM, Mcmullan RK (1984) The crystal structure and molecular thermal motion of urea at 12, 60 and 123 K from neutron diffraction. Acta Cryst B 40:300–306
124. Hagler AT, Lifson S (1974) Energy functions for peptides and proteins. II. The amide hydrogen bond and calculation of amide crystal properties. J Am Chem Soc 96:5327–5335
125. Zaitsau D, Kabo G, Kozyro A, Sevruk V (2003) The effect of the failure of isotropy of a gas in an effusion cell on the vapor pressure and enthalpy of sublimation for alkyl derivatives of carbamide. Thermochim Acta 406:17–28
126. Piana S, Donchev AG, Robustelli P, Shaw DE (2015) Water dispersion interactions strongly influence simulated structural properties of disordered protein states. J Phys Chem B 119: 5113–5123
127. Rauscher S et al (2015) Structural ensembles of intrinsically disordered proteins depend strongly on force field: a comparison to experiment. J Chem Theory Comput 11:5513–5524
128. Lindorff-Larsen K et al (2012) Systematic validation of protein force fields against experimental data. PLoS ONE 7:e32131
129. Li DW, Brüschweiler R (2010) NMR-based protein potentials. Angew Chemie 49:6778–6780
130. Waldman M, Hagler AT (1993) New combining rules for rare gas van der waals parameters. J Comput Chem 14:1077–1084

131. Song W, Rossky PJ, Maroncelli M (2003) Modeling alkane + perfluoroalkane interactions using all-atom potentials: failure of the usual combining rules. J Chem Phys 119:9145
132. Nikitin A, Milchevskiy Y, Lyubartsev A (2015) AMBER-II: new combining rules and force field for perfluoroalkanes. J Phys Chem B 119:14563–14573
133. Best RB, Hummer G (2009) Optimized molecular dynamics force fields applied to the helix-coil transition of polypeptides. J Phys Chem B 113:9004–9015
134. Yin J, Henriksen NM, Slochower DR, Gilson MK (2017) The SAMPL5 host–guest challenge: computing binding free energies and enthalpies from explicit solvent simulations by the attach-pull-release (APR) method. J Comput Aided Mol Des 31:133–145
135. Lindorff-Larsen K et al (2010) Improved side-chain torsion potentials for the Amber ff99SB protein force field. Proteins 78:1950–1958
136. Kubelka J, Chiu TK, Davies DR, Eaton WA, Hofrichter J (2006) Sub-microsecond protein folding. J Mol Biol 359:546–553
137. Rohl CA, Baldwin RL (1997) Comparison of NH exchange and circular dichroism as techniques for measuring the parameters of the helix-coil transition in peptides. Biochemistry 36:8435–8442
138. Izadi S, Anandakrishnan R, Onufriev AV (2014) Building water models: a different approach. J Phys Chem Lett 5:3863–3871
139. Sullivan MR, Sokkalingam P, Nguyen T, Donahue JP, Gibb BC (2017) Binding of carboxylate and trimethylammonium salts to octa-acid and TEMOA deep-cavity cavitands. J Comput Aided Mol Des 31:21–28
140. Stouch TR (2012) The errors of our ways: taking account of error in computer-aided drug design to build confidence intervals for our next 25 years. J Comput Aided Mol Des 26:125–134
141. Chodera JD, Mobley DL (2013) Entropy-enthalpy compensation: Role and ramifications in biomolecular ligand recognition and design. Annu Rev Biophys 2013 42:121–142
142. Ren P, Wu C, Ponder JW (2011) Polarizable atomic multipole-based molecular mechanics for organic molecules. J Chem Theory Comput 7:3143–3161
143. Shaik MS, Liem SY, Popelier PLA (2010) Properties of liquid water from a systematic refinement of a high-rank multipolar electrostatic potential. J Chem Phys 132:174504
144. Morozov AV, Tsemekhman K, Baker D (2006) Electron density redistribution accounts for half the cooperativity of R helix formation. J Phys Chem B 110:4503–4505
145. Wallqvist A (1990) Incorporating intramolecular degrees of freedom in simulations of polarizable liquid water. Chem Phys 148:439–449
146. Yin J et al (2017) Overview of the SAMPL5 host–guest challenge: are we doing better? J Comput Aided Mol Des 31:1–19
147. Lamoureux G, MacKerell AD, Roux B (2003) A simple polarizable model of water based on classical Drude oscillators. J Chem Phys 119:5185
148. Shi Y et al (2013) Polarizable atomic multipole-based amoeba force field for proteins. J Chem Theory Comput 9:4046–4063
149. Schmollngruber M, Lesch V, Schrö C, Heuer A, Steinhauser O (2015) Comparing induced point-dipoles and Drude oscillators. Phys Chem Chem Phys 17:14297–14306
150. Lemkul JA, Huang J, Roux B, MacKerell AD (2016) An empirical polarizable force field based on the classical drude oscillator model: development history and recent applications. Chem Rev 116:4983–5013
151. Bernal JD, Fowler RH (1933) A theory of water and ionic solution, with particular reference to hydrogen and hydroxyl ions. J Chem Phys 1:515–548
152. Jorgensen WL, Chandrasekhar J, Madura JD, Impey RW, Klein ML (1983) Comparison of simple potential functions for simulating liquid water. J Chem Phys 79:926–935
153. Lamoureux G, Harder E, Vorobyov IV, Roux B, MacKerell A (2005) A polarizable model of water for molecular dynamics simulations of biomolecules. Chem Phys Lett 418:2006
154. Corongiu G, Clementi E (1993) Molecular dynamics simulations with a flexible and polarizable potential: density of states for liquid water at different temperatures. J Chem Phys 98:4984–4990
155. Dinur U, Hagler AT (1992) The role of nonbond and charge flux in hydrogen bond interactions. The effect on structural changes and spectral shifts in water dimer. J Chem Phys 97:9161–9172
156. Kitano M, Kuchitsu K (1974) Molecular Structure Of Formamide As Studied By Gas Phase Electron Diffraction. Bull Chem Soc Jpn 47:67–72
157. Vorobyov IV, Anisimov VM, MacKerell AD (2005) Polarizable empirical force field for alkanes based on the classical Drude oscillator model. J Phys Chem B 109:18988–18999
158. Steiner T (1996) C–H–O hydrogen bondiong in crystals. Cryst Rev 6:1–57
159. Bernstein J (2013) 'It Isn't'. Cryst Growth Des 13:961–964
160. Harder E, Anisimov VM, Whitfield T, MacKerell AD, Roux B (2008) Understanding the dielectric properties of liquid amides from a polarizable force field. J Phys Chem B 112:3509–3521
161. Maple JR, Hwang M, Stockfisch TP, Hagler AT (1994) Derivation of class II force fields. III. Characterization of a quantum force field for alkanes. Isr J Chem 34:195–231
162. Klauda JB, Brooks BR, MacKerell AD, Venable RM, Pastor RW (2005) An ab initio study on the torsional surface of alkanes and its effect on molecular simulations of alkanes and a DPPC bilayer. J Phys Chem B 109:5300–5311
163. Shivakumar D, Harder E, Damm W, Friesner RA, Sherman W (2012) Improving the prediction of absolute solvation free energies using the next generation OPLS force field. | Chem Theory Comput 8:2553–2558
164. Lopes PEM, Lamoureux G, Roux B, MacKerell AD (2007) Polarizable empirical force field for aromatic compounds based on the classical Drude oscillator. J Phys Chem B 111:2873–2885
165. Hall D, Williams DE (1974) The effect of coulombic interactions on the calculated crystal structures of benzene at atmospheric and 25 kbar pressure. Acta Cryst A 31:56–58
166. Dzyabchenko AV, Bazilevskii MV (1985) Theoretical structures of crystalline benzene II. Verification of atom–atom potentials. J Struct Chem 26:558–564
167. Allinger NL, Lii J-H (1987) Benzene, aromatic rings, van der Waals molecules, and crystals of aromatic molecules in molecular mechanics (MM3). J Comput Chem 8:1146–1153
168. van Eijck BP, Spek aL, Mooij WTM, Kroon J (1998) Hypothetical crystal structures of benzene at 0 and 30 kbar. Acta Crystallogr B 54:291–299
169. Orabi EA, Lamoureux G (2012) Cation-π and π–π interactions in aqueous solution studied using polarizable potential models. J Chem Theory Comput 8:182–193
170. Nevins N, Chen K, Allinger NL (1996) Molecular mechanics (MM4) calculations on alkenes. J Comput Chem 17:669–694
171. Vorobyov I et al (2007) Additive and classical Drude polarizable force fields for linear and cyclic ethers. J Chem Theory Comput 3:1120–1133
172. Baker CM, MacKerell AD (2010) Polarizability rescaling and atom-based Thole scaling in the CHARMM Drude polarizable force field for ethers. J Mol Model 16:567–576
173. Anisimov VM, Vorobyov IV, Roux B, MacKerell AD (2007) Polarizable empirical force field for the primary and secondary alcohol series based on the classical Drude model. J Chem Theory Comput 3:1927–1946
174. Lin B, Lopes PEM, Roux B, MacKerell AD (2013) Kirkwood-Buff analysis of aqueous *N*-methylacetamide and acetamide solutions modeled by the CHARMM additive and Drude polarizable force fields. J Chem Phys 139:08B624_1

175. Jorgensen WL, Swenson CJ (1985) Optimized intermolecular potential functions for amides and peptides. Structure and properties of liquid amides. J Am Chem Soc 107:569–578
176. Wang J, Hou T (2011) Application of molecular dynamics simulations in molecular property prediction II: Diffusion coefficient. J Comput Chem 32:3505–3519
177. Distasio RA, Jung Y, Head-Gordon MA (2005) Resolution-of-the-identity implementation of the local triatomics-in-molecules model for second-order Møller-Plesset perturbation theory with application to alanine tetrapeptide conformational energies. J Chem Theory Comput 1:862–876
178. Robertson MJ, Tirado-Rives J, Jorgensen WL (2015) Improved peptide and protein torsional energetics with the OPLS-AA force field. J Chem Theory Comput 11:3499–3509
179. Lopes PEM et al (2013) Polarizable Force Field for Peptides and Proteins based on the Classical Drude Oscillator. J Chem Theory Comput 9:5430–5449
180. Li H et al (2015) Representation of ion—protein interactions using the Drude polarizable force-field. J Phys Chem B 8:9401–9416
181. Ermer O, Lifson S (1973) Consistent force field calculations. III. Vibrations, conformations, and heats of hydrogenation of nonconjugated olefins. J Am Chem Soc 95:4121–4132
182. Maple JR, Hwang MJ, Jalkanen KJ, Stockfisch TP, Hagler AT (1998) Derivation of class ii force fields: V. Quantum force field for amides, peptides, and related compounds. J Comput Chem 19:430–458
183. Patel S, Brooks CL (2004) CHARMM fluctuating charge force field for proteins: I parameterization and application to bulk organic liquid simulations. J Comput Chem 25:1–15
184. Rick SW, Stuart SJ (2002) Potentials and algorithms for incorporating polarizability in computer simulations. Rev Comput Chem 18:89–146
185. Bauer Ba, Patel S (2012) Recent applications and developments of charge equilibration force fields for modeling dynamical charges in classical molecular dynamics simulations. Theor Chem Acc 131:1153
186. Rablen PR, Lockman JW, Jorgensen WL (1998) Ab initio study of hydrogen-bonded complexes of small organic molecules with Water. J Phys Chem 102:3782–3797
187. Rick SW, Stuart SJ, Berne BJ (1994) Dynamical fluctuating charge force fields: application to liquid water. J Chem Phys 101:6141–6156
188. Zhong Y, Patel S (2010) Nonadditive empirical force fields for short-chain linear alcohols: methanol to butanol. Hydration free energetics and Kirkwood-Buff analysis using charge equilibration models. J Phys Chem B 114:11076–11092
189. Patel S, Brooks CL III (2005) Structure, thermodynamics, and liquid–vapor equilibrium of ethanol from molecular- dynamics simulations using nonadditive interactions. J Chem Phys 123:164502
190. Halgren TA (1992) The representation of van der Waals (vdW) interactions in molecular mechanics force fields: potential form, combination rules, and vdW parameters. J Am Chem Soc 114:7827–7843
191. Ponder JW et al (2010) Current status of the AMOEBA polarizable force field. J Phys Chem B 114:2549–2564
192. Kumar R, Wang F-F, Jenness GR, Jordan K (2010) A second generation distributed point polarizable water model. J Chem Phys 132:14309
193. Naserifar S, Brooks DJ, Goddard WA, Cvicek V (2017) Polarizable charge equilibration model for predicting accurate electrostatic interactions in molecules and solids. J Chem Phys 146:124117–124117
194. Santos LHR, Krawczuk A, Macchi P (2015) Distributed atomic polarizabilities of amino acids and their hydrogen-bonded aggregates. J Phys Chem A 119:3285–3298
195. Palmo K, Mannfors B, Mirkin NG, Krimm S (2006) Inclusion of charge and polarizability fluxes provides needed physical accuracy in molecular mechanics force fields. Chem Phys Lett 429:628–632
196. Harder E et al (2016) OPLS3: a force field providing broad coverage of drug-like small molecules and proteins. J Chem Theory Comput 12:281–296
197. Storer JW, Giesen DJ, Cramer CJ, Truhlar DG (1995) Class IV charge models: a new semiempirical approach in quantum chemistry. J Comput Aided Mol Des 9:87–110
198. Jakalian A, Jack DB, Bayly CI (2002) Fast, efficient generation of high-quality atomic charges. AM1-BCC model: II. Parameterization and validation. J Comput Chem 23:1623–1641
199. Distasio RA, Steele RP, Rhee YM, Shao Y, Head-Gordon M (2007) An improved algorithm for analytical gradient evaluation in resolution-of-the-identity second-order Møller-Plesset perturbation theory: application to alanine tetrapeptide conformational analysis. J Comput Chem 28:839–856
200. Graf J, Nguyen PH, Stock G, Schwalbe H (2007) Structure and dynamics of the homologous series of alanine peptides: a joint molecular dynamics/NMR study. J Am Chem Soc 129:1179–1189
201. Dodda LS, Vilseck JZ, Tirado-Rives J, Jorgensen WL (2017) 14*CM1A-LBCC: localized bond-charge corrected CM1A charges for condensed-phase simulations. J Phys Chem B 121:3864–3870
202. Choudhary A, Gandla D, Krow GR, Raines RT (2009) Nature of amide carbonyl–carbonyl interactions in proteins. J Am Chem Soc 131:7244–7246
203. Wang L et al (2015) Accurate and reliable prediction of relative ligand binding potency in prospective drug discovery by way of a modern free-energy calculation protocol and force field. J Am Chem Soc 137:2695–2703
204. Maple JR et al (1994) Derivation of class II force fields. 1. Methodology and quantum force-field for the alkyl functional group and alkane molecules. J Comput Chem 15:162–182
205. Palmo K, Mannfors B, Mirkin NG, Krimm S (2003) Potential energy functions: from consistent force fields to spectroscopically determined polarizable force fields. Biopolymers 68:383–394
206. Kolă M, Hobza P (2012) On extension of the current biomolecular empirical force field for the description of halogen bonds. J Chem Theory Comput 8:1325–1333
207. Doig AJ, Baldwin RL (1995) N- and C-capping preferences for all 20 amino acids in alpha-helical peptides. Protein Sci 4:1325–1336
208. Shalongo W, Dugad L, Stellwagen' E (1994) Distribution of helicity within the model peptide acetyl(AAQAA)3amide. J Am Chem Soc 116:8288–8293
209. Lifson S, Hagler AT, Dauber P (1979) Consistent force field studies of intermolecular forces in hydrogen-bonded crystals. 1. Carboxylic acids, amides, and the C=O… H–hydrogen bonds. JAm Chem Soc 101:5111
210. Dunitz JD, Gavezzotti A (2005) Molecular recognition in organic crystals: directed intermolecular bonds or nonlocalized bonding? Angew Chem Int Ed Engl 44:1766–1787
211. Kazantsev AV et al (2011) Successful prediction of a model pharmaceutical in the fifth blind test of crystal structure prediction. Int J Pharm 418:168–178
212. Kuhn B et al (2017) Prospective evaluation of free energy calculations for the prioritization of cathepsin L inhibitors. J Med Chem 60:2485–2497

213. Baliban SM et al (2017) Development of a glycoconjugate vaccine to prevent invasive *Salmonella typhimurium* infections in sub-Saharan Africa. PLoS Negl Trop Dis 11:1–27
214. Robinson D et al (2016) Differential water thermodynamics determine PI3K-Beta/Delta selectivity for solvent-exposed ligand modi fi cations. J Chem Inf Model 6:886–894
215. Dinur U, Hagler AT (1989) Determination of atomic point charges and point dipoles from the Cartesian derivatives of the molecular dipole moment and second moments, and from energy second derivatives of planar dimers II. Applications to model systems. J Chem Phys 91:2959–2970
216. Dinur U, Hagler AT (1991) New approaches to empirical force fields. In: Lipkowitz KB, Boyd DB (eds) Reviews in Computational Chemistry. VCH Publisher2, New Jersey pp 99–164
217. Dinur U, Hagler AT (1995) Geometry-dependent atomic charges—methodology and application to alkanes, aldehydes, ketones, and amides. J Comput Chem 16:154–170
218. Decius JC (1975) An effective atomic charge model for infrared intensities. J Mol Spec 362:348–362
219. Person WB, Zerbi G (1982) Vibrational intensities in infrared and raman spectroscopy. Elsevier, Amsterdam
220. Miwa Y, Machida K (1988) Molecular mechanics simulations of thermodynamic functions and infrared spectra of alkanes. J Am Chem Soc 110:5183–5189
221. Gussoni M, Castiglioni C, Ramos MN, Rui M, Zerbi G (1990) Infrared intensities: from intensity parameters to an overall understanding of the spectrum. J Mol Struc 224:445–470
222. Stern PS, Chorev M, Goodman M, Hagler AT (1983) Computer-simulation of the conformational properties of retro-inverso peptides. 2. Abinitio study, spatial electron-distribution, and population analysis of *N*-formylglycine methylamide, *N*-formyl N'-acetyldiaminomethane, and N-methylmalonamide. Biopolymers 22:1885–1900
223. Cieplak P, Kollman P (1991) On the use of electrostatic potential derived charges in molecular mechanics force-fields—relative solvation free-energy of Cis-N-methyl-acetamide and trans-N-methyl-acetamide. J Comput Chem 12:1232–1236
224. Stouch TR, Williams DE (1992) Conformational dependence of electrostatic potential derived charges of a lipid headgroup: glycerylphosphorylcholine. J Comput Chem 13:622–632
225. Reynolds CA, Essex JW, Richards WG (1992) Atomic charges for variable molecular conformations. J Am Chem Soc 114:9075–9079
226. Dinur U (1990) 'Flexible' water molecules in external electrostatic potentials. J Phys Chem 94:5669–5671
227. Dinur U, Hagler AT (1989) Direct evaluation of nonbonding interactions from ab initio calculations. J Am Chem Soc 111:5149–5151
228. Wallqvist A, Ahlstrom P, Karlstroms GA (1990) New intermolecular energy calculation scheme: applications to potential surface and liquid properties of water. J Phys Chem 94:1649–1656
229. Breneman CM, Wiberg KB (1990) Determining atom-centered monopoles from molecular electrostatic potentials. The need for high sampling density in formamide conformational analysis. J Comput Chem 11:361–373
230. Hagler AT, Leiserowitz L, Tuval M (1976) Experimental and theoretical studies of barrier to rotation about N-C-Alpha and C-Alpha-C' bonds (Phi and Psi) in amides and peptides. J Am Chem Soc 98:4600–4612
231. Wei D, Guo H, Salahub DR (2001) Conformational dynamics of an alanine dipeptide analog: An ab initio molecular dynamics study. Phys Rev E 64:11907
232. Palmo K, Mirkin NG, Krimm S (1998) Spectroscopically determined force fields for macromolecules. 2. saturated hydrocarbon chains. J Phys Chem A 102:6448–6456
233. Pietilä L-O (1989) Molecular mechanics and force field calculations in vibrational spectroscopy. J Mol Struct 195:111–132
234. Palmö K, Pietilä L-O, Krimm S (1991) Construction of molecular mechanics energy functions by mathematical transformation of ab initio force fields and structures. J Comput Chem 12:385–390
235. Hagler AT, Huler E, Lifson S (1974) Energy functions for peptides and proteins. 1. Derivation of a consistent force-field including the hydrogen-bond from amide crystals. J Am Chem Soc 96:5319–5327
236. Mannfors B, Palmo K, Krimm S (2008) Spectroscopically determined force field for water dimer: Physically enhanced treatment of hydrogen bonding in molecular mechanics energy functions. J Phys Chem A 112:12667–12678
237. Mannfors B, Mirkin NG, Palmo K, Krimm S (2001) A polarizable electrostatic model of the N-methylacetamide dimer. J Comput Chem 22:1933–1943
238. Mannfors B, Palmo K, Krimm S (2000) A new electrostatic model for molecular mechanics force fields. J Mol Struct 556:1–21
239. Ewig CS, Waldman M, Maple JR (2002) Ab initio atomic polarizability tensors for organic molecules. J Phys Chem A 106:326–334
240. Albaugh A et al (2016) Advanced potential energy surfaces for molecular simulation. J Phys Chem B. https://doi.org/10.1021/acs.jpcb.6b06414
241. Kratz EG et al (2016) LICHEM: a QM/MM program for simulations with multipolar and polarizable force fields. J Comput Chem 37:1019–1029
242. Loboda O, Ingrosso F, Ruiz-López MF, Reis H, Millot C (2016) Dipole and quadrupole polarizabilities of the water molecule as a function of geometry. J Comput Chem 37:2125–2132
243. Hobza P, Havlas Z (2000) Blue-shifting hydrogen bonds. Chem Rev 100:4253–4264
244. Honda K (2002) An effective potential function with enhanced charge-transfer-type interaction for hydrogen-bonding liquids. J Chem Phys 117:3558
245. Řezác J, Hobza P (2016) Benchmark calculations of interaction energies in noncovalent complexes and their applications. Chem Rev 116:5038–5071
246. Mirkin NG, Krimm S (2014) Note: charge transfer in a hydrated peptide group is determined mainly by its intrinsic hydrogen-bond energetics. J Chem Phys 140:46101
247. Ren P, Ponder JW (2002) Consistent treatment of inter- and intramolecular polarization in molecular mechanics calculations. J Comp Chem 23:1497–1506
248. Dudek MJ, Ponder JW (1995) Accurate modeling of the intramolecular electrostatic energy of proteins. J Comput Chem 16:791–816
249. Rasmussen TD, Ren P, Ponder JW, Jensen F (2007) Force field modeling of conformational energies: importance of multipole moments and intramolecular polarization. Int J Quantum Chem 107:1390–1395
250. Rowlinson JS (1951) The lattice energy of ice and the second virial coefficient of water vapour. Trans Faraday Soc 47:120–129
251. Berkovitch-yellin Z, Leiserowitz L (1980) The role of coulomb forces in the crystal packing of amides. A study based on experimental electron densities. J Am Chem Soc 102:7677–7690
252. Stone AJ (1981) Distributed multipole analysis, or how to describe a molecular charge distribution. Chem Phys Lett 83:233–239
253. Stone AJ, Price SL (1988) Some new ideas in the theory of intermolecular forces: anisotropic atom–atom. J Phys Chem 92:3325–3335
254. Price SL (2000) Review in computational chemistry. Wiley, New Jersey pp 225–289
255. Gresh N, Claverie P, Pullman A (1984) Theoretical studies of molecular conformation. Derivation of an additive procedure for

the computation of intramolecular interaction energies. Comparison with ab initio SCF computations. Theor Chim Acta 66:1–20
256. Gresh N et al (1986) Intermolecular interactions: elaboration on an additive procedure including an explicit charge-transfer contribution. Int J Quantum Chem 24:101–118
257. Piquemal J-P, Cisneros GA, Reinhardt P, Gresh N, Darden TA (2006) Towards a force field based on density fitting. J Chem Phys 124:104101
258. Zhang C, Lu C, Wang Q, Ponder JW, Ren P (2015) Polarizable multipole-based force field for dimethyl and trimethyl phosphate. J Chem Theory Comput 11:5326–5339
259. Thole BT (1981) Molecular polarization calculated with a modified dipole interaction. Chem Phys 59:341–350
260. Geballe MT, Skillman AG, Nicholls A, Guthrie JP, Taylor PJ (2010) The SAMPL2 blind prediction challenge: introduction and overview. J Comput Aided Mol Des 24:259–279
261. Gresh N, Kafafi S, Truchon J-F, Salahub DR (2004) Intramolecular interaction energies in model alanine and glycine tetrapeptides. Evaluation of anisotropy, polarization, and correlation effects. A parallel ab initio HF/MP2, DFT, and polarizable molecular mechanics study. J Comput Chem 25:823–834
262. Shi Y, Schnieders MJ, Ren P (2009) Trypsin-ligand binding free energy calculation with AMOEBA. In: 2009 Annual International Conference of the IEEE Engineering in Medicine and Biology Society, IEEE. pp 2328–2331. https://doi.org/10.1109/IEMBS.2009.5335108
263. Gresh N, Cisneros GA, Darden T, Piquemal J-P, Anisotropic (2007) Polarizable molecular mechanics studies of inter- and intramolecular interactions and ligand-macromolecule complexes. A bottom–up strategy. J Chem Theory Comput 3:1960–1986
264. de Courcy B, Piquemal J-P, Garbay C, Gresh N (2010) Polarizable water molecules in ligand—macromolecule recognition. Impact on the relative affinities of competing pyrrolopyrimidine inhibitors for FAK kinase. J Am Chem Soc 132:3312–3320
265. Zhang J, Yang W, Piquemal JP, Ren P (2012) Modeling structural coordination and ligand binding in zinc proteins with a polarizable potential. J Chem Theory Comput 8:1314–1324
266. Avbelj F, Moult J, Kitson DH, James MNG, Hagler AT (1990) Molecular-dynamics study of the structure and dynamics of a protein molecule in a crystalline ionic environment, streptomyces-griseus protease-A. Biochemistry 29:8658–8676
267. Kitson DH et al (1993) On achieving better than 1-Angstrom accuracy in a simulation of a large protein—Streptomyces–Griseus protease-A. Proc Natl Acad Sci USA. 90:8920–8924
268. Cerutti DS, Freddolino PL, Duke RE Jr, Case DA (2010) Simulations of a protein crystal with a high resolution X-ray structure: evaluation of force fields and water models. J Phys Chem B 114:12811–12824
269. Cao L et al (2016) Validation of polarizable force field parameters for nucleic acids by inter-molecular interactions. Front Chem Sci Eng 10:203–212
270. Muddana HS, Fenley AT, Mobley DL, Gilson MK (2014) The SAMPL4 host–guest blind prediction challenge: an overview. J Comput Aided Mol Des 28:305–317
271. Bell DR et al (2016) Calculating binding free energies of host–guest systems using the AMOEBA polarizable force field. Phys Chem Chem Phys. https://doi.org/10.1039/C6CP02509A
272. Hirshfeld FL (1977) Bonded-atom fragments for describing molecular charge densities. Theor Chim Acta 44:129–138
273. Koritsanszky TS, Coppens P (2001) Chemical applications of X-ray charge-density analysis. Chem Rev 101:1583–1627
274. Halgren TA (1996) Merck Molecular force field. II. MMFF94 van der Waals and electrostatic parameters for intermolecular interactions. J Comput Chem 17:520–552
275. Bordner AJ, Cavasotto CN, Abagyan RA (2003) Direct derivation of van der Waals force field parameters from quantum mechanical interaction energies. J Phys Chem B 107:9601–9609
276. Langley CH, Allinger NL (2002) Molecular mechanics (MM4) calculations on amides. J Phys Chem A 106:5638–5652
277. Uzoh OG, Galek PTA, Price SL (2015) Analysis of the conformational profiles of fenamates shows route towards novel, higher accuracy, force-fields for pharmaceuticals. Phys Chem Chem Phys 17:7936–7948
278. Perez A, Morrone JA, Simmerling C, Dill K (2016) A. Advances in free-energy-based simulations of protein folding and ligand binding. Curr Opin Struct Biol 36:25–31
279. Schroeder R, Lippincott ER (1957) Potential function model of hydrogen bonds. J Phys Chem 61:921
280. Chidambaram R, Balasubramanian R, Ramachandran GN (1970) Potential functions for hydrogen bond interactions I. A modified lippincott-schroeder potential function for NH–O interaction between peptide groups. Biochim Biophys Acta 221:182–195
281. Momany FA, Carruthers LM, McGuire RF, Scheraga HA (1974) Intermolecular potentials from crystal data. III. Determination of empirical potentials and applications to the packing configurations and lattice energies in crystals of hydrocarbons, carboxylic acids, amines, and amides. J Phys Chem 78:1595–1620
282. Ewig CS et al (2001) Derivation of class II force fields. VIII. Derivation of a general quantum mechanical force field for organic compounds. J Comput Chem 22:1782–1800
283. Cerutti DS, Swope WC, Rice JE, Case DA (2014) ff14ipq: A self-consistent force field for condensed-phase simulations of proteins. J Chem Theory Comput 10:4515–4534
284. Maier JA et al (2015) ff14SB: improving the accuracy of protein side chain and backbone parameters from ff99SB. J Chem Theory Comput 11:3696–3713
285. Demerdash O, Yap E-H, Head-Gordon T (2014) Advanced potential energy surfaces for condensed phase simulation. Annu Rev Phys Chem 65:149–174
286. Friesner RA (2005) Modeling polarization in proteins and protein-ligand complexes: methods and preliminary results. Adv Protein Chem 72:79–104
287. Mohamed NA, Essex JW, Bradshaw RT (2016) Evaluation of solvation free energies for small molecules with the AMOEBA polarizable force field. J Comp Chem 37:2749–2758
288. Ren P, Wu C, Ponder JW (2012) Polarizable atomic multipole-based molecular mechanics for organic molecules. J Chem Theory Comput 7:3143–3161
289. Dinur U (1991) Charge flux and electrostatlc forces in planar molecules. J Phys Chem 95:6201–6211
290. Dinur U, Hagler AT (1990) A novel decomposition of torsional potentials into pairwise interactions—a study of energy 2nd derivatives. J Comput Chem 11:1234–1246
291. Dinur U, Hagler AT (1994) On the functional representation of bond-energy functions. J Comput Chem 15:919–924
292. Mannfors B, Sundius T, Palmo K, Pietila L-O, Krimm S (2000) Spectroscopically determined force fields for macromolecules. Part 3. Alkene chains. J Mol Struc 521:49–75
293. Wang Q et al (2015) A general model for treating short-range electrostatic penetration in a molecular mechanics force field. J Chem Theory Comput 11:2609–2618
294. Narth C et al (2016) Scalable improvement of SPME multipolar electrostatics in anisotropic polarizable molecular mechanics using a general short-range penetration correction up to quadrupoles. J Comp Chem 37:494–505
295. Rackers JA et al (2017) An optimized charge penetration model for use with the AMOEBA force field. Phys Chem Chem Phys 19:276–291

296. Qi R, Wang Q, Ren P (2016) General van der Waals potential for common organic molecules. Bioorg Med Chem. https://doi.org/10.1016/j.bmc.2016.07.062
297. Ren P, Wu C, Ponder JA (2012) Polarizable atomic multipole-based molecular mechanics for organic molecules. J Chem Theory Comput 7:3143–3161
298. Galimberti D, Milani A, Castiglioni C (2013) Charge mobility in molecules: charge fluxes from second derivatives of the molecular dipole. J Chem Phys 138:164115
299. Tafipolsky M, Ansorg K (2016) Toward a physically motivated force field: hydrogen bond directionality from a symmetry-adapted perturbation theory perspective. J Chem Theory Comput 12:1267–1279
300. Eramian H, Tian Y-H, Fox Z, Beneberu HZ, Kertesz M, Se S (2013) On the anisotropy of van der Waals atomic radii of O. F, Cl, Br, and I. J Phys Chem A 117:14184–14190